Impact of viral infections on Natural Killer cell frequencies and recognition

Dissertation

with the aim of achieving a doctoral degree at the Faculty of Mathematics, Informatics and Natural Sciences Department of Chemistry, University of Hamburg

submitted by

Maja Christiane Ziegler

Kiel/Hamburg, 2020

Reviewer:

Prof. Dr. Marcus Altfeld, Department of Virus Immunology, Heinrich Pette Institute, Leibniz Institute for Experimental Virology, Hamburg, Germany.

Prof. Dr. Wolfram Brune, Virus-Host Interaction, Heinrich Pette Institute, Leibniz Institute for Experimental Virology and MIN-Faculty University Hamburg, Hamburg, Germany.

Date of thesis defense: 23rd October, 2020

Publications

Ziegler MC, Naidoo K, Chapel A, Nkotwana S, Mann J, Goulder P, Ndung' T, Altfeld M and Thobakgale CF; HIV-1 clade C evades a p24 Gag mutation that Abrogates Binding to KIR2DL2 and Disinhibits NK cells in infected Individuals with KIR2DL2^{+}/HLA C*03:04^{+} genotype. Under Review

Ziegler MC, Nelde A, Weber JK, Schreitmüller CM, Martrus G, Huynh T, Bunders MJ, Lunemann S, Stevanović S, Zhou R, Altfeld M; HIV‑1-induced changes in HLA‑C*03:04-presented peptide repertoires lead to reduced engagement of inhibitory NK cell receptors. AIDS 2020 Jun 4. doi: 10.1097/QAD.0000000000002596. Online ahead of print.

Ziegler MC, Grañana FB, Garcia-Beltran WF, Schulze zur Wiesch J, Hoffmann C, Rechtien A, et al. Stable Frequencies of HLA-C*03:04/Peptide-Binding KIR2DL2/3^{+} Natural Killer Cells Following Vaccination. Front Immunol. 2018 Oct 17; 9:2361.

Chapel A, Garcia-Beltran WF, Hölzemer A, **Ziegler M**, Lunemann S, Martrus G, et al. Peptide-specific engagement of the activating NK cell receptor KIR2DS1. Sci Rep. 2017 Dec 25; 7(1):2414.

Körner C, Simoneau CR, Schommers P, Granoff M, **Ziegler M**, Hölzemer A, et al. HIV-1-Mediated Downmodulation of HLA-C Impacts Target Cell Recognition and Antiviral Activity of NK Cells. Cell Host Microbe. 2017 Jul; 22(1):111–119.e4.

Lunemann S, Martrus G, Hölzemer A, Chapel A, **Ziegler M**, Körner C, et al. Sequence variations in HCV core-derived epitopes alter binding of KIR2DL3 to HLA-C∗03:04 and modulate NK cell function. J Hepatol. 2016 Aug; 65(2):252–8.

Contents

Index of abbreviations

(+)ssRNA ..... Single-stranded positive sense RNA-genome
aa ..... Amino acid
ADCC ..... Antibody dependent cellular cytotoxicity
AIDS ..... Acquired Immunodeficiency Syndrome
CLRS ..... C type lectin receptor
DAA ..... Direct-Acting Antiviral therapy
DC ..... Dentritic cell
ER ..... Endoplasmic reticulum
GWAS ..... Genome wide association studies
HAART ..... Highly active antiretroviral therapy, Highly Active Antiretroviral Therapy
HCC ..... Hepatocellular carcinoma
HCMV ..... Human Cytomegalovirus
HCV ..... Hepatitis C Virus
HIV-1 ..... Human Immunodeficiency Virus type 1
IFN-α ..... Interferon-α
Ig ..... Immunoglobulin
IL ..... Interleukin
IN ..... Integrase
IRE ..... Internal ribosome entry site
ITAM ..... Immunoreceptor tyrosine based activating motif
ITIM ..... Immunoreceptor tyrosine based inhibitory motif
KIR ..... Killer cell immunoglobuline receptor
LS-MS/MS ..... Liquid chromatography coupled tandem mass spectrometry
LTR ..... Long terminal repeat sequences
MAPK ..... Mitogen activated protein kinase
MHC ..... Major histocompatibility complex
NCR ..... Natural cytotoxicity receptors
NF-κB ..... Nuclear factor κB
NK cells ..... Natural killer cells
NKG2 ..... C type lectins
P2 ..... Anchor position at N-Terminus
PR ..... Protease
PRR ..... Germline encoded pattern recognition receptor
PΩ ..... Anchor position at C-Terminus
RT ..... Reverse transcriptase
SNP ..... Single nucleotide polymorphism
TAP ..... Transporter associated with antigen processing
T_H1 cell ..... Type 1 helper T-cell
Th17 cell ..... T helper 17 cell
T_H2 cell ..... Type 2 helper T-cell
TLR ..... Toll-like receptor
TNF-α ..... Tumor necrosis factor-α
TRAIL ..... TNF related apoptosis inducing ligand
T_{reg} ..... Regulatory T-cell
UTR ..... Short untranslated region

List of tables

Table of figures

Zusammenfassung

Natürliche Killerzellen (NK-Zellen) spielen eine wichtige Rolle in der Bekämpfung viraler Infektionen. Sie tragen hemmende Killerzell Immunglobulin-ähnliche Rezeptoren (KIRs) auf der Zelloberfläche, welche die Aktivität der Zelle durch die Interaktion mit humanen Leukozytenantigenen der Klasse I (HLA-I) regulieren können. Virale Infektionen können diese Interaktion beeinflussen, indem sie die intrazellulären Peptide verändern, die für die Präsentation durch HLA-I Moleküle zur Verfügung stehen. HLA-C ist der Ligand für KIR2DL2/3, aber die genauen Mechanismen wie diese Interaktion von viralen Infektionen beeinflusst wird, wurde bisher noch nicht genauer untersucht. Im ersten Teil dieser Arbeit habe ich die Häufigkeit von KIR2DL2/3$^+$ NK-Zellen, die HLA-C*03:04 im Komplex mit spezifischen viralen Peptiden erkennen können, in gelbfiebergeimpften Personen und HIV-1 oder HCV infizierten Menschen untersucht. E*x vivo* Färbungen von NK-Zellen mit HLA-I Tetrameren haben ergeben, dass die Anzahl an Tetramer$^+$KIR2DL2/3$^+$ NK-Zellen auch über einen längeren Zeitraum nach Antigen-Kontakt stabil bleibt und die Avidität des Tetramers zu KIR2DL2/3 bestimmt, wie viele KIR2DL2/3$^+$ NK-Zellen das Tetramer binden. Im zweiten Teil dieser Arbeit habe ich die durch eine HIV-1 Infektion auftretenden Veränderungen in den HLA-I präsentierten Peptiden und deren Einfluss auf die Aktivität von NK-Zellen untersucht. Mittels massenspektrometrischer Analyse wurden 533 Peptide identifiziert, die ausschließlich auf HIV-1 infizierten Zellen präsentiert wurden und von denen 8 viralen Ursprungs waren. *In vitro* Experimente zeigten, dass HLA-C*03:04 präsentierte Peptide, die auf uninfizierten Zellen identifiziert wurden, eine stärkere Bindung an KIR2DL3 vermitteln, als Peptide die auf HIV-1 infizierten Zellen präsentiert wurden. Zusammengefasst zeigen diese Daten, dass die HLA-C*03:04/Peptid/KIR2DL2/3 Interaktion keine Veränderung der Anzahl von spezifischen KIR$^+$ NK-Zellen bewirkt. Durch eine HIV-1 Infektion herbeigeführte Veränderungen in HLA-I präsentierten Peptiden kann jedoch dazu führen, dass die Bindung an hemmende KIRs reduziert wird. Dies eröffnet einen möglichen Mechanismus, wie NK-Zellen von virusinfizierten Zellen aktiviert werden und somit zu einem positiveren Krankheitsverlauf beitragen können.

Abstract

Natural killer cells (NK cells) are known to play a crucial role in the control of viral infections. It is described that inhibitory killer cell immunoglobuline-like receptors (KIRs) expressed on NK cells modulate NK cell activity through the binding to human leukocyte antigen class I (HLA-I). These interactions are influenced by viral infections altering intracellular peptide repertoires available for presentation by HLA-I. KIR2DL2/3 binds to HLA-C molecules, but the exact mechanisms how this interaction is modulated by viral infections remains incompletely understood. In the first part of this thesis, I investigated whether frequencies of KIR2DL2/3$^+$ NK cells recognizing HLA-C*03:04/viral peptide complexes are impacted by Yellow Fever Virus vaccination and HIV-1 or HCV infection. *Ex vivo* HLA-I tetramer staining of primary human NK cells revealed that the proportion of teramer$^+$KIR2DL2/3$^+$ NK cells remained stable over time after antigen exposure and that the avidity of the tetramer to KIR2DL2/3 dictated the frequency of tetramer$^+$KIR2DL2/3$^+$ NK cells. In the second part, I focused on HIV-1-induced alterations in the HLA-I-presented peptide repertoire and how these changes modulate the function of NK cells. Using mass spectrometric analysis, I identified a total of 533 peptides exclusively presented on HIV-1-infected cells, of which only 0.2 % represented HIV-1-derived peptides. Cell-based *in vitro* assays focusing on HLA-C*03:04/KIR2DL3 interactions revealed that HLA-C*03:04-presented peptides derived from non-infected CD4$^+$ T cells mediated stronger binding of inhibitory KIR2DL3 than peptides derived from HIV-1-infected cells. All in all these data show that interactions between inhibitory KIRs and their HLA-I ligands are modulated by the HLA-presented peptide, but that these interactions do not result in the expansion or accumulation of specific inhibitory KIR$^+$ NK cell subpopulations. But, HIV-1-infection-induced changes in HLA-I-presented peptides can reduce engagement of inhibitory KIRs, providing a mechanism for enhanced activation of NK cells by virus-infected cells leading to a more favorable disease outcome.

Introduction

First described in 1983, Human Immunodeficiency Virus type 1 (HIV-1) infection remains a major public health problem, especially in countries of the global south (1). In 2018, approximately 37.9 million people were suffering from infection with HIV-1 all over the world, with highest prevalence in southern sub-Saharan Africa (WHO, UNAIDS). In the absence of treatment, infection with HIV-1 results in the development of Acquired Immunodeficiency Syndrome (AIDS), which ultimately can lead to death. Due to the introduction of Highly Active Antiretroviral Therapy (HAART) in 1995, the HIV-1-related mortality declined and the progression to the later stages of AIDS are being reduced. In 2017, 1.7% of all deaths globally were caused by HIV-1, with very high variations across the world. In South Africa and Botswana HIV-1-related mortality was still the fourth leading cause of death in 2017 (WHO). Like HIV-1, infection with Hepatitis C Virus (HCV) leads to clinically relevant persistent infections. In 2015, an estimated 71 million people suffered from chronic HCV infection most prevalent in the Eastern Mediterranean Region and the European Region (WHO, 2017). In 2016, 399 000 individuals died of HCV infection-related diseases like cirrhosis and hepatocellular carcinoma, making HCV infection the leading cause for liver transplantation. For HCV, a recent breakthrough in treatment , the newly Direct-Acting Antiviral therapy (DAA therapy), has led to an effective cure of chronic HCV infection in about 95 % of infected individuals, but DAA therapy fails to prevent re-infection. However, for HIV-1 as well as for HCV, access to diagnosis is low and therapies remain costly limiting their availability to developed countries. Extensive efforts have been made to develop prophylactic vaccines to effectively reduce HCV and HIV-1 infection rates. Due to high genetic diversity and strategies of the viruses to evade the host immune response these attempts, have so far failed (2,3). On the contrary, numerous studies highlight the role of the innate immune system to determine the clinical outcome of HCV and HIV-1 infections (4–7). The innate immune response plays a crucial role in controlling viral infections in the acute phase of infection and helps to initiate and direct the adaptive immune response (4,8–10). In this context, NK cells are of special interest, as several epidemiological studies have shown that expression of specific NK cell receptors in combination with their

respective HLA-I ligands can be beneficial in the context of HIV-1 and HCV infections (4,5,11). Therefore, further investigations to improve the understanding of the NK cell response to HIV-1 and HCV infections might open new perspectives for the development of immunotherapies.

1. Human immunodeficiency virus type 1

HIV-1 is an enveloped retrovirus belonging to the genus of *Lentivirus*. HIV-1 is transmitted mainly through contact with body fluids, through sexual behavior, by sharing needles with an infected individual during intravenous drug use or vertically from mother-to-child at birth or through breast-feeding (12). Acute infection is followed, in the large majority of cases, by a chronic infection and the establishment of a persistent viral reservoir. HIV-1 infects cells of the human immune system such as $CD4^+$ T cells, macrophages and dendritic cells (DCs). Thereby, persistent infection leads to an impairment of cell-mediated immunity characterized by a massive decline of $CD4^+$ T cells. Subsequently the host becomes progressively more susceptible to opportunistic infections, as well as cancer. Clinical outcome of HIV-1 infection is very heterogeneous depending on the immune status and genotype/phenotype of the infected individual, ranging from progression to AIDS within a year after infection to the control of the infection without drugs for more than twenty years (13). HIV-1 enters the host cell using receptor-mediated endocytosis, involving CD4, CCR5 and CXCR4. The single-stranded positive sense RNA-genome ((+)ssRNA) of the virus is transcribed via the viral reverse transcriptase into cDNA, which is subsequently integrated in the host genome. Utilization of the promotor in the 5' long terminal repeat sequences (LTRs) drives transcription. The copies of viral mRNA are translated into newly synthesized viral proteins, and, together with the genomic RNA, move to the cell surface. After assembly of the viral particle and budding from the infected cell, new viral particles are released (14). The HIV-1 genome consists of nine genes, flanked by LTRs. LTRs contain binding sites for gene regulatory proteins and are necessary for the integration in the host genome. The three major genes are *gag*, *pol* and *env*. *Gag* is highly conserved and codes for structural proteins of the viral core, such as the capsid protein p24 (CA), the matrix protein

p17 (MA) and the nucleocapsidprotein p9 (NC). *Pol* is translated into the three enzymes necessary for the viral replication such as the reverse transcriptase (RT), protease (PR) and integrase (IN). The gene product of *env* is cleaved into gp120 and gp41, two glycoproteins located in the envelope and responsible for the cellular tropism of the virus (13). The most effective treatment of HIV-1 is the highly active antiretroviral therapy (HAART), which allows HIV-1-infected individuals to survive and have a good life expectancy and quality. HAART is a combination of several antiretroviral drugs, which slows down the replication rate of the virus thereby helping to control viral load. They act mostly through inhibition of the important viral enzymes reverse transcriptase, integrase and protease. Newly synthesized drugs also interfere with viral binding, fusion and entry to the host cell or viral maturation (15). Although this antiretroviral medication is quite successful to control the virus, until now, there is neither a cure nor an effective vaccine against HIV-1 available.

2. Hepatitis C virus

HCV is an enveloped (+)ssRNA virus and belongs to the *Flaviviridae* family of the genus *Hepacivirus* (16). It mainly targets cells of the liver, the hepatocytes, causing acute as well as chronic infection. While chronic infections are established in majority of infected individuals, 25% clear HCV infection during acute phase of infection. Persistent infection can cause severe liver disease including fibrosis, cirrhosis and liver cancer such as hepatocellular carcinoma (HCC). HCV is a blood-borne virus and therefore transmitted through infected blood or blood products. The main risks for HCV infection are intravenous drug use, the use of contaminated blood products, unsafe medical procedures and from mother to child at birth. The HCV virion circulates in the blood as free-particle or surrounded by host low-density lipoproteins highly associated with infectivity (17). After attaching to the target cell by binding of various receptor molecules, the viral particle enters the cell via clathrin–mediated endocytosis. Following uncoating, the (+)ssRNA is released in the cytoplasm and directly translated into a single precursor polyprotein and subsequently cleaved into ten mature proteins. New virions are assembled in an ER-derived compartment, transported to the cell membrane via the Golgi-dependent secretory pathway and released through exocytosis (18). The HCV genome encodes for one single open reading frame flanked by short untranslated regions (5’

UTR and 3'UTR) containing internal ribosome entry sites (IREs) necessary for protein translation. The encoded polyprotein delivers three structural proteins (core, E1, E2) and seven non-structural proteins (p7, NS2, NS3, NS4A, NS4B, NS5A and NS5B) (19). In chronically HCV-infected patients, the main goal of therapy is to cure the infection and therefore prevent HCV-related diseases. Since the late 1980s Interferon-α (IFN-α) was used as an antiviral treatment, bearing a lot of side effects. Since then, therapy improved by the combination of IFN-α with ribavirin, a nucleoside analogue, or protease inhibitors. Between 2011 and 2015 the introduction of IFN-free DAAs changed HCV therapy dramatically. DAAs have been shown to effectively cure chronic HCV infections with an infection cure rate of more than 95% (20,21). DAAs target three proteins crucial for the HCV life cycle thereby interfering with the NS3/4A protease, NS5A protein and NS5B, the RNA-dependent RNA polymerase.

3. Yellow fever virus vaccine 17D as an *in vivo* model

In this thesis, I used the live attenuated YFV vaccine 17D as a human *in vivo* model to study longitudinally frequencies of NK cell subsets after viral challenge. I therefore mainly focus on the vaccine in this part.

YFV is the type species of the genus Flavivirus, that owes its name to the jaundice associated with the liver dysfunction characteristic for yellow fever disease. In the first phase of infection YFV infects mainly macrophages and dendritic cells causing only mild symptoms, whereas in the second phase hepatocytes are the target of the virus leading to more severe symptoms such as renal failure, severe hepatitis, circulatory shock, hemorrhage and multi-organ failure (22,23). YFV follow the life cycle generic to Flavivirus (24). The main strategy to control yellow fever is vaccination. In 1936 the yellow fever 17D vaccine was developed, which is a live attenuated vaccine injected subcutaneously providing effective immunity within one week in 95% of vaccinees. A single dose provides protection for at least 30 years (23). Vaccination results in a mild or subclinical infection and a transient low-level viremia. The effectiveness of the vaccine is attributed to the induction of both the innate as well as the adaptive immune response. This leads to the production of neutralizing antibodies directed against the envelope

protein of the virus. Additionally, innate immune cells are stimulated to secrete balanced anti-inflammatory and pro-inflammatory cytokines modulating other immune cells and shaping the adaptive immune response (25). More specifically, vaccination with 17D was shown to induce a robust NK cell response *in vivo* with a peak of NK cell function at day 6 and proliferation of NK cells at day 10 post vaccination (26). Individuals vaccinated with YFV 17D are therefore an interesting *in vivo* model to investigate NK cell characteristics after viral infection.

4. The human immune system in viral infections

The human immune system is specialized to protect the host against infection by various pathogens. These pathogens include extracellular bacteria, parasites, fungi, intracellular bacteria, parasites, viruses and parasitic worms (13). The elimination of these pathogens is mediated by leukocytes which arise from precursor cells in the bone marrow and build up the two arms of the immune system: innate and adaptive immunity (Fig. 1).

Viral infections induce similar patterns of immune response .The initiation of the immune response starts once the host senses a virus via germline-encoded pattern recognition receptors (PRR) like C-type lectin receptors (CLRSs) and Toll-like receptors (TLRs), which are expressed highly on DCs (27). These receptors recognize pathogen-associated products or damage-associated molecular patterns. The engagement of PRRs leads to the production of IFN-α/β and Interleukin-15 (IL-15) (28). Subsequently DCs mature and migrate to the lymph nodes, where they present antigens to immature $CD4^+$ and $CD8^+$ T cells via HLA-I and -II molecules. Naive $CD4^+$ T cells subsequently mature into type 1 helper T cells (T_H1 cells), Type 2 helper T cells (T_H2 cells), regulatory T cells (T_{regs}) and T helper 17 cells (Th17 cells). $CD8^+$ T cells differentiate into virus specific cytotoxic cells. In addition to direct stimulation through activation receptors, IFN-α, IFN-β, IL-12 and IL-15 activate NK cells (29). Activated NK cells release perforin and granzyme to kill the virus-infected cell (30). Additionally, cytotoxic cells can release the cytokines IFN-γ and tumor necrosis factor-α (TNF-α), upon stimulation by an infected cell (31,32). IFN-γ boosts killing of virus-infected cells in

various ways including direct induction of apoptosis, the increase of HLA-I and -II presented antigens, upregulation of antiviral proteins and modulation of the expression of proteins interfering with cell cycle and proliferation (33). Additionally, IFN-γ can have immunomodulatory effects through the upregulation of protein, which serve as chemo attractants for various immune cells and can introduce immunoglobulin (Ig) class switch of B cells (34). TNF-α is responsible for multiple signaling events inducing apoptosis or necrosis of virus-infected cells through activation of the nuclear factor κB- (NF-κB) and mitogen-activated protein kinase (MAPK) pathways (35). Moreover production of IL-15 mainly by DC's, monocytes and macrophages induces proliferation of NK cells, $CD8^+$ T cells and B cells and helps maintaining the memory pool of $CD8^+$ T cells (36,37). In addition, macrophages are stimulated to release TNF-α. Th1 and Th2 cells contribute to the differentiation of B cells to antibody-producing plasma cells and long-lived memory cells (38). The overall aim of the immune response is to either clear the virus or reduce viral load in persistent viral infections (39).

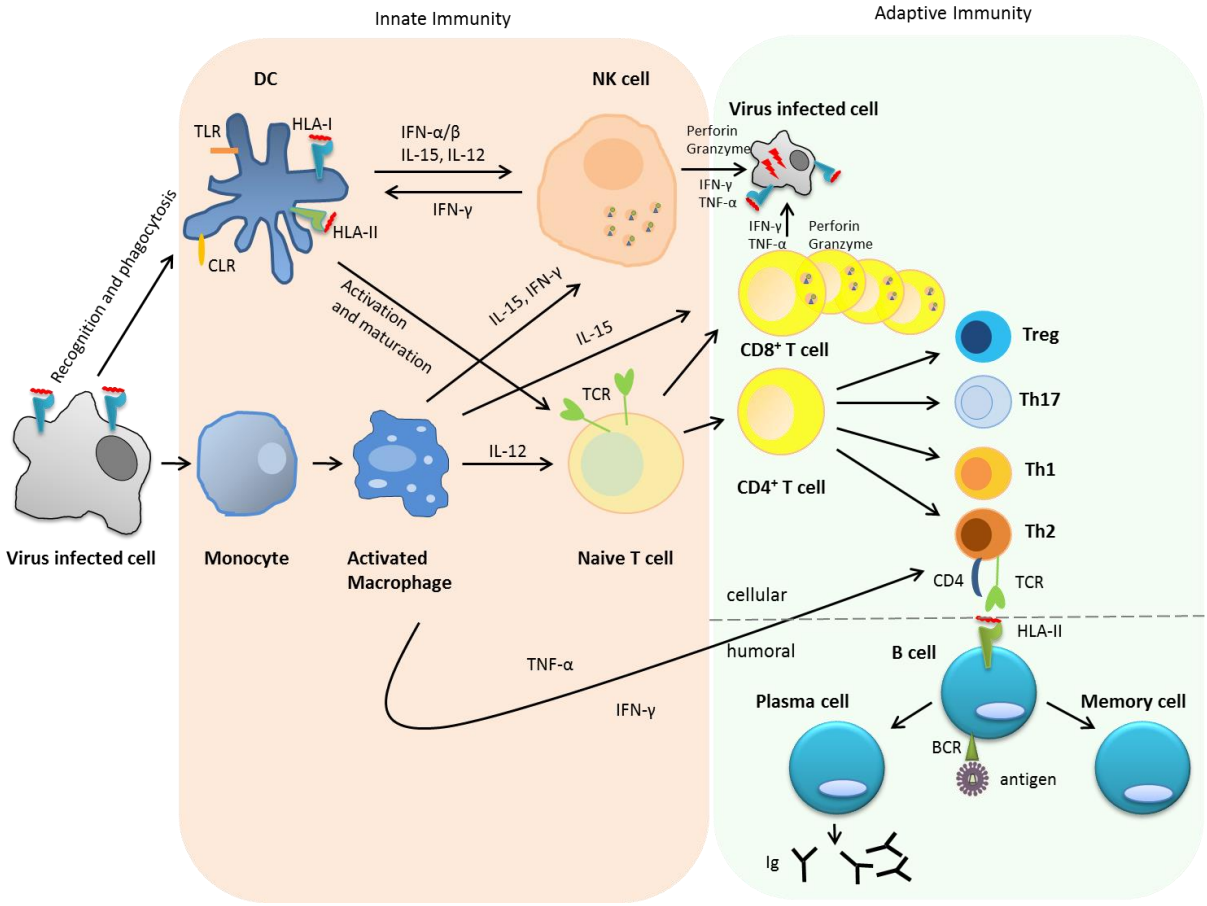

Fig. 1 Simplified illustration of innate and adaptive immune responses to viral infections. Virus-infected cells are recognized via PRR and subsequently engulfed by macrophages and dendritic cells. After activation these antigen presenting cells (APC) release pro-inflammatory cytokines. NK cells are activated by theses cytokines or direct interaction with virus-infected cells. Presentation of antigens via HLA-I and HLA-II induces the maturation of T cells into either $CD8^+$ or $CD4^+$ T cells. $CD4^+$ T cells differentiate further into regulatory T cells (Treg), T-helper 17 cells (Th17), T-helper 1 (Th1) and T-helper 2 type (Th2) cells. IL-15 stimulates proliferation of cytotoxic $CD8^+$ T cells. NK cells and $CD8^+$ T cells kill virus-infected cells through the release of granzyme and perforin. Interactions of Th1 and Th2 cells with B cells via B cell receptor (BCR) and T cell receptor (TCR) lead to differentiation of the B cell into antibody producing plasma cells and long-lived memory cells.

5. Natural killer cells

NK cells are known to play an important role in controlling viral infections. Amongst innate immune cells, NK cells are equipped with the distinctive ability to recognize and kill virus-infected cells without prior sensitization. NK cells are large granular lymphocytes and were initially identified by their ability to kill malignantly transformed cells (40,41). NK cells make up 5-15% of peripheral blood mononuclear cells. Based on their expression levels of CD56 and CD16, NK cells are classically divided into two subsets. The minor subset accounts for $CD3^{neg}CD56^{bright}CD16^{neg}$ NK cells, capable of producing large quantities of

pro-inflammatory cytokines such as IFN-γ and TNF-α. Whereas the major subset consists of $CD3^{neg}CD56^{dim}CD16^{pos}$ NK cells, highly cytolytic through the ability to secret large amounts of perforin and granzyme (42).

The importance of NK cells in the defense against viral infections was initially highlighted by individuals who are NK cell-deficient. These individuals are highly susceptible to viral infections especially infections with herpesviruses (43,44). NK cells have been traditionally classified as part of innate immunity as they act early in infection, do not possess an antigen specific receptor and are able to kill target cells without prior antigen exposure. Nevertheless increasing studies report that NK cells share some features with adaptive lymphocytes. It was shown that NK cells are able to clonally expand and their responsiveness is modulated through an "education" or "licensing" process which can be either antigen-specific or antigen-independent (45–50). The lysis of infected cells is mediated through the secretion of the lytic granules perforin and granzyme (30). Additionally, NK cells express TNF-related apoptosis-inducing ligand (TRAIL) and Fas, both binding to their respective cell-death receptors such as Fas-R and TRAIL-R, inducing caspase-dependent apoptosis of the target cell. The third effector function is antibody-dependent cellular cytotoxicity (ADCC). NK cells thereby recognize target cells coated with IgG antibodies via Fcγ receptors and react by secreting IFN-γ and cytolytic granules (51). Moreover, it was shown that NK cells are able to modulate the adaptive immune response (4). These immunoregulatory effects are mediated through the production of cytokines and chemokines (9) and the interaction with $CD4^+$ T cells, $CD8^+$ T cells and DC's (8,52,53) (Fig. 1). NK cells are furthermore known to be involved in the rejection of bone marrow transplants, autoimmunity, tissue remodeling and the maintenance of pregnancy. This highlights the multiple functions of NK cells in the immune system and development (54).

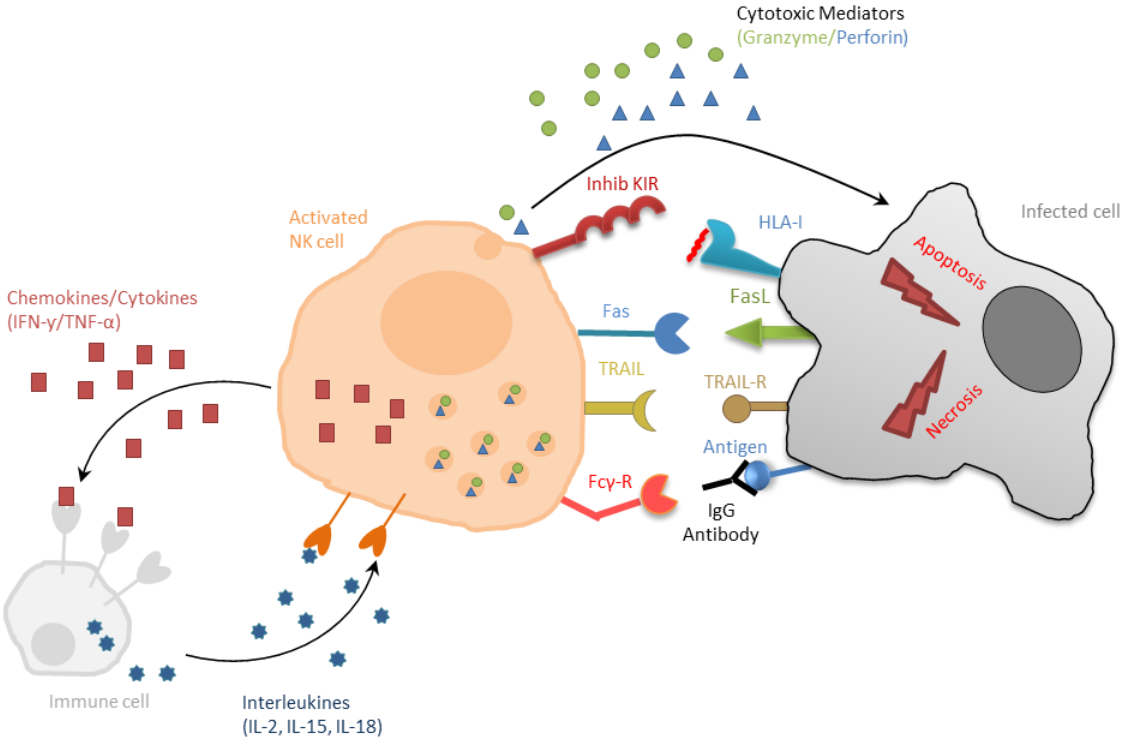

Fig. 2 NK cell effector functions. After receptor-mediated recognition of the infected cell, NK cells are endowed with three effector functions leading to the lysis of the target cell. Firstly, degranulation with release of granzyme and perforin, secondly death-Receptor mediated induction of apoptosis and thirdly Antibody-dependent cellular cytotoxicity (ADCC). Additionally NK cells have immunomodulatory functions through the secretion of IFN-γ and TFN-α.

5.1 Regulation of NK cell activity

Due to their potent effector function, NK cell activity has to be tightly regulated by a balanced interplay between activating and inhibitory receptors. An important step in the understanding of how NK cells are regulated was the observation that NK cells preferentially kill cells with low or no HLA-I expression. This led to the formulation of the “missing-self hypothesis” of NK cell killing (55). This hypothesis describes the ability of NK cells to discriminate between infected or altered and normal cells through monitoring the peptide state of the cell. Besides receptor-mediated activation of NK cells, cytokines are critical for the synthesis of cytotoxic granules and cytokines, as well as for survival and proliferation.

NK cell activation is determined through the integration of activating and inhibitory signals delivered by different receptor families. Therefore the repertoire of receptors expressed on the NK cell combined with the repertoire of ligands expressed on the target cell determines the fate of the interaction – a balanced

interaction leads to inhibition, an unbalanced one leads to activation of the NK cell (Fig. 3). NK cell receptors are germline-encoded and recognize self-ligands, stress-induced ligands and infection-associated ligands on target cells. The receptors involved in NK cell regulation, can be divided into three major families - natural cytotoxicity receptors (NCR), c-type lectins (NKG2) and KIRs (Fig. 3). NCRs are activating receptors and include the constitutively expressed NKp46 and NKp30. NKp44 is expressed upon IL-2 triggered NK cell activation. The ligands of these receptors are partly unknown, but several viral- and tumor-associated molecules have been identified (56). Recently it was shown, that a subset of HLA-II molecules, HLA-DP, can serve as a ligands for NKp44, triggering functional NK cell responses (57). The receptors of the NKG2 family deliver activating as well as inhibitory signals. The activating receptor NKG2D recognizes the proteins ULBP1 and 2 derived from HCMV and the ligands MIC-A/B, expressed on stressed cells such as virus-infected cells. NKG2A and NKG2C interact with HLA-E, a non-classical HLA-I molecule, loaded with peptides derived from classical HLA-I molecules (58). The KIR family is highly polymorphic and consists of 15 functional activatory and inhibitory receptors. KIRs interact with specific allotypes of classical and non-classical HLA- I molecules (Table 1). So far not every KIR ligand is identified. But, recently it was shown that KIR3DS1 binds to open conformers of the non-classical HLA-I molecule HLA-F (59).

In addition there are a number of other specific receptors, differentially expressed among the various NK cell subsets that play an important role for NK cell function. They give the NK cells the ability to respond in an adequate manner to their target cells (42). As I am focusing on HLA-I/KIR interactions in this thesis I will further describe KIRs in more detail.

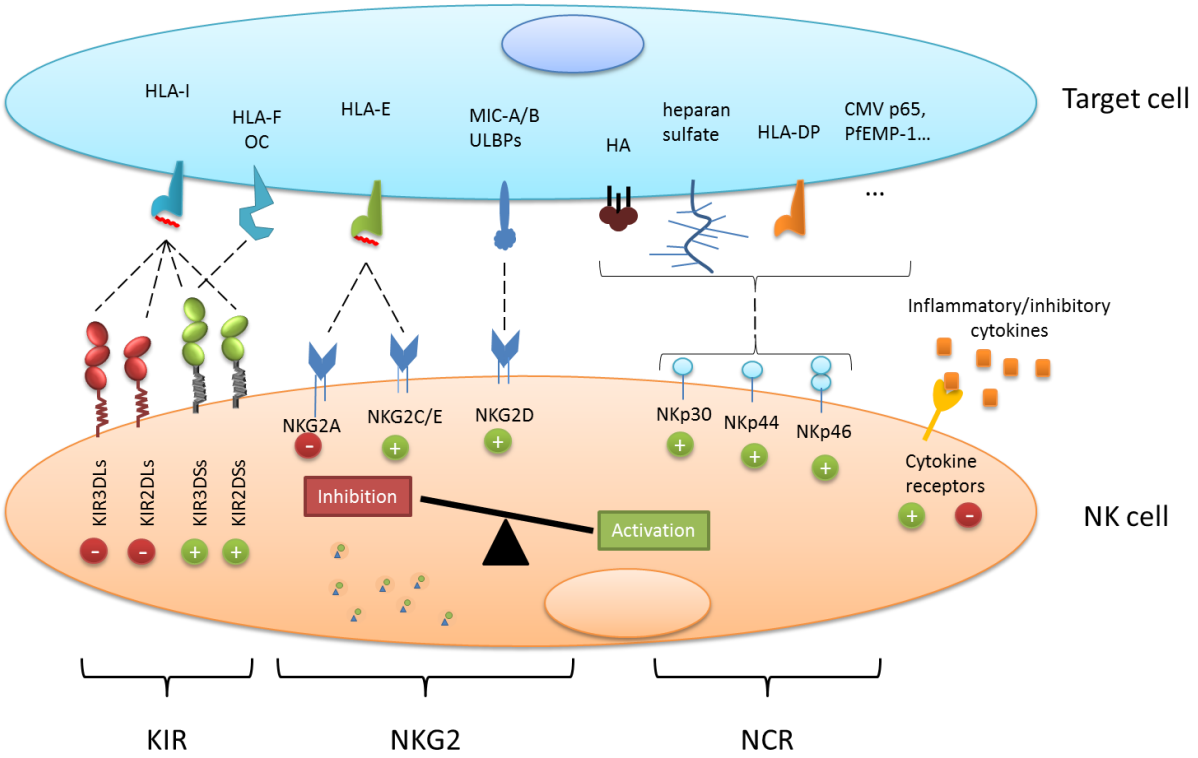

Fig. 3 NK cell receptors and their ligands on target cells. Abbreviations: KIR, killer immunoglobulin-like receptor; NCR, natural cytotoxicity receptor; HLA, human leukocyte Antigen; OC, open conformer; MIC, MHC class I polypeptide-related sequence; ULBP, UL16-binding protein; HA, hemagglutinin; PfEMP-1, Duffy-binding-like (DBL)-1α of Plasmodium falciparum erythrocyte membrane protein-1 (Figure based on (60)).

5.2 Killer cell immunoglobulin-like receptors

KIRs are divided into two structural groups, KIR2D and KIR3D, reflecting the number of immunoglobulin-like domains in the extracellular region. The size of the cytoplasmic tail determines whether the receptor is activating or inhibitory. Activating KIRs exhibit a short cytoplasmic tail (designated "S"), which interacts upon stimulation via a lysine in the transmembrane region of the cell, with the adaptor molecule DAP-12. DAP-12 contains immunoreceptor tyrosine-based activating motifs (ITAMs), which are responsible for the delivery of activating signals to the cell. Inhibitory KIRs possess a long cytoplasmic tail, containing immunoreceptor tyrosine-based inhibitory motifs (ITIMs), which can effectively prevent NK cell activation (61) (Fig. 4).

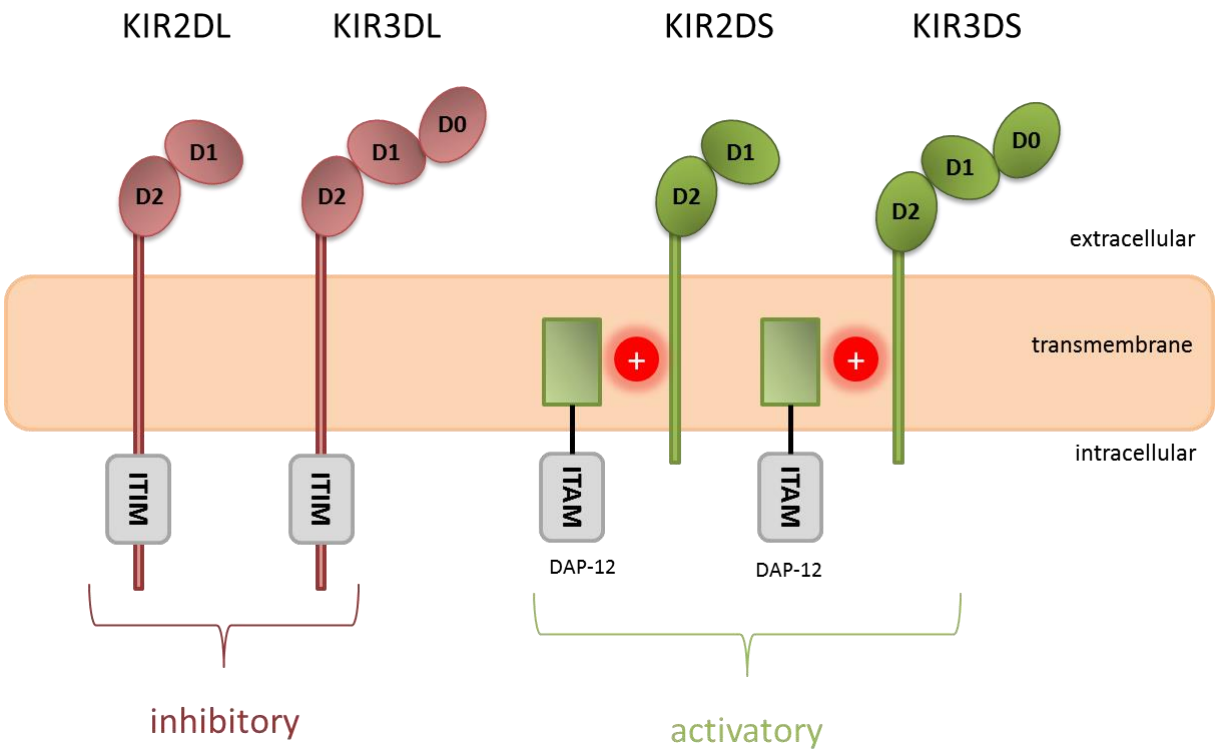

Fig. 4 Structure of Killer cell immunoglobulin-like receptors. Immunoglobulin-like domains are divided into three groups D0, D1 and D2. Inhibitory KIRs exhibit a long cytoplasmic tail, containing ITIMs. Activatory KIRs exhibit a short cytoplasmic tail and the positively charged transmembrane region interacts with the adaptor molecule DAP-12.

5.3 HLA-I molecules presenting peptides are ligands for KIRs

HLAs enable the immune system to distinguish 'self' versus 'non-self' and are therefore classified as the major histocompatibility complexes (MHCs). The HLA system in human is analogous to the MHC system in other animals. HLA alleles are grouped into classical HLA-I (HLA-A, -B, -C), non-classical HLA-I (HLA-E, -F, -G, -H), and HLA-II (HLA-DR, -DQ, -DM, and –DP), all of them are involved in antigen presentation to $CD8^+$ T cells, NK cells and $CD4^+$ T cells (62–65). They are encoded in the most variable region in the human genome, a ~3,500 kb segment located on human chromosome 6p21.3 (66). The function of HLA-I molecules is the presentation of intracellular peptides at the cell surface reflecting the health state of the cell (67,68). HLA-I molecules are formed by two polypeptide chains. The α-chain consists of 3 domains. The α1- and α2- domain form the peptide-binding groove, whereas the α3 domain spans the plasma-membrane and is non-covalently linked with the β2-microglobulin subunit (β2m) (69). Peptide binding to classical HLA-I is fundamental for the proper folding, expression and function of the molecule.

It is estimated that HLA-I molecules, encoded by a single HLA-I allele, are able to present 10^3-10^4 different peptides per cell (70). The potential peptide repertoire is dependent on the peptide-binding groove of the HLA-I molecule. A conserved hydrogen-bonding network at the N- and the C-termini leads to a preferentially binding of peptides with a length of 8 to 11 amino acids (aas), with 9 aa being the optimal length. The peptide is generally fixed at two anchors residues, one at the N-Terminus (P2) and the other at the C-terminus (PΩ), determined by the size, hydrophobicity and electrostatic charge of six pockets within the peptide binding groove (71). The antigen presentation pathway includes a series of proteins that together determine the stable surface expression and antigen presentation of HLA-I molecules. Proteasomal degradation and further amino peptidase-mediated trimming of cytolytic proteins lead to peptides with the optimal size for HLA-I binding. These peptides bind to Transporter associated with antigen processing (TAP) located in the endoplasmic reticulum (ER) membrane and are subsequently translocated into the ER lumen in an ATP-dependent manner. Several proteins, known as the peptide-loading complex, help to load the peptides onto HLA-I/β2m heterodimers. Presentation of the peptides occurs after trafficking of the HLA-I/peptide complex via the secretory pathway to the cell surface (Fig. 5) (72). This process is highly sensitive and influenced by protein abundance and turnover as well as ER stress (73,74). Viral infections lead to accumulation of misfolded dysfunctional proteins as a byproduct of virus replication, which can be toxic to the cell (75). This biological stress let the infected cell respond in a heat shock-like manner and leads to the induction of the intracellular stress response. Which focuses on the removal of misfolded proteins, through the expression of protein chaperones, inhibition of protein synthesis and activation of the ubiquitination machinery (76–79). As viral infections can affect numerous aspects of cellular metabolism, they possess enormous potential to alter the repertoire of peptides in the endogenous antigen presentation pathway to be detected by f the immune system (80). Besides the specificity of KIRs for specific HLA-I molecules, the interaction of both molecules is dependent on the peptide presented by the HLA-I molecule. This was shown in functional studies demonstrating that sequence changes in the presented peptide significantly modulated NK cell function (81,82). Rajagopalan and Long were the first who showed that the binding of KIR2DL1 to HLA-Cw4 is peptide-dependent. This

interaction is abrogated through amino acid exchanges at position 8 of the peptide, while the peptide is still able to bind to HLA-Cw4 (83).

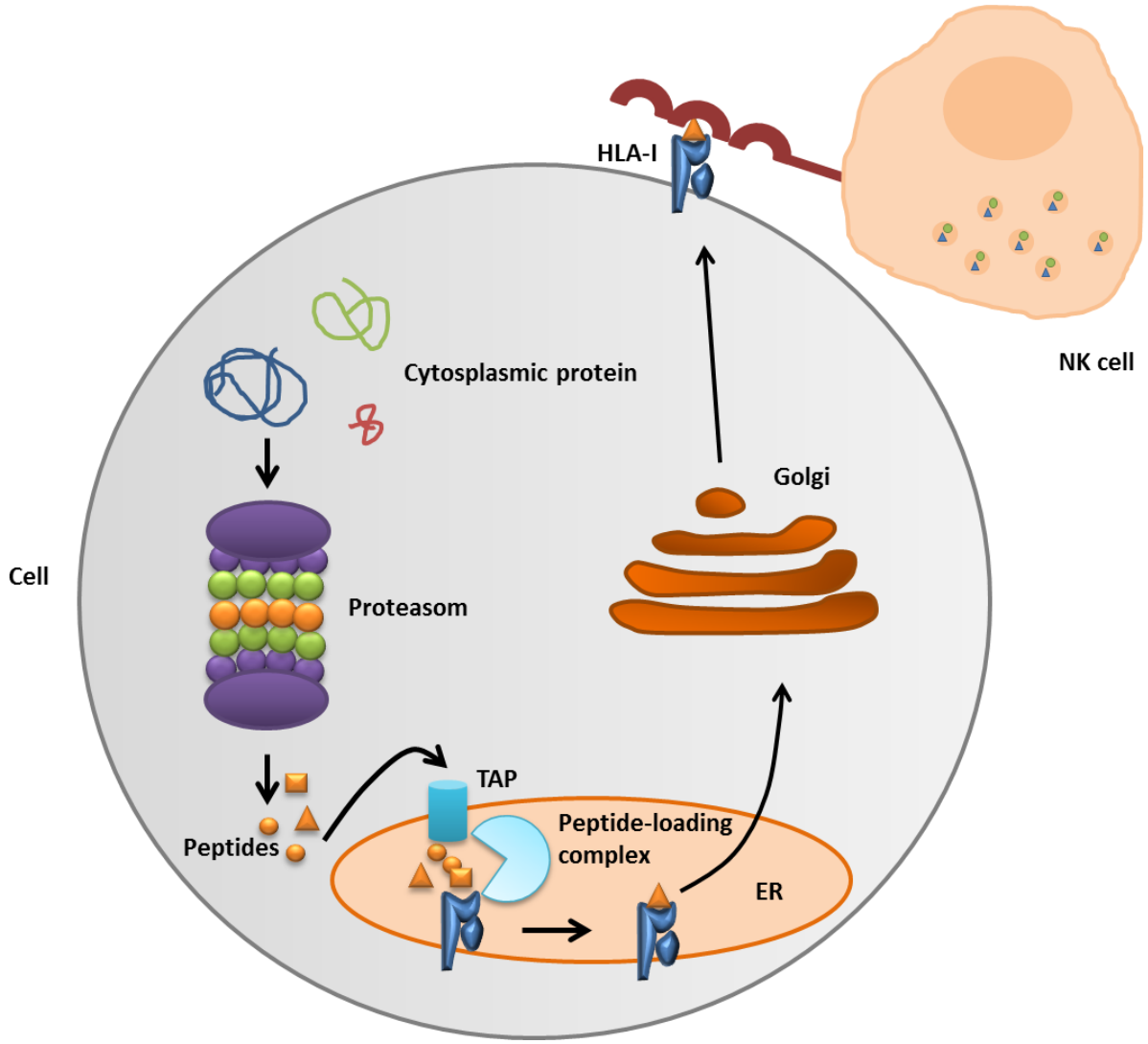

Fig. 5 HLA-I antigen processing. Cytoplasmic proteins are cleaved into peptides by the proteasome. After TAP-dependent translocation into the ER, peptides are loaded onto HLA-I molecules. The peptide-loaded HLA-I molecule traffics via the Golgi complex to the cell surface where it presents the peptide to cytotoxic cells such as NK cells. (Figure based on (72))

Table 1 Killer cell immunoglobulin-like receptors and their ligands. KIR/HLA-I interaction important for this thesis marked in red.

Receptor	Known ligand	Function
KIR2DL1	HLA-C group 2	Inhibitory
KIR2DL2/3	**HLA-C group 1** HLA-B*46:01	**Inhibitory**
KIR2DL4	HLA-G	Activating
KIR2DL5	Unknown	Inhibitory
KIR2DS1	HLA-C group 2	Activating
KIR2DS2	HLA-C group 2, HLA-A*3/A*11	Activating
KIR2DS3	Unknown	Activating
KIR2DS4	HLA-Cw4	Activating
KIR2DS5	Unknown	Activating
KIR3DL1	HLA-Bw4^{I80} HLA-F	Inhibitory
KIR3DS1	HLA-Bw4^{I80}/OC HLA-F	Activating
KIR3DL2	HLA-A*3/A*11 HLA-F	Inhibitory

5.4 HLA-C*03:04/KIR2DL3 in HCV and HIV-1 infections

Discovered in the 1970s (84), HLA loci appeared to be a leading genetic factor for the susceptibility to infectious disease (85,86). Here I focus on the interaction of HLA-C*03:04 and KIR2DL3, as this interaction was shown to be important in HCV as well as HIV-1 infection. HLA-C*03:04 is a member of the HLA-C group 1 and expressed at variable frequencies, ranging from 1% in Saudi Arabian populations up to 54% in Brazilians (allelfrequencies.net). In Caucasian populations in Germany the range is between 14–21%. HLA-C*03:04 is a ligand for the inhibitory receptor KIR2DL3. Expression of KIR2DL3 varies between 57% in Australians up to 100% in Chinese population (87). In this study I focus on KIR2DL3*001, the most common allele in European and North-American populations (88).

Combined expression of KIR2DL3 and HLA-C*03:04 was shown to be beneficial in HCV infection as well as HIV-1 infection. Genetic association studies on HCV-infected individuals showed a consistent association between viral clearance and KIR2DL3 genotype in conjunction with its ligand HLA-C1 (5,89). Additionally

it was shown that better responsiveness to DAA treatment is associated with the expression of KIR2DL3 and HLA-C1 (90). Moreover our recent study suggests that HCV selects for peptides presented by HLA-C*03:04 mediating binding to KIR2DL3 thereby inhibiting KIR2DL3^{+} NK cell activity (91). In the context of HIV-1 it is described that HIV-1-infected individuals can carry sequence mutations in the HIV-1 genome which are associated with *KIR2DL2/3* genotypes (92). Furthermore genome wide association studies (GWAS) showed association between single nucleotide polymorphisms (SNPs), responsible for higher expression of HLA-C and better control of HIV-1 infection (93). Additionally, it was shown that the downmodulation of HLA-C by HIV-1 is associated with reduced binding to KIR2DL3 and reduced activity of HLA-C-licensed NK cells. And also for HIV-1, it is suggested that the virus selects for HLA-C*03:04-presented peptides able to restore engagement of KIR2DL3 and inhibiting KIR2DL3^{+} NK cell activity indicating NK cell-mediated immune pressure on the virus (94).

6. Hypothesis and aims of the work

The aim of this thesis was to gain better insights into the impact of changes in the HLA-I-presented peptide repertoire (referred to as the HLA-I "presentome") resulting from viral infection on the recognition of infected cells by and frequencies of KIR^+NK cells. My hypothesis was that the engagement of inhibitory KIRs to viral peptides presented by HLA-I molecules modulates frequencies of KIR^+NK cells. Furthermore, I hypothesized that the switch of the presentome from "normal self" to "stressed self" reduces the engagement of inhibitory KIRs resulting in NK cell activation and killing of infected cells (Fig. 6). I proposed to test this hypothesis in this thesis project by the following three specific aims:

In **Aim I** I assessed whether NK cell subsets that are able to recognize HLA-C*03:04/viral peptide complexes are present and modulated in their frequency in HIV-1- as well as HCV-infected patients and Yellow Fever vaccinees.

In **Aim II** I identified HLA-I-presented peptides on HIV-1-infected cells in comparison to uninfected cells.

In **Aim III** I investigated the impact of the peptides identified in Aim II on the function of KIR^+ cells in comparison to peptides presented by normal uninfected cells.

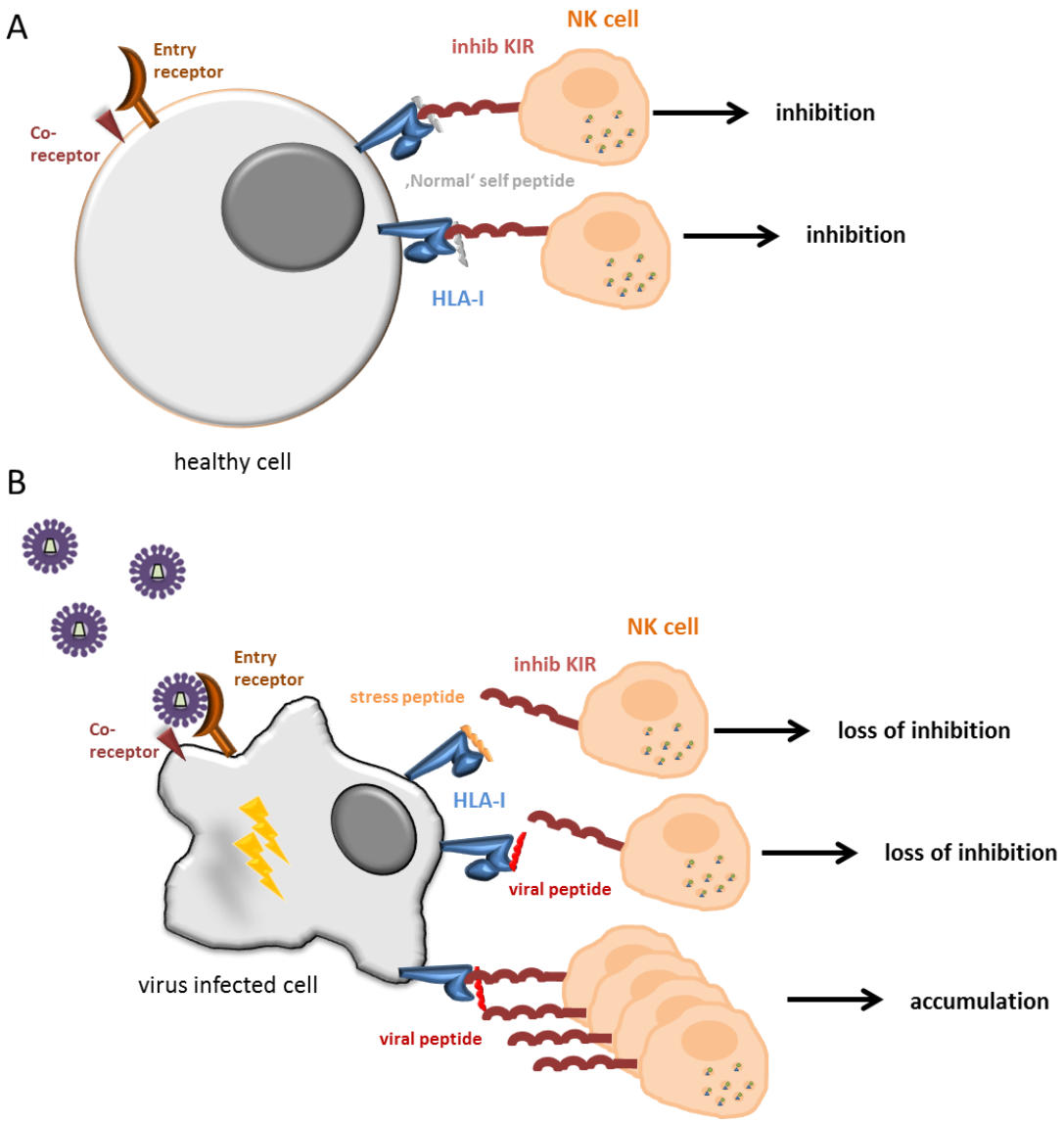

Fig. 6 Hypothesis A) A 'healthy' cell will present 'normal' self-peptides via its HLA-I molecules. This leads to the engagement of inhibitory KIRs expressed on NK cells and NK cell inhibition. B) Infection of a cell by a virus will stress the cell resulting in the presentation of stress peptides as well as viral peptides. On the one hand this will lead to the abrogation of the engagement to inhibitory KIRs expressed on NK cells leading to NK cell activation through loss of inhibition. On the other hand the recognition of viral peptides presented on HLA-I molecules on the infected cell by inhibitory KIRs leads to accumulation of specific NK cell subsets through reduced activation-induced cell death.

Materials and Methods

2.1 Materials

2.1.1 Chemicals and consumables

Table 2 Chemicals and consumables

Name	Company
Dulbecco's Modified Eagle Medium (DMEM)	Sigma-Aldrich Chemie GmbH (St. Louis, USA)
Dimethylsulfoxide (DMSO)	Sigma-Aldrich Chemie GmbH (St. Louis, USA)
Dulbecco's PBS (PBS)	Sigma-Aldrich Chemie GmbH (St. Louis, USA)
Foetal bovine serum (FBS)	Biochrom GmbH (Berlin, Germany)
Paraformaldehyde (PFA)	Sigma-Aldrich Chemie GmbH (St. Louis, USA)
Penicillin-Streptomycin	Sigma-Aldrich Chemie GmbH (St. Louis, USA)
RPMI-1640 Medium with L-glutamine and sodium bicarbonate	Thermo Fisher Scientific (Waltham, Massachusetts, USA)
Trypan Blue solution 0.4%	Sigma-Aldrich Chemie GmbH (St. Louis, USA)
CS&T research beads	BD Biosciences (Franklin Lakes, New Jersey, USA)
BD GolgiStop	BD Biosciences (Franklin Lakes, New Jersey, USA)
Biocoll	Biochrom GmbH, Berlin, Germany
Hank's balanced salt solution (HBSS)	Sigma-Aldrich Chemie GmbH (St. Louis, USA)
Penicillin-streptomycin	Sigma-Aldrich Chemie GmbH (St. Louis, USA)
Dynabeads Human T-Activator CD3/CD28	Thermo Fisher Scientific (Waltham, Massachusetts, USA)
Recombinant human IL-15	PeproTech GmbH (Hamburg, Germany)
Customized peptides	peptides & elephants GmbH (Hennigsdorf, Germany) and GenScript USA Inc (Piscataway, USA)
PE-labeled tetramers (YFV/HLA-C*03:04NS2A$_{4\text{-}13}$, HIV/HLA-C*03:04Gag$_{296\text{-}304}$, HCV/HLA-C*03:04Core$_{136\text{-}144}$)	National Institutes of Health (NIH)

2.1.2 Buffers

Table 3 Buffers

Buffer	Composition
Cell line cultivation medium for non-adhering cells (R10)	RPMI-1640 Medium supplemented with 10 % (v/v) FBS, 10 units/ml penicillin and 1 mg/ml streptomycin
PBMC cultivation medium	RPMI-1640 Medium supplemented with 20 %
Staining buffer	DPBS supplemented with 2 % FBS
Fixation Buffer	DPBS supplemented with 2 % (v/v) PFA
Cryopreservation medium	FBS supplemented with 10 % (v/v) DMSO
CD4$^+$ T-cell isolation buffer	DPBS supplemented with 2 % FBS

Tetramer Buffer	DPBS supplemented with 3 % FBS
Blocking Buffer	DPBS supplemented with 10 % human serum and 3 % FBS

2.1.3 Antibodies

Table 4 Antibodies

Antigen	Conjugate	Clone	Target species	Company
Pan-HLA-I	unconjugated	W6/32	human	University of Tübingen
Pan-HLA-I	APC	W6/32	human	eBioscience (Frankfurt am Main, Germany)
IgG-Fc anti-human	PE	-	human	Life technologies (Carlsbad, USA)
KIR2DL3/CD158k Fc Chimera	pure		human	R&D Systems (Minneapolis, Minnesota, USA)
HIV-1 Core (p24)	FITC	D45F	HIV-1	Beckman Coulter GmbH (Brea, California; USA)
CD3	BV510	UCHT1	human	Biolegend, Inc. (San Diego, California, USA)
CD3	PerCP-CY5.5	UCHT1	human	Biolegend, Inc. (San Diego, California, USA)
CD14	BV510	M5E2	human	Biolegend, Inc. (San Diego, California, USA)
CD19	BV510	HIB19	human	Biolegend, Inc. (San Diego, California, USA)
CD8	PerCP-CY5.5	RPA-T8	human	Biolegend, Inc. (San Diego, California, USA)
CD56	BUV395	NCAM16.2	human	BD Bioscience (Franklin Lakes, New Jersey, USA)
CD16	BV785	B73.1	human	BD Bioscience (Franklin Lakes, New Jersey, USA)
KIR2DL3	APC	REA147	human	Miltenyi Biotech (Bergisch Gladbach, Germany)
KIR2DL3	APC	180701	human	R&D Systems (Minneapolis, Minnesota, USA)
KIR2DL2	FITC	143211	human	R&D Systems (Minneapolis, Minnesota, USA)
CD69	BV421	FN50	human	Biolegend, Inc. (San Diego, California, USA)
CD107a	BV421	LAMP-1	human	Biolegend, Inc. (San Diego, California, USA)

2.1.4 Kits

Table 5 Kits

Name	Company
$CD4^+$ T Cell Isolation Kit, human	Miltenyi Biotech (Bergisch Gladbach, Germany)
Zombie NIR™ Fixable Viability Kit	Biolegend (London, UK)

Fixation & Permeabilization Buffer Set	Thermo Fisher Scientific (Waltham, Massachusetts, USA)

2.1.5 Plastic ware and general materials

Table 6 Plastic ware and general materials

Name	Company
5 ml round bottom FACS sample tubes	Corning Life Sciences (Tewksbury, Massachusetts, USA)
5mL round bottom FACS sample tubes, with cell strainer snap cap	Corning Life Sciences (Tewksbury, Massachusetts, USA)
96 well U-bottom cell culture plates	Greiner Holding (Kremsmünster, Austria)
Cell culture flasks (25cm^2, 75cm^2)	VWR International GmbH (Radnor, USA)
Cell counting slides	BioRad (Hercules, USA)
CombiTips	VWR International GmbH (Radnor, USA)
CryoPure, 2ml, tubes	SARSTEDT (Nümbrecht, Germany)
Disposable Serological pipettes (sterile)	SARSTEDT (Nümbrecht, Germany)
Eppendorf tubes (1.5 ml)	Eppendorf (Hamburg, Germany)
Falcon Tubes (15, 50 ml)	VWR International GmbH (Radnor, USA)
Filter tip (10 µl – 1000 µl)	Sarstedt (Nümbrecht/Rommelsdorf, Germany)
Filter tips ClipTip (200 µl, 300 µl)	VWR International GmbH (Radnor, USA)
Pipetting reservoirs	VWR International GmbH (Radnor, USA)
50 µm x 25 cm PepMap rapid separation liquid chromatography column	Thermo Fisher Scientific (Waltham, Massachusetts, USA)
LS Column	Miltenyi Biotech (Bergisch Gladbach, Germany)

2.1.6 Equipment

Table 7 Equipment

Name	Company
RSLnano	Thermo Fisher Scientific (Waltham, Massachusetts, USA)
online-coupled LTQ Orbitrap Fusion Lumos mass spectrometer	Thermo Fisher Scientific (Waltham, Massachusetts, USA)
BD LSRFortessa	BD Biosciences (Franklin Lakes, New Jersey, USA)
BD FACSCanto II	BD Biosciences (Franklin Lakes, New Jersey, USA)
Sorvall Legend XTR Centrifuge	Thermo Fisher Scientific (Waltham, Massachusetts, USA)
Centrifuge 5810R	Eppendorf (Hamburg, Germany)
HERAcell 150i CO2 Incubator	Thermo Fisher Scientific (Waltham, Massachusetts, USA)
Herasafe™ KS (NSF) Class II, Type A2 Biological Safety Cabinet	Thermo Fisher Scientific (Waltham, Massachusetts, USA)
TC20™ Automated Cell Counter	BioRad (Hercules, USA)
Eppendorf Research Plus Pipette	Eppendorf (Hamburg, Germany)
Multichannel pipetter, 12-channels, 300 µl	Thermo Fisher Scientific (Waltham, Massachusetts, USA)

QuadroMACS™ Separator	Miltenyi Biotech (Bergisch Gladbach, Germany)
Stratacooler	Agilent Technologies (Santa Clara, California, USA)

2.1.7 Cell lines

Table 8 Cell lines

Type	Description	Reference	Source
721.221	No expression of HLA-A, -B, -C	Shimizu Y, DeMars R. (1989)	*Angelique Hölzemer,* Heinrich Pette Institute, Hamburg
721.221-TAPko-HLA-C*03:04 (221-TAPko-C*03:04)	No expression of HLA -A and -B but HLA-C*03:04, TAP knocked out using CRSPR/CAS9 system		*Angelique Hölzemer,* Heinrich Pette Institute, Hamburg
KIR2DL3ζ⁺ Jurkat reporter cells	expressing KIR2DL3, intracellular tail exchanged through CD3ξ chain resulting in activation of the cell after ligand binding		*Angelique Hölzemer,* Heinrich Pette Institute, Hamburg

2.1.8 Software

Table 9 Software

Name	Company
Mendeley Desktop, version 7.0	Mendeley Ltd. (London, United Kingdom)
FACSDiva	BD Biosciences (Heidelberg, Germany)
FlowJo, version 10.4.2	Tree Star Inc. (Ashland, USA)
Graphpad Prism 8	Graphpad Software Inc. (California, USA)
Microsoft Office Professional Plus 2010	Microsoft (Redmond, USA)
MATLAB 2017b	The MathWorks, Inc. (Natick, Massachusetts, United States)
GNU Image Manipulation Program 2.8.16	The GIMP Team, www.gimp.org
NetMHCpan 3.0	Department of Bioinformatics, TU Dänemark (Denmark)
SYFPEITHI	Immunology, University of Tübingen (Tübingen, Germany)
Adobe Illustrator CS 5.1	Adobe Inc (California, USA)

2.2 Methods

2.2.1 Study population and Ethics Statement

All study subjects provided informed consent for participation under protocols approved by the Ärztekammer Hamburg (PV4780). The demographics and clinically characteristics of study subjects of investigation of frequencies of tetramer^{+}KIR2DL2/3^{+} NK cells are summarized in Table 10.

Yellow Fever vaccinated donors

5 individuals enrolled in a Yellow Fever Virus (YFV) vaccine study at the Bernhard-Nocht-Institute for tropical medicine (BNITM) were included in this study. Peripheral blood samples were collected one day prior vaccination and at day 1, day 3 and day 28 post vaccination. The samples were processed freshly at day of blood drawing.

HIV-1-infected donors

The group of HIV-1-infected individuals consisted of 5 chronically HIV-1-infected individuals that were treated with antiretroviral therapy. The PBMCs were isolated, frozen down and stored in liquid nitrogen at -170 °C until processing.

HCV-infected donors

The group of HCV-infected individuals consisted of 5 chronically HCV-infected individuals that were treatment naive at time of blood draw. The samples were processed freshly at day of blood drawing.

HIV-1^{neg} HLA-I-typed donor

For identification of HLA-I-presented peptides on HIV-1-infected primary CD4^{+} T cells one healthy donor was recruited. HLA-I of this donor was as follows (HLA-A*02:01/-A*02:01, -B*27:05/-B*40:01, -C*02:02/-C*03:04). The donor was female and at date of blood draws 34 years of age.

Table 10 Study populations

Cohort	n	Sex (female/male)	Age in years (mean with range)	Viral load in copies/ml (mean with range)	CD4 count (mean with range)
YFV	5	4/1	31 (24-35)	n.a.	n.a.
HIV-1	5	1/4	58 (31-78)	242,000 (140,000-290,000)	353 (251-478)
HCV	5	4/1	49 (29-59)	2,950,000 (450,000-6,300,000)	n.a.

2.2.2 Cell culture

All working steps were performed under sterile conditions using Herasafe™ KS (NSF) Class II, Type A2 Biological Safety Cabinet. Cells were cultured in 75 cm² cell culture flasks with 30 ml of RPMI 1640 medium supplemented with 10 % heat inactivated FCS and 5000 IU penicillin 5000 µg/mL streptomycin in an incubator (37 °C, 5 % CO2, 95 % humidity). Cells were split every two days by a split-ratio of 1:4 when cells were approximately at $4*10^5$ cells/mL.

2.2.3 Isolation of PBMCs by Density Gradient Centrifugation

Isolation of Peripheral Blood Mononuclear Cells (PBMCs) was performed using Density Gradient Centrifugation. This method allows to separate blood components according to their differences in size, density and aggregation behavior. Blood diluted at a ratio of 1:2 with Hanks' balanced salt solution (HBSS) was layered on prewarmed Biocoll. Centrifugation was performed at 500 g for 30 min at RT with a slow start and no brakes. Serum layer was aspirated and the PBMC layer was harvested. PBMCs were washed using prewarmed HBSS and centrifuged for 10 min at 500 g. Supernatant was discarded afterwards. This step was repeated twice.

2.2.4 Cryopreservation of cell samples

Freezing

Cells were centrifuged for 5 min at 500 g. Afterwards supernatant was discarded. Cryopreservation Medium was edited drop-wise. Aliquots of the cell suspension were placed in cryopreservation vials and

immediately placed into a stratacooler box in the -80 °C freezer. After one day cells were transferred to liquid Nitrogen.

Thawing

Frozen vials were thawed in 37 °C water bath until a small pellet of ice remained. The cells were then transferred in R10 and spun down for 5 min at 500 g. Supernatant was discarded and the pellet was resuspended in R10 medium. After a second spin the cells were transferred in a cell culture flask and cultured as described above (2.2.2).

Determination of cell number and viability

To determine the number of living and dead cells, cell samples were added to an equal volume of 0.4 % trypan blue solution, transferred to counting slides and counted with an automated cell counter.

2.2.5 HLA-I-tetramer staining of primary human PBMCs

PE-labeled tetramers of HLA-C*03:04 refolded by either the yellow fever virus-derived peptide HAVPFGLVSM (YFV/HLA-C*03:04NS2A$_{4\text{-}13}$), the HIV-1 derived peptide YVDRFFKVL (HIV/HLA-C*03:04Gag$_{296\text{-}304}$) or the HCV-derived peptide YIPLVGAPL (HCV/HLA-C*03:04Core$_{136\text{-}144}$) were provided by the NIH Tetramer Core Facility. These tetramers were used for staining of primary human PBMCs. Therefore, 1x10^6 cells were stained for 30 min at 4 °C with a mixture of live/dead marker, anti-CD14-BV510, anti-CD19-BV510, anti-CD8-PerCP-Cy5.5, anti-CD3-PB, anti-CD56-BUV395, anti-CD16-BV785, anti-KIR2DL3-APC, anti-KIR2DL1-FITC. The cells were washed with Tetramer Buffer and incubated twice on ice with 50 µl Blocking Buffer in a 96 well plate. After blocking the cells were stained with the corresponding tetramer at a 1/100 dilution in 50 µl Blocking Buffer resulting in a concentration of 11 ng/ml and incubated on ice for 60 min. After two washing steps the cells were fixed with Fixation Buffer and analyzed by flow cytometry. Gates were set to only include CD3$^-$ CD8$^-$ CD14$^-$ CD19$^-$ CD56$^+$ CD16$^+$ KIR2DL3$^+$ NK cells, while all CD3$^+$, CD8$^+$, CD14$^+$ CD19$^+$ KIR2DL3$^-$ cells were excluded. Tetramer binding was assessed as percentage of PE positive cells (Fig. 7).

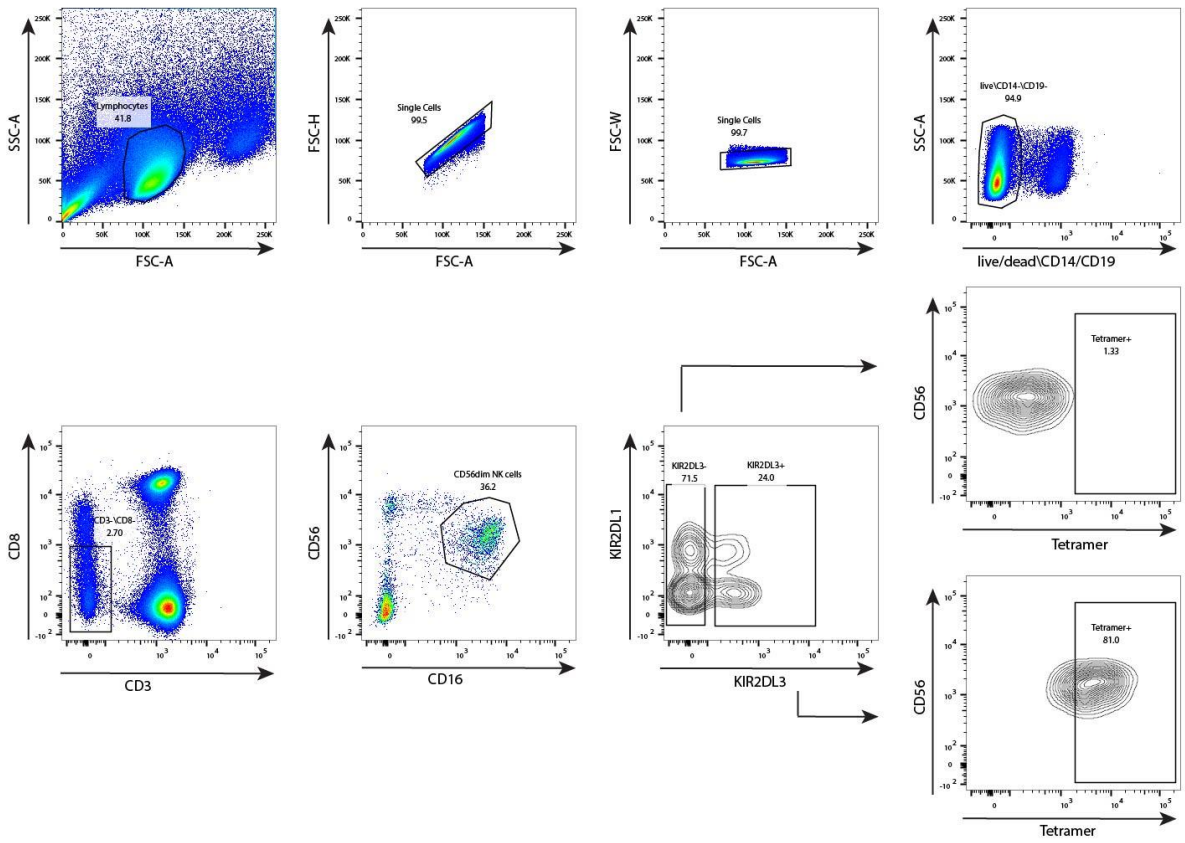

Fig. 7 Gating strategy used to identify tetramer$^+$KIR2DL2/3$^+$ NK cells. Gates were set to only include live CD3$^-$ CD8$^-$ CD14$^-$ CD19$^-$ CD56$^+$ CD16$^+$ KIR2DL3$^+$ NK cells, while all CD3$^+$, CD8$^+$, CD14$^+$ CD19$^+$ KIR2DL3$^-$ cells were excluded (95).

2.2.6 Isolation and infection of primary human CD4$^+$ T cells

500 mL blood was drawn from one HIV-1^{neg} HLA-I-typed donor two times 6 months apart. Blood was processed directly after collection. After PBMC isolation (2.2.3), CD4$^+$ T cells were isolated using positive selection MACS cell separation kits. 50 x 10^6 cells were immediately cryopreserved and stored at -80 °C as non-stimulated control samples (nCD4$^+$ T cells). Remaining cells were stimulated for 72 h using Dynabeads Human T Activator CD3/CD28 in RPMI 1640 $^+$ 20 % FBS $^+$ 100 U IL2. 80 x 10^6 cells were frozen after stimulation and stored at -80 °C, serving as stimulated control samples (sCD4$^+$ T cells). At least 100 x 10^6 stimulated cells were used for infection using the laboratory adapted HIV-1 strain NL_{4-3}. Cells were resuspended in virus stock at MOi = 0.01 and spinoculated for 2 h at 1200 g, 26 °C. Cells were cultured in T75 flasks for 72 h at 39.5 °C yielding highest infections rates in cell incubator, and subsequently cryopreserved (sHIVCD4$^+$ T cells).

2.2.7 Assessment of infection rate of HIV-1 infected primary CD4$^+$ T cells

Intracellular p24 expression was used as infection marker as described before (96). For intracellular p24 staining 2 x 10^5 cells were prepared using Intracellular Fixation & Permeabilization Buffer Set. Cells were subsequently stained using anti-HIV-1 Core Antigen-FITC for 30 min at 4 °C. After two washing steps with Staining Buffer and fixation with Fixation Buffer, cells were analyzed by flow cytometry. Infection rate was assessed as percentage of FITC- positive cells, yielding 65 % and 40 % for the two experiments, respectively.

2.2.8 Isolation of HLA-I molecules from primary CD4$^+$ T cell samples

HLA-I molecules were isolated using standard immunoaffinity purification as described before (97) using the pan-HLA-I specific monoclonal antibody W6/32 to extract HLA-I molecules.

2.2.9 Mass spectrometric analysis of HLA-I-presented peptides

Mass spectrometric analysis was performed by Annika Nelde at the Institute for Cell Biology, Department of Immunology, University of Tübingen, Germany. Identification of HLA-I-presented peptides was performed using liquid chromatography-coupled tandem mass spectrometry (LS-MS/MS). Therefore HLA-I extracts were analyzed in five technical replicates as described previously (98,99). In brief, peptide samples were separated by nanoflow high-performance liquid chromatography using a 50 µm x 25 cm PepMap rapid separation liquid chromatography column and a gradient ranging from 2.4 % to 32.0 % acetonitrile over the course of 90 min. Eluted peptides were analyzed in an online coupled LTQ Orbitrap Fusion Lumos mass spectrometer using a top speed collision induced dissociation fragmentation method.

2.2.10 Database search and HLA-I annotation

Data processing was performed as described previously (64). In brief, the SEQUEST HT search engine (University of Washington) (100) was used to search the human and the HIV-1 proteome as comprised in the Swiss-Prot database (20.197 reviewed human protein sequences, August 30th 2016) without enzymatic restriction. Precursor mass tolerance was set to 5 ppm, and fragment mass tolerance to 0.02 Da. Oxidized methionine was allowed as a dynamic modification. The false discovery rate (FDR) was

estimated using the Percolator algorithm (101) and limited to 5 %. Peptide lengths were limited to 8-12 amino acids. Protein inference was disabled, allowing for multiple protein annotations of peptides. HLA-I annotation was performed using NetMHCpan 3.0 (102,103) annotating peptides with IC50 scores or percentile rank below 500 nM or 2 %, respectively. In cases of multiple possible annotations, the HLA allotype yielding the lowest rank was selected.

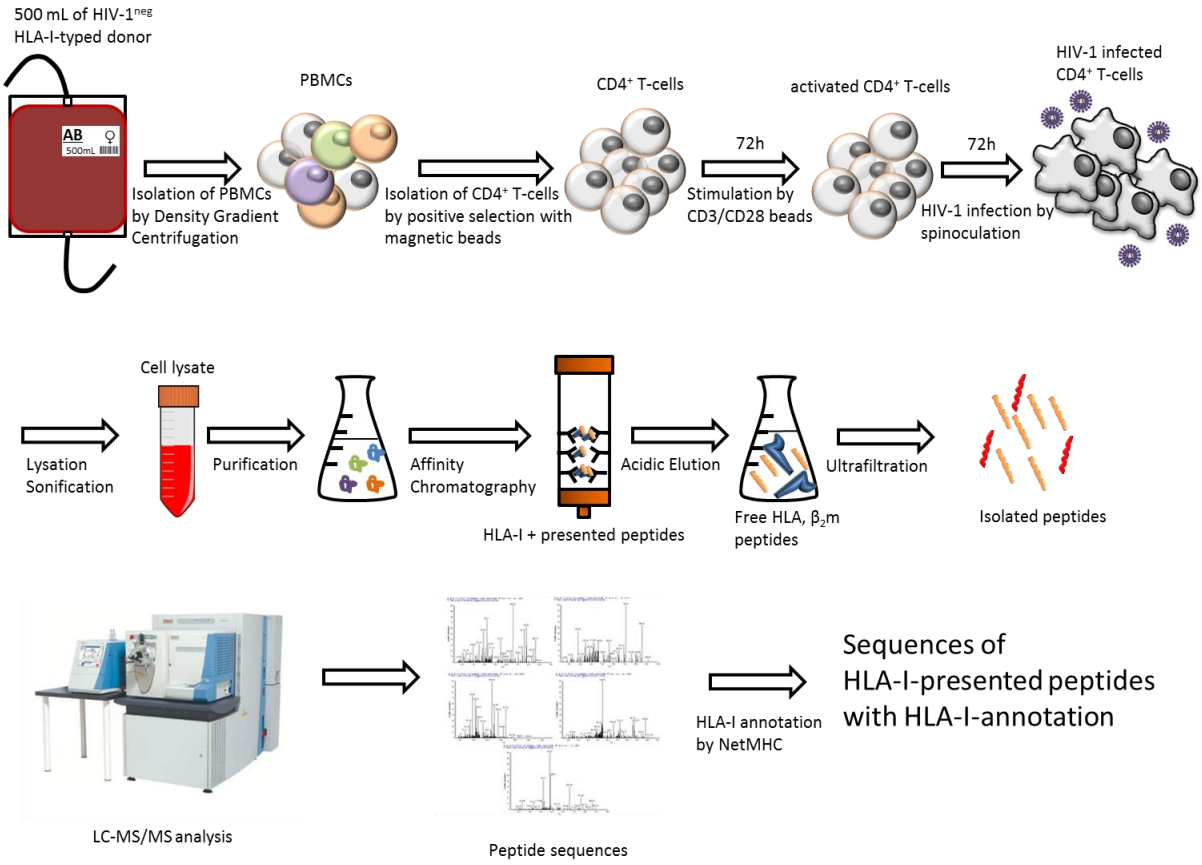

Fig. 8 Experimental setup for the identification of HLA-I-presented peptides on HIV-1-infected primary CD4⁺ T cells. After Isolation, activated CD4⁺ T cells are infected with HIV-1. Infected cells are lysed and HLA-I-presented peptides are isolated. Isolated peptides are subsequently analyzed by LC-MS/MS. Computational annotation reveals sequences of HLA-I-presented peptides with their respective HLA-I-annotation.

Identification of HLA-I presented peptides of HIV-1 infected and non-infected cells was carried out in collaboration with the Institute for Cell Biology, Department of Immunology, University of Tübingen, Germany. I performed blood processing (2.2.3) as well as isolation of CD4⁺ T cells (2.2.6), HIV-1 infection (2.2.6) and validation (2.2.7) and lysation of the cells (parts of 2.2.8). Immunopurification of HLA-I/peptide complexes (parts of 2.2.8), elution and isolation of peptides (parts of 2.2.8), masspectrometric analysis

(2.2.9) as well as HLA-I annotation of peptides (2.2.10) was performed by Christian Schreitmüller and Annika Nelde at the Department of Immunology in Tübingen, Germany.

2.2.11 Cell-based assays

Assessment of in vitro binding of peptides to HLA-C*03:04

For verification of peptide binding to HLA-C*03:04, a subset of selected peptides were synthetically synthesized and validated by LC-MS/MS. Subsequently, peptides were loaded on 221-TAPko-HLA-C*03:04. Cells were starved for 4 h in FBS free RPMI 1640, and the corresponding peptides were added to the cell culture medium in concentration of 100 µM and incubated for 21 h at 26 °C. To determine HLA-C*03:04 stabilization, cells were stained with anti-pan-HLA-I-APC, washed twice with Staining Buffer, fixed with Fixation Buffer, and analyzed by flow cytometry. HLA-I-stabilization was assessed as median MFI of APC and normalized to background expression.

Assessment of binding affinities of peptides to HLA-C*03:04

For peptide titration the corresponding peptides were synthetically synthesized and loaded on 221-TAPko-HLA-C*03:04. Therefore the cells were starved for 4h in FBS-free RPMI 1640. Following peptides were added to the cell culture medium in concentrations of 0 µM, 5 µM, 10 µM, 50 µM, 100 µM, 200 µM and 250 µM and incubated for 21 h at 26 °C. After stabilization the cells were stained with anti-pan-HLA-I-APC. Cells were washed with FACS-Buffer, fixed using Fixation Buffer and analyzed by flow cytometry. HLA-C*03:04-stabilization was assessed as median MFI of APC and normalized to background.

Assessment of binding avidities of HLA-I-tetramers to KIR2DL2/L3

PBMCs of 3 KIR2DL2/3^{+} healthy donors were isolated as described above (2.2.4). PBMCs were subsequently stained with the corresponding tetramers at increasing concentrations of 1-1000 ng/ml as described above (2.2.5) and analyzed by flow cytometry. Tetramer binding was assessed as percentage of PE positive cells.

Functional assessment KIR2DL3 binding to HLA C*03:04/peptide complex

To assess the functionality of KIR2DL3 binding to HLA-C*03:04/peptide complex 2.5 x 10^5 221-TAPko-HLA-C*03:04 cells per sample were starved for 4 h and pulsed with the corresponding peptides at the given concentrations calculated due to their relative quantity measured with LC-MS/MS. Peptide loaded cells were coincubated with Jurkat Reporter cells expressing KIR2DL3, with the intracellular tail exchanged through CD3ξ chain (KIR2DL3ζ$^+$ Jurkat reporter cells) resulting in activation of the cell after ligand binding in a ratio of 1:10. After 5 h of incubation at 37 °C/5% CO_2 cells were stained with anti-CD69-BV421 (Biolegend), anti-CD3-PerCP-Cy5.5 (Biolegend) and anti-KIR2DL3-APC (Miltenyi Biotec) for 30 min at 4 °C. After washing with ice cold 2% FBS/PBS cells were fixed with Fixation Buffer and analyzed using flow cytometry (BD LSR Fortessa). Gates were set to only include CD3$^+$/KIR2DL3$^+$ cells. Activation of the reporter cells was assessed as median MFI of CD69 and normalized to background expression.

Functional assessment of tetramer-binding NK cell population

For functional assessment of tetramer$^+$ and tetramer^{neg} KIR2DL3$^+$ NK cell populations PBMCs were isolated from whole blood and rested overnight in R20 (RPMI 1640 containing 20% FBS) and 1 ng/ml IL-15. 1 M PBMCs per sample were stained with anti-KIR2DL3-APC and anti-KIR2DL1-FITC (R&D) for 30 min at 4°C. After washing, cells were blocked and stained with 1/100 dilution of YFV/HLA-C*03:04NS2A$_{4\text{-}13}$. After staining, cells were coincubated with 721.221 cells or 221-TAPko-HLA-C*03:04 cells pulsed with either no peptide or YFV/NSA2A$_{4\text{-}13}$, HIV/Gag$_{296\text{-}303}$ or HCV/Core$_{136\text{-}144}$. After one hour incubation at 37°C Golgistop was added (BD Bioscience) and transferred to 26°C. After incubation for 5 h surface staining was performed with a mixture of live/dead dye, anti-CD14-BV510, anti-CD19-BV510, anti-CD3-BV510, anti-CD8-PerCP-Cy5.5, anti-CD56-BUV785, anti-CD16-BV785 and anti-CD107a-BV421. After two washing steps the cells were fixed with 4% paraformaldehyde in sterile PBS and analyzed by flow cytometry (BD LSR Fortessa). Gates were set to only include CD3^{neg} CD8^{neg} CD14^{neg} CD19^{neg} CD56$^+$ CD16$^+$ KIR2DL3$^+$ NK

cells, while all $CD3^+$ $CD8^+$ $CD14^+$ $CD19^+$ $KIR2DL3^{neg}$ cells were excluded. Degranulation of NK cells was assessed as percentage of CD107a positive cells.

2.2.12 Molecular dynamics simulations of HLA C*03:04/peptide/KIR2DL3 complexes

Molecular dynamics simulations were performed by Jeffrey K. Weber at the Computational Biology Center (IBM Thomas J. Watson Research Center). Initial structures for molecular dynamics simulations were generated from PDBs 1EFX (59) and 1B6U (60), starting with an alignment of the KIR2DL3 structure present in 1B6U with the KIR2DL2 structure engaged with an HLA-C*03:04/peptide complex. The resulting HLA-C*03:04/peptide/KIR2DL3 ternary complex was solvated in TIP3P (69) water and ionized with Na^+ and Cl^- to a neutral ionic strength of 150 mM. The simulation system was then annealed over three iterations of 10000 steepest descent minimization steps and 5 ns equilibration at 310 K at 1 atm, and subsequently equilibrated at 310 K for an additional 50 ns. The 1EFX source peptide was next mutated to either VIYPARISL or YAIQATETL within an equilibrated ternary complex snapshot, and these new complex structures were subjected to same solvation, ionization, and annealing procedures described above, equilibrated for 100 ns at 310 K and 1 atm, and then run at production for 200 ns under the same conditions. Peptide residue solvent-accessible surface areas (SASAs) as well as single point peptide-KIR van der Waals and electrostatic energies were computed for each production frame.

All molecular dynamics simulations were conducted with NAMD2.12 (70) using the CHARMM27 (71,72) force field; temperature and pressure were controlled with a Langevin thermostat (with a damping coefficient of 1/ps) and a Langevin Piston barostat, respectively (73). The rigidBonds option in NAMD was selected to enable 2 fs molecular dynamics time steps. Single point energies were computed using the NAMD Energy plugin in VMD, and SASAs were calculated with VMD's measure tool. Mutations were carried out using the MUTATOR plugin of VMD. Subfigures including molecular structural representations were generated with VMD 1.9.2 (74).

Results

In the first part of this thesis I focused on frequencies of KIR$^+$ NK cells after viral challenge. In the second part I investigated HIV-1-mediated alterations of HLA-I presented peptide repertoire and their impact on HLA-I/KIR interactions.

*Proportion of HLA-C*03:04/Tetramer$^+$ KIR2DL3$^+$ NK cells do not differ between YFV vaccinees and HIV-1- or HCV-infected individuals*

HLA-I tetramer-binding to primary human KIR$^+$ NK cells has been previously described (104), but it remains unknown whether the frequencies of HLA-C tetramer-binding to KIR2DL2/3$^+$ NK cells are modulated by the HLA-I-presented peptide. To investigate whether the frequency of KIR2DL2/3$^+$ NK cells able to recognize HLA-C*03:04 presenting either the YFV-derived peptide NS2A$_{4\text{-}13}$ (1), the HIV-1-derived peptide Gag$_{296\text{-}304}$ (94) or the HCV-derived peptide Core$_{136\text{-}144}$ (91) differ in YFV vaccinees, HIV-1- or HCV-infected individuals, I used HLA-C*03:04-tetramers refolded with the respective peptides, previously described to bind to HLA-C*03:04 and enable KIR2DL3-binding (91,94,106). These tetramers were used to *ex vivo* stain primary human NK cells of YFV vaccine recipients (28 days post vaccination), HIV-1-infected or HCV-infected individuals (Table 10). Stainings were performed using freshly isolated PBMCs for healthy controls, YFV vaccinees and HCV-infected individuals and frozen PBMCs derived from HIV-1-infected individuals. Even though the frequency of tetramer$^+$ KIR2DL2/3$^+$ NK cells differed for every viral setting, the relative hierarchy of tetramer$^+$ NK cells did not vary between the different study groups. YFV/HLA-C*03:04-NS2A$_{4\text{-}13}$ showed consistently the highest binding to KIR2DL2/3$^+$ NK cells (average of 52%, ranging from 26%-72%), whereas HIV/HLA-C*03:04-Gag$_{296\text{-}304}$ (average of 6%, ranging from 4%-8%) and HCV/HLA-C*03:04-Core$_{136\text{-}144}$ (average of 10%, ranging from 3%-14%) did bind to a significantly lower degree (Fig. 9). Taken together, these data show that KIR2DL3$^+$ NK cells follow a consistent peptide-dependent hierarchy in their binding to HLA-C*03:04, which is independent of the underlying viral background, indicating a lack of antigen-dependent expansion of these NK cell populations.

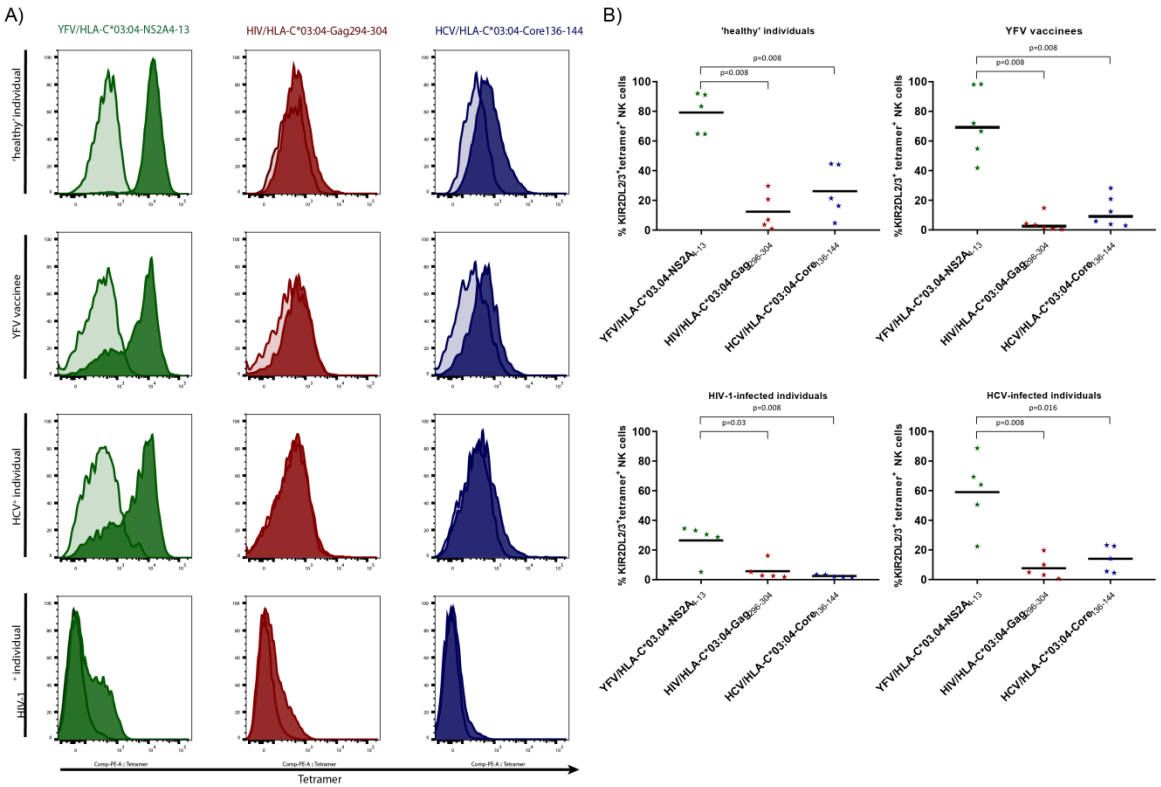

Fig. 9 Frequency of tetramer$^+$ KIR2DL3$^+$ NK cells in YFV vaccines, HIV-1-infected individuals and HCV-infected individuals. Staining with YFV/HLA-C*03:04-NS2A$_{4-13}$, HIV/HLA-C*03:04-$_{Gag296-304}$ and HCV/HLA-C*03:04-Core$_{136-144}$ depicted in green, red and blue respectively. A) Histograms of one representative individual for each viral setting and one unvaccinated, healthy control donor. KIR2DL2/3$^+$ NK cells tinted, KIR2DL2/3^{neg} NK cells transparent. B) Scatter Plots of frequencies of tetramer$^+$ KIR2DL2/3$^+$ NK cells in YFV vaccinees, HIV-1- and HCV-infected individuals with unvaccinated, healthy donors as control. P-values calculated using Mann-Whitney test. Black bar represents median of each group (Figure based on (95)).

Frequencies of YFV-specific tetramer$^+$ KIR2DL2/3$^+$ NK cells in YFV vaccinees remain stable over time

To address the question whether the frequency of KIR2DL2/3$^+$ NK cells able to recognize HLA-C*03:04/NS2A$_{4-13}$ changes after antigen challenge, I performed HLA-I-tetramer staining of primary human PBMCs using YFV/HLA-C*03:04-NS2A$_{4-13}$-tetramers in 5 YFV vaccinees at day 0, day 1, day 3 and day 28 before and after vaccination with YFV-17D. HIV/HLA-C*03:04-Gag$_{296-304}$- and HCV/HLA-C*03:04-Core$_{136-144}$-tetramer-stainings were used as controls. As it is described that human cytomegalovirus (HCMV) infection can influence the proportion of NK cell subsets (107), YFV vaccinees were tested for HCMV infection (3 individuals were positive and 2 negative for HCMV IgG or IgM, Fig. 10

B). I did not observe an increase in the average frequency of YFV/HLA-C*03:04-NSA_{4-13}-tetramer$^+$ KIR2DL3$^+$ NK cells (Fig. 10 A+B). Already before vaccination YFV/HLA-C*03:04-$NS2A_{4-13}$-tetramers bound to majority of KIR2DL2/3$^+$ NK cells (mean 74% range 57%-90) and did not significantly change after vaccination. Binding of the HIV-1- and the HCV-specific tetramers HIV/HLA-C*03:04-$Gag_{296-304}$ and HCV/HLA-C*03:04-$Core_{136-144}$ showed the same tendency with binding of an average of 2.9% and 9.8% respectively, which did not significantly differ between the different time points. Even though the tetramers bound to a lower degree, the amount of tetramer$^+$ KIR2DL2/3$^+$ NK cells did not change over time (Fig. 10). In addition, the overall frequency of KIR2DL2/3$^+$ NK cells did not change following YFV vaccination (Fig. 10 C). These data demonstrate that the proportion of KIR2DL2/3$^+$ NK cells binding to HLA-C*03:04 is dictated by the presented viral peptide, and that this proportion does not change following YFV vaccination.

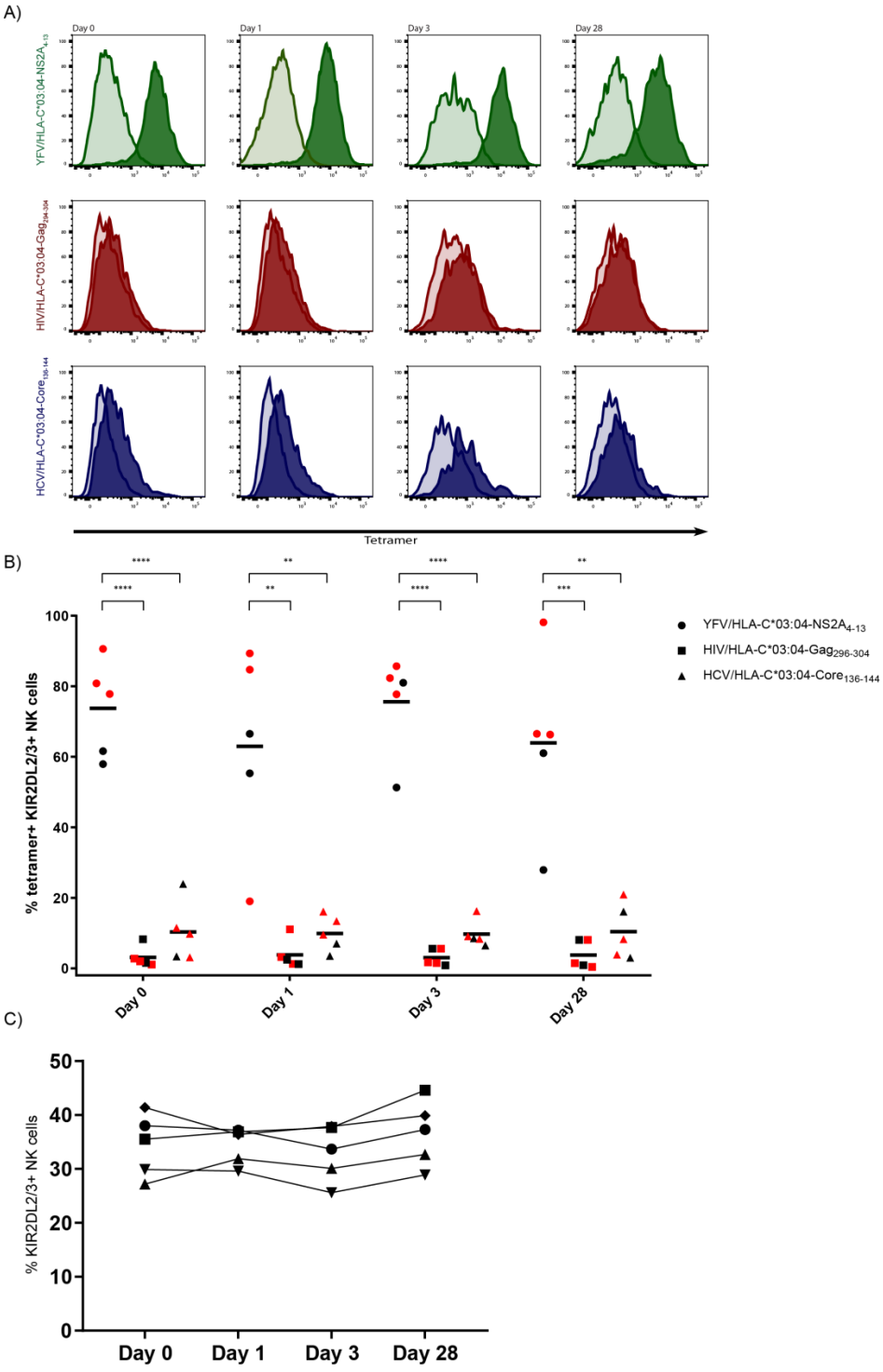

Fig. 10 Frequency of Tetramer^{+} KIR2DL2/3^{+} NK cells in YFV vaccinees over time. A) Histograms of one exemplary YFV-vaccinated donor stained with the respective tetramers at day 0, day 1, day 3 and day 28 before and after vaccination. KIR2D2/L3^{+} NK cells tinted, KIR2DL3^{neg} NK cells transparent. B) Scatter Plot of all 5 tested YFV vaccinees stained with the respective tetramers at day 0, day 1, day 3 and day 28. HCMV^{+} individuals depicted in red. Bar represents mean of each group. P-value calculated using unpaired t-test. C) Frequencies of total KIR2DL2/3^{+} NK cells at 0, 1, 3, and day 28 after vaccination. Freshly isolated PBMCs were used for all experiments (Figure based on (95)).

Results

*Peptide-dependent hierarchies of tetramer-binding follow affinity of HLA-C*03:04/peptide complex to KIR2DL2/3*

To assess whether the observed hierarchal binding of the different tetramers is influenced by the affinity of either the peptide to the HLA-I molecule or the HLA-I/peptide complex to KIR, I performed *in vitro* assays measuring the binding affinity of the peptides YFV/NSA2A$_{4\text{-}13}$, HIV/Gag$_{296\text{-}303}$, HCV/Core$_{136\text{-}144}$ to HLA-C*03:04, the binding avidity of the tetramers YFV/HLA-C*03:04-NS2A$_{4\text{-}13}$, HIV/HLA-C*03:04-Gag$_{296\text{-}304}$ and HCV/HLA-C*03:04-Core$_{136\text{-}144}$ to KIR2DL2/3 and KIR2DL3-binding to HLA-C*03:04 expressing cells presenting YFV/NSA2A$_{4\text{-}13}$, HIV/Gag$_{296\text{-}303}$ or HCV/Core$_{136\text{-}144}$.

For evaluation of the binding affinity of YFV/NSA2A$_{4\text{-}13}$, HIV/Gag$_{296\text{-}303}$, HCV/Core$_{136\text{-}144}$ peptides to HLA-C*03:04, I analysed 721.221 cells, which are deficient of classical HLA-I molecules and TAP, but transfected with HLA-C*03:04 (221-TAPko-HLA-C*03:04) pulsed with increasing concentration of the respective peptides. All three peptides peaked at 10 µM and showed saturation for concentrations >50 µM, indicating similar binding affinities to HLA-C*03:04 (Fig. 11 A). These results confirmed online predicted HLA-C*03:04 binding scores calculated with the NetMHCpan 4.0 program, which showed similar scores for all three peptides ranging from 0.3 to 0.5 (103). These data indicated that the observed hierarchies of tetramer$^+$ KIR2DL2/3$^+$ NK cells were independent of peptide-binding affinities to HLA-C*03:04. I next assessed binding avidities of the HLA-I/peptide tetramers to KIR2DL2/3$^+$ NK cells. The YFV/HLA-C*03:04-NS2A$_{4\text{-}13}$ tetramer showed a significantly stronger avidity to KIR2DL2/3$^+$ NK cells compared to HIV/HLA-C*03:04-Gag$_{296\text{-}304}$ and HCV/HLA-C*03:04-Core$_{136\text{-}144}$ (p=0.005) which bound to a similar level (Fig. 11 B). This observation was confirmed using KIR2DL3 (CD158b2) Fc Chimera Protein (KIR2DL3-Fc) constructs to stain 221-TAPko-HLA-C*03:04 cells pulsed with the respective peptides. The HLA-C*03:04-presented GAVDPLLAL (GAL) peptide known to bind KIR2DL3 was used as positive control, whereas the variant GAVDPLLKL (GKL) peptide which stabilizes HLA-C*03:04 at similar levels but does not bind KIR2DL3 was used as a negative control (108). In line with the tetramer titration, I observed the highest binding of KIR2DL3-Fc to YFV/NSA2A$_{4\text{-}13}$ in complex with HLA-C*03:04. 221-TAPko-HLA-C*03:04 cells pulsed with HCV/Core$_{136\text{-}144}$ showed the second highest binding to KIR2DL3-Fc and KIR2DL2-Fc. These

data suggest that the hierarchical binding of YFV/HLA-C*03:04-NS2A$_{4-13}$, HIV/HLA-C*03:04-Gag$_{296-304}$ and HCV/HLA-C*03:04-Core$_{136-144}$ to KIR2DL2/3^{+} NK cells in virus-infected individuals or vaccine recipients is determined by the binding avidity of the tetramer to KIR2DL2/3 and that this binding is independent of the binding affinity of the corresponding peptide to HLA-C*03:04.

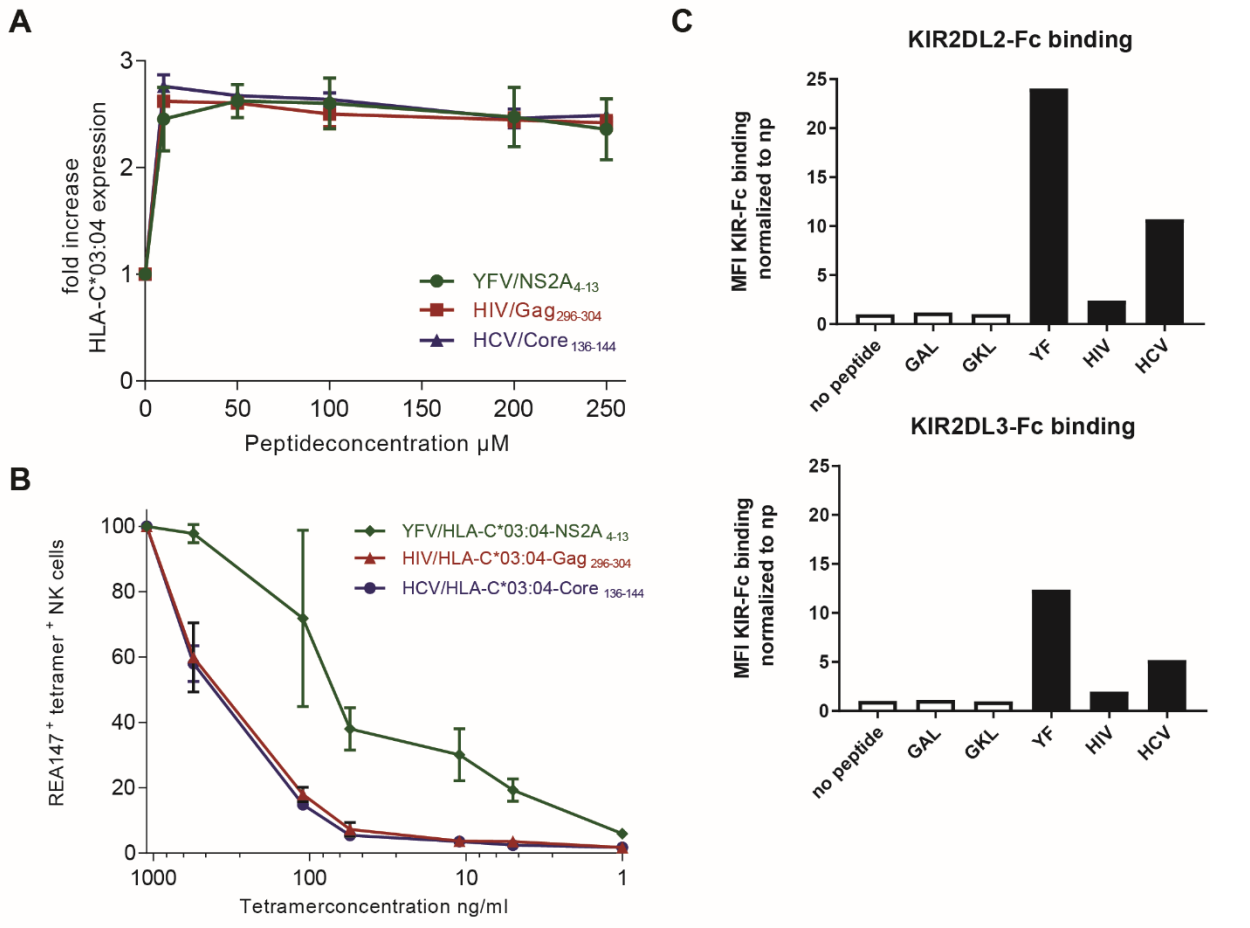

Fig. 11 *In vitro* determination of the affinity of peptides to HLA-C*03:04, avidity of tetramers to KIR2DL2/3 and KIR2DL2/3-Fc-binding to HLA-C*03:04/peptide complex. A) Binding of YFV/NSA2A$_{4-13}$ (green), HIV/Gag$_{296-303}$ (red), HCV/Core$_{136-144}$ (blue) to 221-TAPko-HLA-C*03:04 cells at concentrations of 0-250µM. B) Titration of YFV/HLA-C*03:04-NS2A$_{4-13}$, HIV/HLA-C*03:04-Gag$_{296-304}$ and HCV/HLA-C*03:04-Core$_{136-144}$ KIR2DL3^{+} NK cells at concentrations of 1-1000 ng/ml. C) KIR2DL2/3-Fc binding to 221-TAPko-HLA-C*03:04 cells pulsed with YFV/NSA2A$_{4-13}$, HIV/Gag$_{296-303}$, HCV/Core$_{136-144}$. GAL was used as positive control, GKL as negative control (Figure based on (95)).

Binding to HLA-I/peptide complex reverts higher functional capacity of tetramer^{+} KIR2DL3^{+} NK cell subpopulations

While most study subjects showed one major population of YFV/HLA-C*03:04-NS2A$_{4-13}$-tetramer^{+} NK cells (Fig. 12 A, donor 1), some study subjects exhibited both YFV/HLA-C*03:04-NS2A$_{4-13}$-tetramer^{+} and

YFV/HLA-C*03:04-NS2A$_{4-13}$-tetramer^{neg} KIR2DL3^{+} NK cell populations (Fig. 12 A, donor 2). This provides an opportunity to compare the functional activity of tetramer^{+} and tetramer^{neg} KIR2DL3^{+} NK cells, using an antibody previously described as being KIR2DL3-specific (clone #180701) (109). To assess whether the binding of YFV/HLA-C*03:04-NS2A$_{4-13}$-tetramer correlates with increased functionality of KIR2DL3^{+} NK cells, I compared CD107a expression of YFV/HLA-C*03:04-NS2A$_{4-13}$-tetramer^{+} and tetramer^{neg} KIR2DL3^{+} NK cell subpopulations of donor 2 after challenge with classical HLA-I deficient 721.221 cells (.221) (110)(Fig. 12 B). Expression of CD107a has been described to directly correlate with NK cell activity such as degranulation and lysis of target cells, offering a marker to measure NK cell activity (111). PBMCs were stained with YFV/HLA-C*03:04-NS2A$_{4-1}$ and coincubated with either 221 cells or 221-TAPko-HLA-C*03:04 cells pulsed with YFV/NSA2A$_{4-13}$, HIV/Gag$_{296-303}$ or HCV/Core$_{136-144}$ peptide. The tetramer^{+} NK cell population exhibited higher CD107a expression after stimulation with 221 cells in comparison to the tetramer^{neg} NK cell population (35% vs 25%). Co-incubation of KIR2DL3^{+} NK cells with peptide pulsed 221-TAPko-HLA-C*03:04 cells however reverted higher degranulation levels. YFV/NSA2A$_{4-13}$- and HCV/Core$_{136-144}$-peptide pulsed 221-TAPko-HLA-C*03:04 cells reduced YFV/HLA-C*03:04-NS2A$_{4-13}$-tetramer^{+} KIR2DL3^{+} NK cell CD107a expression levels strongest (19% vs. 35% (YFV) and 18% vs. 35% (HCV) respectively), whereas HIV/Gag$_{296-303}$-peptide pulsed 221-TAPko-HLA-C*03:04 cells had the lowest ability to inhibit degranulation (26% vs. 35%) (Fig. 12 B, left column). While I did not observe an impact of peptide-pulsed 221-TAPko-HLA-C*03:04 cells on CD107a expression levels of YFV/HLA-C*03:04-NS2A$_{4-13}$-tetramer^{neg} KIR2DL3^{+} NK cell populations, which remained stable at around 25% (range 21–25%, Fig. 12 B, right column). These data show that the capacity of KIR2DL3^{+} NK cells to bind to YFV/HLA-C*03:04-NS2A$_{4-13}$ correlates with a higher functionality, consistent with NK cell licensing, and that binding of the respective HLA-C*03:04/peptide ligand can inhibit KIR2DL3^{+} NK cell function.

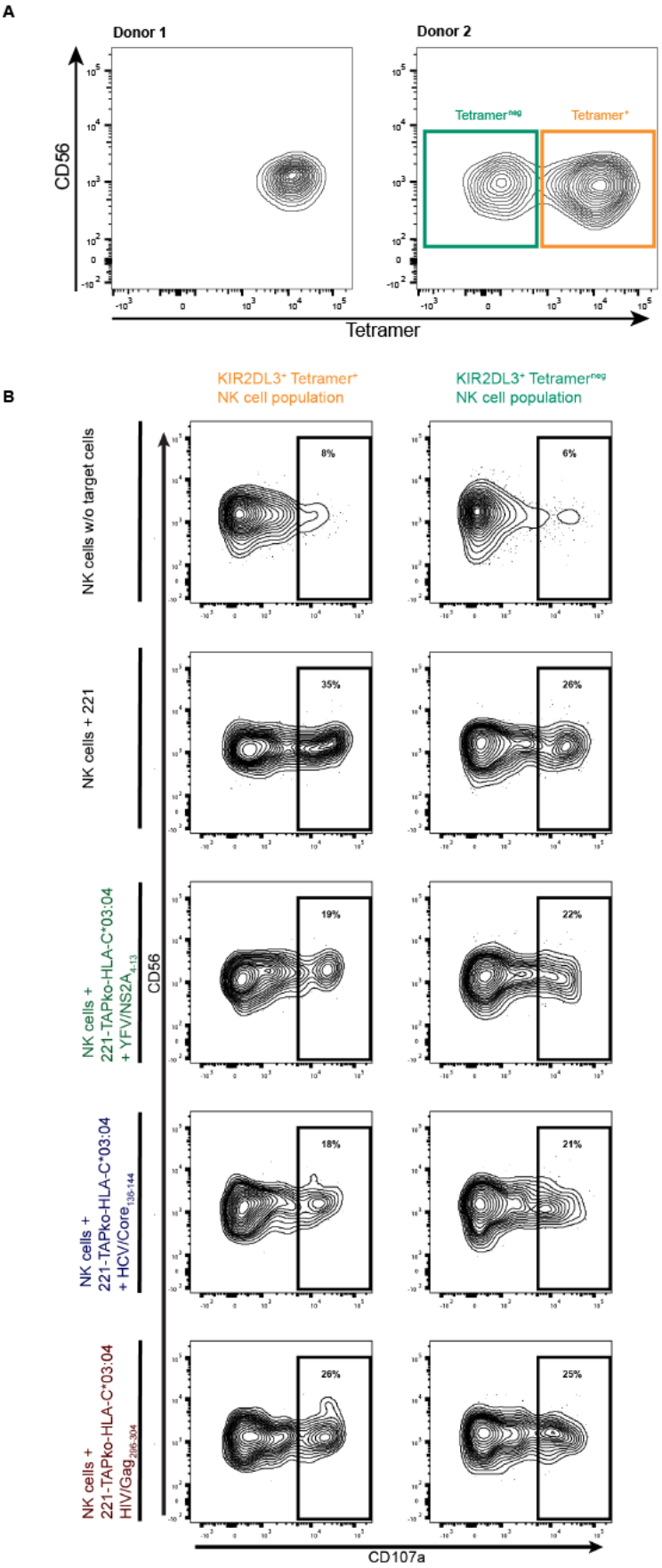

Fig. 12 Functional determination of tetramer^{+} and tetramer^{neg} KIR2DL3^{+} NK cell subpopulations.

A) YFV/HLA-C*03:04-NS2A$_{4-13}$-tetramer binding to KIR2DL3^{+} (clone #180701) NK cells in two donors. The right flow plot shows two KIR2DL3^{+} NK cell populations either binding the YFV/HLA-C*03:04-NS2A$_{4-13}$-tetramer (orange, tetramer^{+}) or not (teal, tetramer^{neg}) in donor 2. B) PBMCs from donor 2 were incubated with either no other cells, 221 cells, or 221-TAPko-HLA-C*03:04 cells pulsed with YFV/NSA2A$_{4-13}$- (green), HCV/Core$_{136-144}$- (blue) and HIV/Gag$_{296-303}$- (red) peptide. The gates show the percentage of CD107a^{+} from either YFV/HLA-C*03:04-NS2A$_{4-13}$-tetramer^{+} (orange) or tetramer^{neg} (teal) KIR2DL3^{+} (clone #180701) NK cells (95).

In summary, these data show that the viral background does not influence the proportion of tetramer$^+$KIR2DL2/3$^+$ NK cells which remains stable over time after viral challenge. Rather, the affinity of the respective tetramer to KIR2DL2/3 dictates the number of tetramer-binding KIR2DL2/3$^+$ NK cells, which show higher cytotoxicity, reverted through the interaction of HLA-C*03:04/peptide complex and KIR2DL3.

Following the analysis of frequencies of KIR2DL3$^+$ NK cells able to recognize HLA-C*03:06/viral peptide complexes in HIV-1- or HCV-infected and YFV-vaccinated individuals, I investigated HIV-1-induced changes in the presentome of primary CD4$^+$ T cells on the binding of HLA-C*03:04 to KIR2DL3 and the subsequent functional and structural consequences as a potential mechanisms of NK cell activation by infected cells.

Mass spectrometric analysis identifies alterations in the presentome of HIV-1-infected primary CD4$^+$ T cells

HLA-I-presented peptides on infected cells are critical for recognition by immune cells, but which peptides are naturally presented by HLA-I molecules and how presentation changes during viral infections remains incompletely understood. To reveal changes in HLA-I-presented peptide repertoire, I infected primary human CD4$^+$ T cells with HIV-1 *in vitro*. CD4$^+$ T cells were pre-stimulated using CD3/CD28 bead prior to infection to guarantee HIV-1 infection (stimulated and HIV-1-infected CD4$^+$ T cells short sHIVCD4$^+$ T cells), as previously described (32). HLA-I-presented peptides were analyzed using liquid chromatography-coupled tandem mass spectrometry (LC-MS/MS). As control populations, I used both untreated CD4$^+$ T cells (non-infected/non-stimulated CD4$^+$ T cells short nCD4$^+$ T cells) and CD3/CD28 bead stimulated CD4$^+$ T cells (stimulated CD4$^+$ T cells short sCD4$^+$ T cells) to control for activation induced changes resulting from stimulation prior to HIV-1 infection. Experiments were performed twice 6 months apart using PBMCs derived from the same study subject with the following HLA-I genotype: HLA-A*02:01/-A*02:01, -B*27:05/-B*40:01, -C*02:02/-C*03:04.

Figure 13 A shows an overview of the results from the two independent experiments for nCD4$^+$ T cells, sCD4$^+$ T cells and sHIVCD4$^+$ T cells. In total more than 12.000 HLA-I-presented peptides were identified,

out of those 1.369 were presented on nCD4$^+$ T cells, 4.716 on sCD4$^+$ T cells and 3.962 on sHIVCD4$^+$ T cells. HIV-1-derived peptides were only detected on HIV-1-infected cells (Fig. 13 A).

To investigate whether HIV-1 infection influences peptide length distribution on infected cells, I compared peptide length between the different conditions and HLA-I allotypes (Fig. 13 B). 9aa long peptides represented the most abundant peptides for all HLA-I molecules followed by 10meres. For HLA-A*02:01, -B*40:01 and -B*27:05, the presentome of sHIVCD4$^+$ T cells and sCD4$^+$ T cells shifted towards the presentation of longer peptides, ranging from 9 to 11aa length. No difference in peptide lengths occurred between the different conditions for HLA-C*02:02- and HLA-C*03:04-presented peptides. These HLA-C molecules almost exclusively presented 9 aa long peptides (Fig. 13 B). I subsequently assessed whether the proportional distribution of peptides allocated to HLA-I molecules was affected by HIV-1 infection. The highest proportion of HLA-I-presented peptides were restricted to HLA-A*02:01 (average of 44%), followed by HLA-B*40:01 (average of 36%). HLA-B*27:05-presented peptides contributed very little (average of 7%) to the total number of detected peptides, while HLA-C*02:02 (average of 6%) and HLA-C*03:04 (average of 7%) contributed with similar proportions. The two experiments and the different conditions showed high consistency in regard to the contributions of individual HLA-I molecules to the detected HLA-I-presented peptides, with a small reduction of HLA-C-presented peptides on sCD4$^+$ T cells and sHIVCD4$^+$ T cells (average of 8.5%/9.5% for nCD4$^+$ T cells, average of 4%/5% on sCD4$^+$ T cells and average of 5%/6% on sHIVCD4$^+$ T cells; for HLA-C*02:02 and HLA-C*03:04 respectively), while the contribution of HLA-B*40:01-presented peptides increased (average of 30.5% for nCD4$^+$ T cells, average of 35.5% on sCD4$^+$ T cells and average of 42.5% on sHIVCD4$^+$ T cells) (Fig. 13 C). All in all these data show that HIV-1 infection alone has no significant effect on the peptide length distribution of HLA-I-presented peptides, but led to an increase in the proportion of HLA-B*40:01-restricted peptides.

A)

	Run 1			Run 2			Run 1+2	
	unique peptides	HLA-I restricted peptides	HIV-1 pNL_{4-3} peptides	unique peptides	HLA-I restricted peptides	HIV-1 pNL_{4-3} peptides	HLA-I restricted peptides	HIV-1 pNL_{4-3} peptides
non-inf/non-stim	1233	972	0	674	593	0	1369	0
stimulated	4048	3574	0	2403	2211	0	4716	0
HIV-1 infected	2443	2222	6	3238	2837	8	3962	8

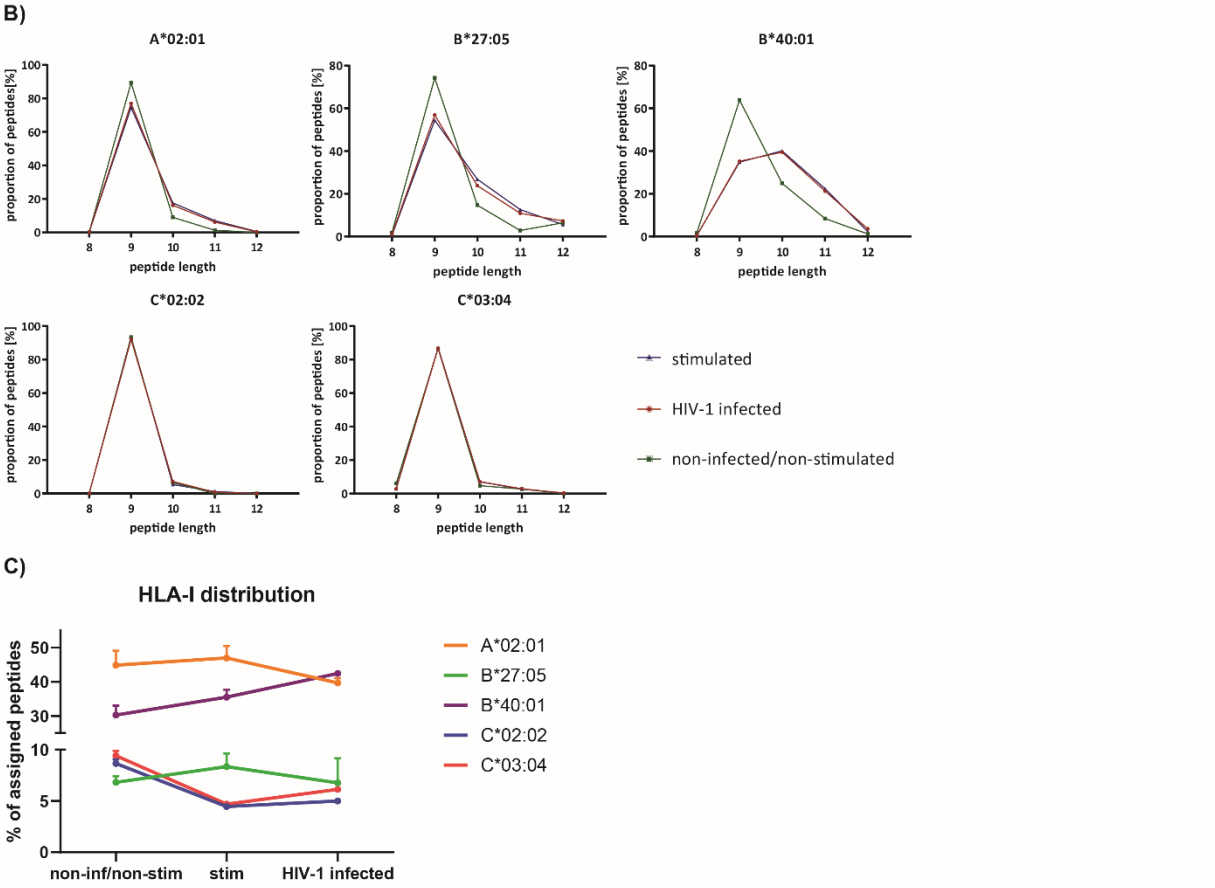

Fig. 13 Analysis of the immunopeptidome of primary HIV-1-infected CD4⁺ T cells by mass spectrometry. A) Table shows results of LC-MS/MS analysis of non-infected/non-stimulated CD4⁺ T cells (non-stimulated), stimulated but not infected CD4⁺ T cells (stimulated) and stimulated and HIV-1-infected CD4⁺ T cells (HIV-1 infected). B) Proportional distribution of peptide length for non-infected/non-stimulated CD4⁺ T cells (green), stimulated but not infected CD4⁺ T cells (blue) and stimulated and HIV-1-infected CD4⁺ T cells (red) for the different HLA-I alleles. C) Distribution of HLA-I-restricted peptides according to HLA-I alleles analyzing non-stimulated/non-infected CD4⁺ T cells (non-inf/non-stim), stimulated but not infected CD4⁺ T cells (stim) and stimulated and HIV-1 infected CD4⁺ T cells (HIV-1 infected) (Figure based on (112)).

HIV-1-infected CD4⁺ T cells present distinct host-derived peptides by HLA-I including a small subset of HIV-1-derived peptides

While virus-derived peptides presented by HLA-I molecules are essential for the recognition of HIV-1-infected cells by CD8⁺ T cells, it becomes more and more evident that the proportion of virus-derived peptides presented on virus infected cells is very little. Indeed, only 0.2% of the peptides I

identified on HIV-1-infected cells were of viral origin, in line with previous studies (33–36). Three of the identified HIV-1 peptides were restricted to HLA-A*02:01 and four to HLA-B*40:01. All of them were 8-12 aa in length. Two of the identified peptides represented overlapping peptides (SESARINTIL and SESARINTI). According to NetMHC 3 prediction, one HIV-1-derived peptide did not show any known HLA-I binding motif (RSLFGSDPSSQ) (102). The six HIV-1-derived peptides identified in the first experiment were also present in the second experiment 6 months later, during which 2 additional peptides were identified, representing an inter-experimental overlap of 100% (Fig. 14 A). This indicates a very consistent pattern of the presentation of viral peptides. Four peptides were derived from Gag and clustered at the end of the protein between aa 362-500. One peptide was derived from Env, one from Nef and two from Vif (Fig. 14 A). Comparison of relative quantity of HIV-1- and host-derived peptides showed that the HLA-B*40:01-restricted peptide SESARINTIL was presented at very high quantities in both experiments (Fig. 14 B). Relative quantities for the other HIV-1 peptides differed between the two experiments but showed moderate levels for both experiments (Fig. 14 B). Taken together, these data show that the HLA-I-presented peptide repertoire of HIV-1-infected $CD4^+$ T cells includes only a small minority of HIV-1-derived peptides, indicating that HIV-1-induced alterations in HLA-I-presented host-derived peptides may play a more prominent role in activation of NK cells by virus infected cells.

A)

Sequence	Identified in	Protein	Position in Protein	HLA-I restriction
AVLSIVNRV	both runs	ENV	Env 700→708	A*02:01
FLGKIWPS	run 2	GAG	Gag 433→440	A*02:01
VLAEAMSQV	both runs	GAG/POL	Gag 362→370	A*02:01
KELYPLASL	both runs	GAG	Gag 481→489	B*40:01
GENTSLLHPVSL	both runs	NEF	Nef 159→170	B*40:01
SESAIRNTI	both runs	VIF	Vif 116→124	B*40:01
SESAIRNTIL	both runs	VIF	Vif 116→125	B*40:01
RSLFGSDPSSQ	run 2	GAG	Gag 490→500	non

B)

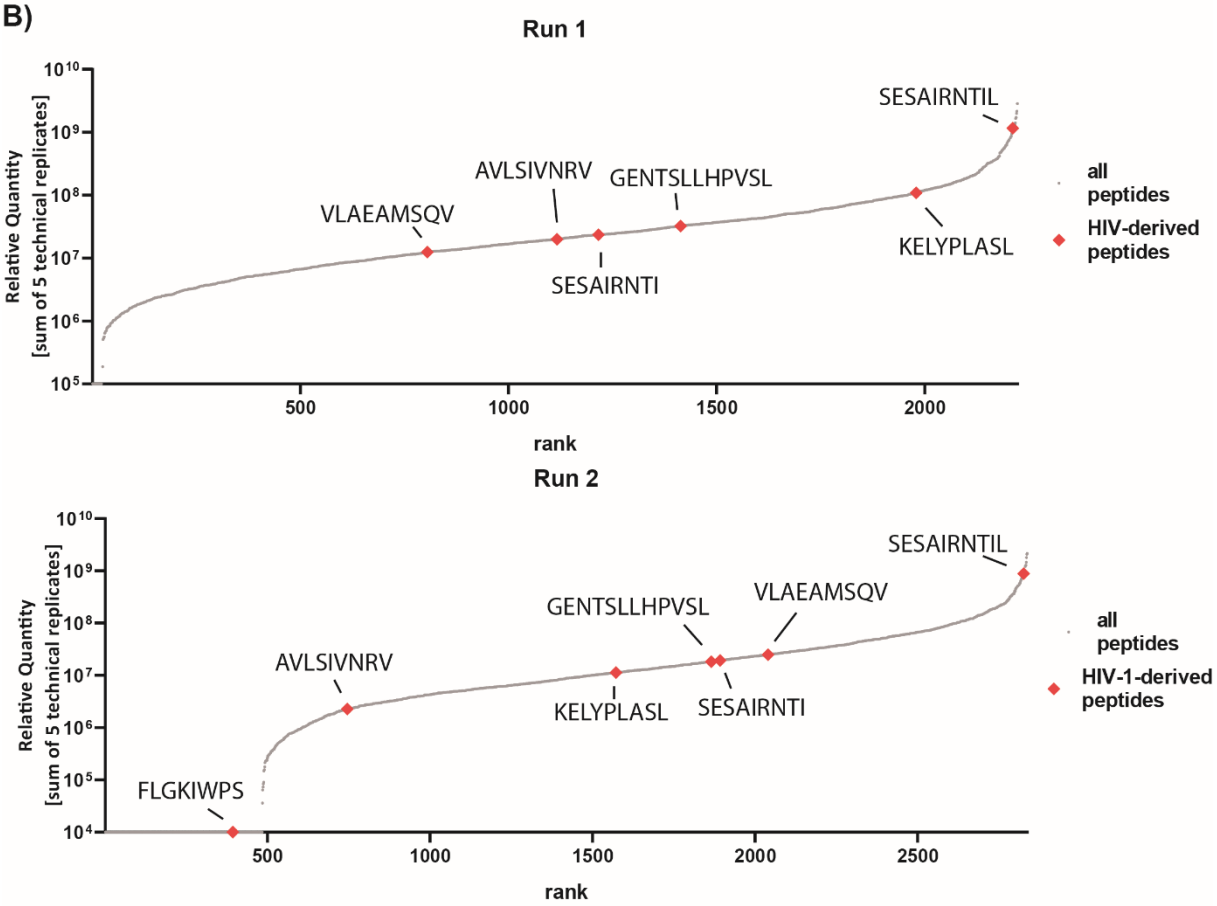

Fig. 14 HLA-I-presented peptides derived from HIV-1. A) Sequence, occurrence, source protein and HLA-I-restriction of the identified peptides. B) Relative quantity of HIV-1 peptides compared to host-derived peptides (112).

To further assess HIV-1-induced alterations in host-derived peptides presented by HLA-I, I compared peptide repertoires between nCD4$^+$ T cells and sHIVCD4$^+$ T cells. I excluded any peptides presented on sCD4$^+$ T cells to control for stimulation-induced changes in the presentome. Venn Diagram in Fig. 15 A show all peptides identified on nCD4$^+$ T cells, sCD4$^+$ T cells and sHIVCD4$^+$ T cells of both experiments with their inter-conditional overlap independent of their annotated HLA-I restriction. 833 host-derived peptides were uniquely presented on sHIVCD4$^+$ T cells and were therefore classified as HIV-1

infection-induced host-derived stress peptides. 282 peptides were unique to nCD4$^+$ T cells and were therefore classified as naturally presented self-peptides (Fig. 15 A).

Previous studies have shown that HLA-C/KIR2DL interactions can modulate NK cell-mediated inhibition of HIV-1 replication *in vitro*, and that peptides presented by HLA-C molecules can significantly impact binding of inhibitory KIR2DL receptors (13,14,37,38). I therefore focused subsequent analyses on 43 and 30 HLA-C*03:04-restricted peptides uniquely presented on sHIVCD4$^+$ T cells and nCD4$^+$ T cells, respectively (Fig. 15 B, **Fehler! Verweisquelle konnte nicht gefunden werden.**).

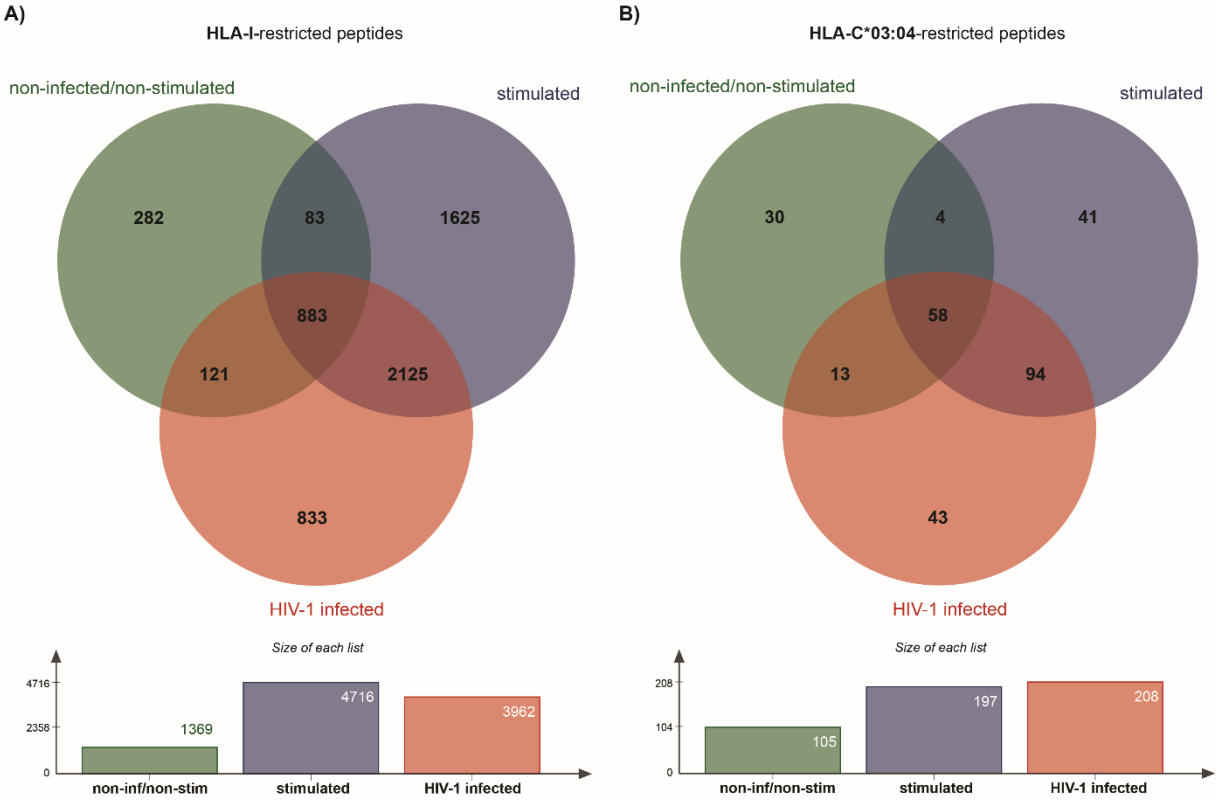

Fig. 15 Overlap analysis illustrating the numbers of HLA-I/HLA-C*03:04-restricted peptides identified under the different conditions. Peptides identified on non-infected/non-stimulated cells in green, peptides identified on stimulated cells in blue and peptides identified on HIV-1-infected cells in red. A) All HLA-I-restricted peptides B) HLA-C*03:04-restricted peptides (112).

*The most abundant peptide presented on non-infected cells and restricted to HLA-C*03:04 mediated strongest binding to inhibitory KIR2DL3*

To evaluate whether HIV-1-induced alterations in HLA-C*03:04-restricted host-derived peptides have an impact on KIR2DL3-binding and KIR2DL3$^+$ cell activation, I first validated *in vitro* binding of the identified

peptides to HLA-C*03:04. Of the 73 HLA-C*03:04-restricted peptides that were unique to either nCD4$^+$ T cells or sHIVCD4$^+$ T cells, I selected 32 peptides (16 for nCD4$^+$ T cells, n1-n16 and 16 for sHIVCD4$^+$ T cells, h1-h16) for functional studies. These included the peptides consistently detected in the two independent experiments and additional peptides that exhibit high binding scores for HLA-C*03:04 using MHC rank (rank of the predicted affinity compared to a set of 400.000 random natural peptides). To confirm HLA-C*03:04-stabilization of the peptides, 221-TAPko-HLA-C*03:04 cells were pulsed with the selected 32 peptides. All 32 peptides stabilized HLA-C*03:04 expression on 221 cells *in vitro* with an average increase of 3.3-fold compared to HLA-I expression of cells when no peptide was added (Fig. 16 A). I subsequently assessed whether these HLA-C*03:04-presented peptides are able to modulate the binding capacity of KIR2DL3 by staining peptide pulsed 221-TAPko-HLA-C*03:04 cells with recombinant KIR2DL3 (CD158b2) Fc Chimera Protein (KIR2DL3-Fc). Despite similar binding affinities to HLA-C*03:04, the different tested peptides exhibited strong differences in their ability to mediate KIR2DL3-Fc-binding (Fig. 16 B). In particular, one peptide identified uniquely on nCD4$^+$ T cells (peptide n3, VIYPARISL) enabled very high engagement of KIR2DL3 (36.9%), while also a number of additional peptides (n4, n8, n9 and n10) showed high binding of KIR2DL3-Fc, ranging from 9.3% to 14.6%. In contrast HLA-C*03:04-restricted peptides identified exclusively on sHIVCD4$^+$ T cells enabled lower binding of KIR2DL3-Fc (average of 3.5%). Overall peptides identified exclusively on sHIVCD4$^+$ T cells led to a 53% decrease in overall KIR2DL3-Fc binding when compared to peptides identified uniquely on nCD4$^+$ T cells, which showed an average of 6.6% KIR2DL3-Fc binding (Fig. 16 B, $p = 0.042$).

Given the variances between different HLA-C*03:04-restricted peptides to mediate KIR2DL3-binding, I next analyzed KIR2DL3-binding in relation to the relative quantity by which peptides were presented by HLA-C*03:04 (Fig. 16 C). Notably, the peptide which mediated strongest KIR2DL3-Fc binding (peptide n3) was also presented at highest quantities on nCD4$^+$ T cells, while the most abundant HLA-C*03:04-restricted peptide presented on sHIVCD4$^+$ T cells only showed no or very minimal KIR2DL3-Fc-binding (Fig. 16 B+C). Lastly, I analyzed activation of KIR2DL3ζ$^+$ Jurkat reporter cells by

HLA-C*03:04-restricted peptides derived from nCD4$^+$ T cells or sHIVCD4$^+$ T cells. KIR2DL3ζ$^+$ Jurkat reporter cells express KIR2DL3 with the intracellular tail exchanged by the CD3ξ chain, resulting in activation of the cell after KIR2DL3 binding, which can be measured by CD69 expression (113). Merging all 16 peptides derived either from nCD4$^+$ or sHIVCD4$^+$ T cells, respectively, or only the 3 to 4 most abundant peptides identified under each condition (n3/n14/n11 for nCD4$^+$ T cells or h9/h1/h4/h3 for sHIVCD4$^+$ T cells), I observed higher CD69 expression of KIR2DL3ζ$^+$ Jurkat reporter cells by peptides derived from nCD4$^+$ T cells (Fig. 16 D), in line with the results using KIR2DL3-Fc. Concentrations of peptides used in this experiment were based on their relative quantity. All in all, these data show that the most abundant peptides presented by HLA-C*03:04 on nCD4$^+$ T cells bind the inhibitory KIR2DL3 receptor more strongly than the most abundantly HLA-C*03:04-presented peptides on sHIVCD4$^+$ T cells.

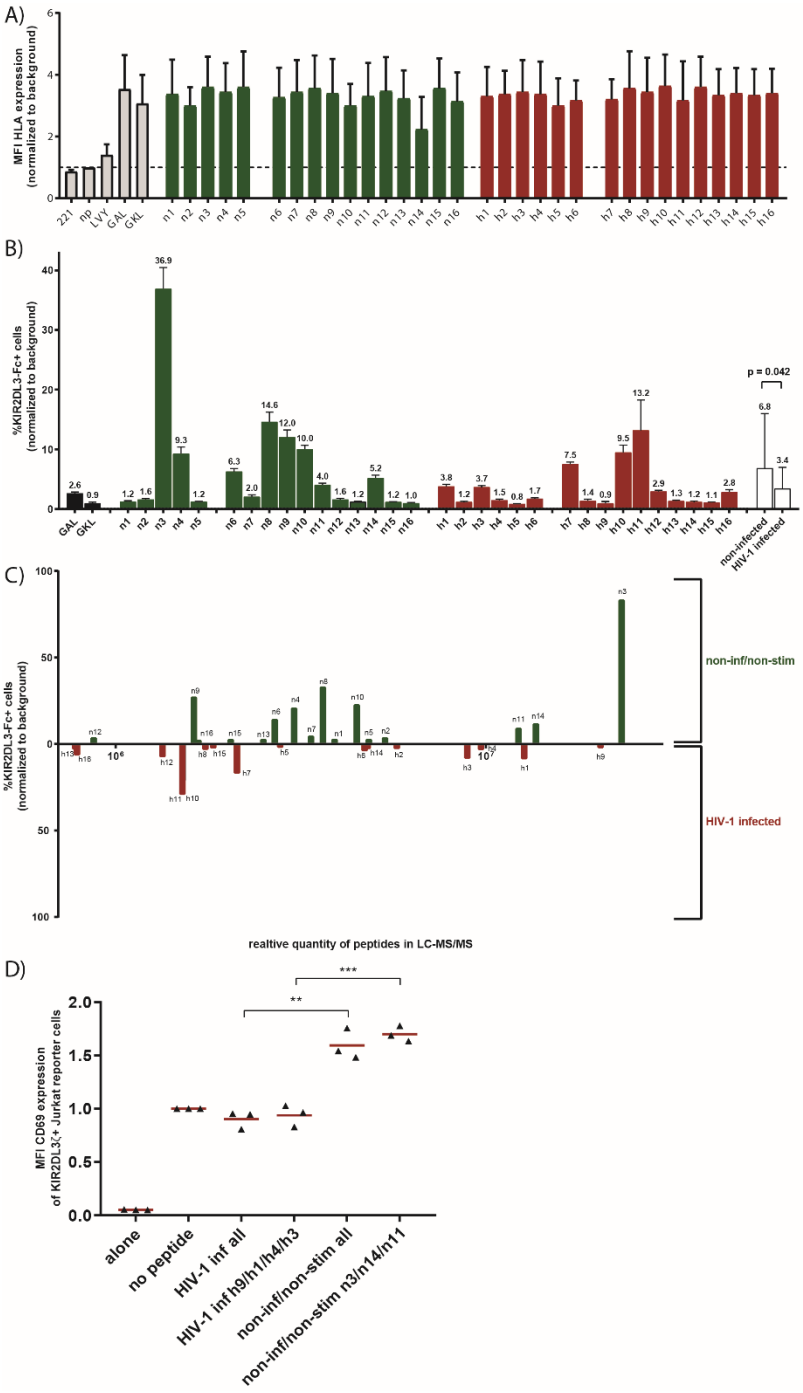

Fig. 16 Interaction of peptides, HLA-C*03:04 and KIR2DL3 *in vitro*. Peptides identified on non-infected/non-stimulated cells in green, peptides identified on HIV-1-infected cells in red. A) Peptide-mediated stabilization of HLA-C*03:04 expressed on 221-TAPko-HLA-C*03:04 cells B) Binding of KIR2DL3-Fc to HLA-C*03:04/peptide complex. Average of KIR2DL3 positive cells of non-infected/non-stimulated peptides and HIV-1-infected peptides in white. P-value calculated using Mann-Whitney Test. C) KIR2DL3-binding capacity of HLA-C*03:04-presented peptides relative to their relative quantity as identified in LC-MS/MS. D) Scatter Plots of CD69 expression of KIR2DL3ζ^{+} Jurkat reporter cells coincubated with 221-TAPko-HLA-C*03:04 cells pulsed with the different combinations of peptides for each group. Red bar demonstrates median of each group. *P*-values were calculated using unpaired, two-tailed t-test (112).

*Molecular dynamics simulations of HLA-C*03:04/n3/KIR2DL3 and HLA-C*03:04/h9/KIR2DL3 show structural evidence for peptide-mediated functional differences*

In an attempt to establish a structural and mechanistic basis for the observed differences between HLA-C*03:04-restricted peptides identified on nCD4$^+$ T cells and sHIVCD4$^+$ T cells in enabling KIR2DL3-binding, I, in collaboration with the Computational Biology Center (IBM Thomas J. Watson Research Center), carried out atomistic molecular dynamics simulations of HLA-C*03:04/KIR2DL3 complexes refolded either with the n3 (VIYPARISL) or the h9 (YAIQATETL) peptide. Initial complex structures were generated in the canonical HLA-peptide-KIR configuration (Fig. 17 A), with each peptide anchored in the HLA-C*03:04 peptide-binding groove and presented to the KIR interface. Simulation trajectories showed strong differences between the n3 and h9 peptides (Fig. 17 B-D). Most significantly, binding between the HLA-C*03:04/n3 complex and KIR2DL3 was dominated by both electrostatic and van der Waals interactions involving the arginine in position 6 of the n3 peptide (VIYPA**R**ISL), which facilitated additional interactions at positions 7, 8 and 9. In contrast, the HLA-C*03:04-presented h9 peptide was defined by van der Waals interactions most prominent at the threonine in position 8 (YAIQATE**T**L) (Fig. 17 C).

In the case of peptide n3, the side chain of the arginine in position 6 (R6) formed a persistent salt bridge with E21 of KIR2DL3, a glutamate near the KIR-peptide interaction interface. This salt bridge led to a side chain extension of R6 which had the effect of “flattening” the peptide KIR interface, enabling a multitude of peptide backbone and side chain interactions between peptide positions 6-9 and KIR2DL3 (Fig. 17 B). The resulting HLA-C*03:04/peptide complex contained a number of hydrophobic and van der Waals interactions, as well as an additional salt bridge between the peptide’s C-terminal carboxylate and K44 of KIR2DL3 (which competes with pre-existing salt bridges between K44 and D183/E187 of KIR2DL3). The two salt bridges at P6 and P9 served to staple the n3 C terminus in place, and are responsible for a large amount of favorable binding free energy. In contrast no net stabilizing electrostatic interactions with KIR2DL3 were observed for peptide h9, despite the presence of polar and charged groups at positions 6-8 (Fig. 17 D). Rather, the h9 peptide led to the burial of the T8 side chain methyl group in a generic

hydrophobic pocket in KIR2DL3 and some additional contacts between T6/KIR2DL3 M70 and E7/KIR2DL3 Q71. This combination of interactions places the h9 C-terminal carboxylate in close proximity to KIR2DL3 D183, partially accounting for the lack of favorable electrostatics interactions (Fig. 17 B). While peptide n3 only exhibited a small surplus of van der Waals interaction energy over peptide h9, on average, peptide n3 did engage the KIR2DL3 with ~60% more contact area which was stabilized by electrostatic groups (Fig. 17 D). Considered together, these observations derived from atomistic molecular dynamics simulations provide a structural correlate for the observed stronger binding of KIR2DL3 to the HLA-C*03:04/n3 complex compared to the HLA-C*03:04/h9 complex.

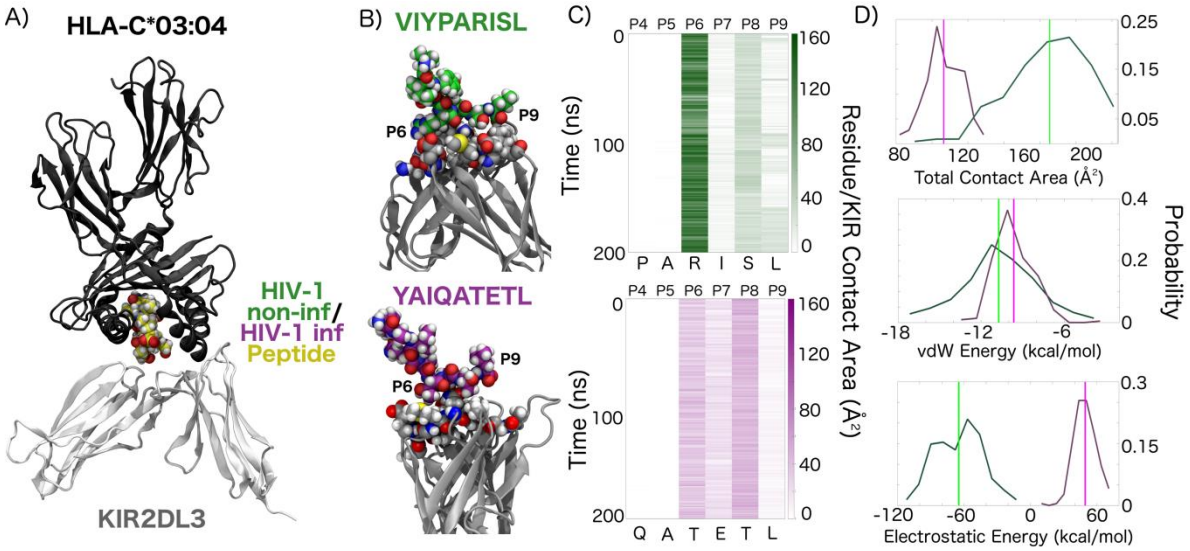

Fig. 17 Molecular dynamics simulations of HLA-C*03:04/peptide-KIR2DL3 complexes. A) Illustration of canonical HLA-I-peptide-KIR arrangement, featuring peptide n3 (VIYPARISL) being presented by HLA-C*03:04 to KIR2DL3. B) Equilibrated peptide-KIR2DL3 interactions for peptides n3 (VIYPARISL – green) and h9 (YAIQATETL – purple). C) KIR2DL3-peptide contact area, as a function of time and peptide residue position over the course of respective 200 ns production simulations. D) Histograms of total peptide-KIR2DL3 contact area, peptide-KIR2DL3 vdW interaction energy, and peptide-KIR2DL3 electrostatic energy, binned over respective 200 ns production trajectories. Mean values are indicated by vertical lines that are color-coded according to the convention established in B) (112).

In summary I was able to identify 833 peptides exclusively presented on HIV-1-infected cells containing 8 viral peptides vs 282 peptides exclusively presented on non-infected cells. The analysis of these peptides revealed that HIV-1 infection did not significantly impact peptide length distribution but lead to an increase in the proportion of peptides restricted to HLA-B*40:01. However, HLA-C*03:04-restricted peptides exclusively presented on infected cells significantly reduced binding to KIR2DL3 when compared

to peptides exclusively presented on uninfected cells. Furthermore the most abundant HLA-C*03:04-restricted peptide on non-infected cells (n3) led to highest binding of KIR2DL3 whereas the most abundant HLA-C*03:04-restricted peptide on HIV-1 infected cells (h8) did not mediate KIR2DL3-binding. These functional differences are likely due to an increased contact area between KIR2DL3 and HLA-C*03:04 caused by peptide n3.

Discussion

The decline of viral load in early stages of viral infections correlates with activation and expansion of NK cells, but the exact mechanism driving this activation and expansion of NK cells is incompletely understood (114–117). A large number of epidemiological studies demonstrated a strong association of combined HLA-I/KIR genotypes and the rate of virus disease progression (5,118,119). It is known that the peptide bound to HLA-I impacts the HLA-I/KIR interaction (91,120,121), but whether virus-induced changes in the HLA-I presented peptide repertoire are able to impact NK cell function and frequencies is largely unknown. In this thesis I sought to unravel mechanisms of the contribution of NK cells to combat viral infections and hypothesized that viral peptides presented by HLA-I are able to induce an inhibitory KIR-mediated accumulation of NK cells. As an additional mechanism, I investigated whether NK cells are able to monitor infection-induced alterations in the presentome of HIV-1 infected cells resulting in elimination of these cells.

*Stable Frequencies of HLA-C*03:04/Peptide-Binding KIR2DL2/3^{+} Natural Killer Cells Following Vaccination*

KIR/HLA-I interactions are highly susceptible to changes in the sequence of the HLA-I-presented peptide, which has been highlighted by crystal structures of KIR2DL2 and KIR3DL1 in complex with HLA-I/peptide complex (122,123). While it is well established that these interactions are peptide-dependent, it remains unknown whether HLA-I-presented peptides can modulate frequencies of KIR^{+} NK cell populations binding specific HLA-I/peptide complexes. To test the hypothesis that KIR2DL2/3^{+} NK cells recognizing HLA-C*03:04 molecules presenting a specific viral peptide would accumulate *in vivo* in response to exposure to the respective antigen, I used HLA-C*03:04/peptide tetramer staining of primary human KIR2DL2/3^{+} NK cells derived from healthy participants in a YFV vaccine trial and from HCV- and HIV-1-infected individuals. The study cohorts included HLA-C*03:04^{+} and HLA-C*03:04^{neg} individuals, and the selected peptides were previously described to induce specific CD8^{+} T cell responses indicating natural processing and presentation by HLA-I (91,124,125). The initial hypothesis was not supported by the results

from this study. I rather showed that KIR2DL2/3^{+} NK cells follow a consistent peptide-dependent hierarchy in their binding to HLA-C*03:04, which is independent of the underlying viral infection or vaccination and the HLA-I genotype (SUP1), but determined by the binding affinity of the respective HLA-C*03:04/peptide complex to KIR2DL2/3. Similar observations were made in a previous study comparing frequencies of HLA-B57/DENV peptide tetramer^{+} CD56^{dim} NK cells in Dengue Virus-infected versus uninfected individuals, demonstrating comparable frequencies of tetramer-binding NK cells in both study groups (126). Additionally one study showed staining of KIR2D^{+} NK cells with tetramers refolded by the SIV-derived peptide $GAG_{71\text{-}79}$ GY9 in a previously non-exposed rhesus macaque (127). These data show that HLA-C group 1/peptide tetramers can be used to identify KIR2DL2/3^{+} NK cell populations, but also suggest that an antigen-dependent expansion or contraction of the respective NK cell populations does not occur.

Viral infections influence frequencies of specific NK cell subsets. This includes expansion of Ly49H^{+} NK cells in MCMV infected mice (128), NKG2C in HCMV- and HCV-infected individuals (129,130) and KIR3DS1 in acute HIV-1 infection (131). Furthermore, contraction of NK cells was observed in HIV-1, HCV and varicella zoster virus infection (132–134). Nevertheless, the molecular mechanisms driving these expansions or contractions remain uncertain, with some studies suggesting a role of licensing/education through HLA-I/inhib KIR interactions (135,136). I longitudinally assessed the frequency of KIR2DL2/3^{+} NK cells able to bind a YFV-derived peptide presented by HLA-C*03:04 in individuals receiving the YFV-17D vaccine to examine whether KIR2DL2/3 are able to mediate an antigen-specific NK cell expansion or contraction *in vivo*. I observed stable frequencies of both total KIR2DL2/3^{+} NK cells as well as tetramer^{+} KIR2DL2/3^{+} NK cells over time. This is in contrast to a study reporting an increased expression of KIR2DL3 mRNA following vaccination with YFV-17D at day 7 (137). In that study the described gene induction of *KIR2DL3* after YFV vaccination might therefore have been restricted to other KIR expressing cell populations, such as T-cells, as only bulk KIR2DL3 mRNA levels on whole blood were quantified. As previous studies also suggested an influence of HCMV infection on NK cell expansion (47,128,138), the HCMV status of the study subjects was assessed, which did not show any differences in frequencies of tetramer^{+} KIR2DL2/3^{+} NK cells between HCMV^{+} and HCMV^{neg} individuals. Infection-induced expansion of NK cells has been

largely described for activating NK cell receptors, including KIR3DS1 and NKG2C in humans and Ly49H in mice (47,135,138,139). Therefore NK cell expansion might be attributed to DAP-12, the adaptor molecule mediating signal transduction of activating receptors (47). Notably these expansions are not purely dependent on KIR/HLA-I interactions, as in TAP-deficient patients an expansion of NKG2C^{+} NK cells was observed albeit these patients express less than 10% of normal HLA-I levels (140). However, receptors such as KIR2DL2/3 signal through ITIMs located in their intracellular tail (141), and given their inhibitory function, it is unclear if they (or any inhibitory NK cell receptor in general) can mediate NK cell expansion or an "accumulation" of cells in the host organism due to prevention of activation-induced cell death, as occurs for T-cells (138,142). These data suggest that the interaction of KIR2DL2/3 and HLA-C*03:04/viral peptide complex does not lead to inhibitory KIR-driven peptide-dependant changes in NK cell frequencies. This is further supported by the observation that frequencies of HLA-C*03:04/peptide complex-binding KIR2DL2/3^{+} NK cells did not differ between *HLA-C*03:04^{+}* and *HLA-C*03:04^{neg}* individuals (SUP 1). However, these data need to be interpreted in the context of the modest size of the study cohorts used. Therefore confirmatory studies in larger cohorts are required to better control for additional factors that may influence KIR^{+} NK cell frequencies, such as specific KIR2DL2/3 and HLA-C subtypes, as well as HCMV serostatus. Furthermore, not all KIR2DL2/3^{+} NK cells bound to HLA-C*03:04/peptide tetramers, suggesting that additional factors, such as KIR2DS2 genotype, surface KIR-expression levels or the ability of KIRs to cluster on the cell surface might impact HLA-C binding.

Furthermore the results of this study show that binding of HLA-C*03:04/peptide complex to KIR2DL2/3^{+} NK cells is impacted by the biochemical properties of the HLA-I-bound peptide. I observed reciprocal concordance between the binding affinities of KIR2DL2/3-Fc to HLA-C*03:04/peptide complex and the avidity of HLA-C*03:04 tetramers to KIR2DL2/3^{+} NK cells. The higher binding of YFV/HLA-C*03:04-NS2A$_{4-13}$- compared to HIV/HLA-C*03:04-Gag$_{296-304}$- and HCV/HLA-C*03:04-Core$_{136-144}$-tetramers to KIR2DL2/3^{+} NK cells was associated with the higher binding avidity of YFV/HLA-C*03:04-NS2A$_{4-13}$ complexes to KIR2DL2/3. This observation is in line with a previous study showing the influence of the HLA-I bound peptide on KIR avidity by mapping binding avidity and peptide selectivity of Mamu-KIR3DL05

to the same domain of the receptor (127). Furthermore the results show that binding affinity of the corresponding peptide to HLA-C*03:04 did not influence the binding of YFV/HLA-C*03:04-NS2A$_{4-13}$-, HIV/HLA-C*03:04-Gag$_{296-304}$- and HCV/HLA-C*03:04-Core$_{136-144}$-tetramers to KIR2DL2/3^{+} NK cells. This highlights the fact that HLA-I, peptide, and KIR are all equally important for binding and have their own unique characteristics depending on each respective sequence.

It has been shown that the binding of inhibitory KIRs to HLA-I molecules during NK cell development plays a critical role in determining the functionality of KIR^{+} NK cells, a process referred to as NK cell licensing or education (49,50). To assess functionality of KIR2DL2/3^{+} NK cells in the context of KIR2DL2/3^{+}/HLA-C*03:04 interactions, I compared tetramer^{+} and tetramer^{neg} KIR2DL2/3^{+} NK cells of one individual due to their ability to degranulate in response to HLA-I deficient target cells. The results showed that the ability of KIR2DL2/3^{+} NK cells to bind to YFV/HLA-C*03:04-NS2A$_{4-13}$-tetramer correlated with a higher functional capacity of these cells, which is consistent with NK cell licensing/education. Therefore the system provided the possibility to clearly identify licensed/educated NK cells *in vivo* and may help to understand the mechanistic basis of licensing.

I furthermore observed that the higher functional capacity of tetramer^{+} KIR2DL3^{+} NK cells was highly influenced by the engagement of KIR2DL2/3 to HLA-C*03:04 presenting the respective peptides. When tetramer^{+} KIR2DL3^{+} NK cells were exposed to 221 cells presenting either the YFV/NS2A$_{4–13}$- or the HCV/Core$_{136–144}$-peptide via HLA-C*03:04, degranulation was reduced, while 221 cells presenting the HIV/Gag$_{296–303}$-peptide inhibited NK cell degranulation less. These data were in line with the low binding of HIV/HLA-C*03:04-Gag$_{296–304}$-tetramers to KIR2DL3^{+} NK cells. Additionally, I observed a tetramer^{+} and tetramer^{neg} population within KIR2DL3^{+} NK cells, which might suggest differential HLA-C*03:04-binding to different KIR2DL3 subtypes, as most NK cells will only express one of the two alleles (143). It has been suggested that viruses, expressing peptides presented by HLA-I able to restore the engagement of inhibitory KIRs and subsequently prevent NK cell killing, accumulate in virus-infected individuals (82,91,94). All in all these observations may suggest that viruses, through selection of specific peptides,

furthermore target cytotoxic competent NK cell populations efficiently avoiding NK cell killing of the virus-infected cell. However, one limitation of studying KIR^+ NK cells is the cross-reactivity of several of the available antibodies, in particular between closely related activating and inhibitory KIRs. While the antibody used to identify $KIR2DL3^+$ NK cells (clone #180701) was described not to cross-react with KIR2DL2 and KIR2DS2 (109), I cannot completely rule out cross-reactivity with these receptors. In conclusion, the findings in this study demonstrate consistent hierarchies in the frequencies of $KIR2DL2/3^+$ NK cells binding HLA-C*03:04/peptide complexes that were not changed by an underlying viral infection or vaccination.

*HIV-1-induced changes in HLA-C*03:04-presented peptide repertoires lead to reduced engagement of inhibitory NK cell receptors*

During acute HIV-1 infection, a drop of viral load occurs before first virus-specific $CD8^+$ T cell responses are established, this decline in viral load is attributed to NK cells, but the exact mechanism still needs to be elucidated (39). It is meanwhile well established that it is not only the loss or insufficient amount of HLA-I expression on virus infected cells that can trigger NK cells, but also the presentation of specific peptides by HLA-I leading to activation of NK cells through abrogation of the engagement to inhibitory KIRs such as KIR2DL3 (91,94,120,144). I investigated HIV-1-induced changes in the presentome of infected cells by mass spectrometry and their impact on the binding to the inhibitory KIR2DL3, and observed reduced KIR2DL3-binding to HLA-C*03:04/peptide complex expressed on HIV-1-infected cells in comparison to uninfected cells.

Intracellular infections, such as HIV-1 infection, lead to massive changes of cell metabolism, resulting in differences of endogenously produced peptides presented by HLA-I molecules on infected cells, enabling recognition by immune cells. Using LC-MS/MS, I compared naturally HLA-I-presented peptides from HIV-1-infected, activated but non-infected and non-activated $CD4^+$ T cells. The results showed that HIV-1 infection induces changes in HLA-I-presented peptides, in line with previous studies (145,146). An initial comparison of the length of detected peptides showed that activation and HIV-1 infection, as well as activation alone, resulted in the presentation of longer peptides by HLA-A*02:01, -B*40:01 and -B*27:05.

$CD4^+$ T cells were activated using anti-CD3/CD28, which is described to induce production of IFN-γ (147), facilitating the presentation of longer peptides by HLA-I molecules (148). In contrast, activation did not change the length of peptides presented by HLA-C. These data are in line with previous studies reporting that HLA-C*02:02 and HLA-C*03:04 preferentially sample 9meres, whereas HLA-A*02:01, HLA-B*27:05 and HLA-B*40:01 are known to sample longer peptides in addition to 9meres (149), in particular following activation (150). Several crystal structures show that KIRs bind to HLA-I molecules on top of the F-pocket (122,151–153). Longer peptides overhanging or extending at the C terminus (154,155) may therefore interfere with the engagement of KIRs (151). As HLA-C is an important KIR ligand, this might explain why HLA-C-restricted peptides are not affected by IFN-γ. Besides changes in peptide length, activation with and without HIV-1 infection also caused moderate shifts in the allocation of peptides presented by respective HLA-I molecules. The number of identified peptides restricted by a given HLA-I molecule can be used as indication for HLA-I expression levels but is not directly equitable. This is because post-translational modified peptides are not included. Cysteine-carrying peptides are underrepresented due to the likelihood of cysteine to be modified. Some peptides are less potent for ionization or fragmentation and are therefore underrepresented. And with the method used, intracellular HLA-I/peptide complex are included in the measurement. Taken together these data suggest that potential effects of HIV-1 proteins on HLA-I expression had no direct effect on the proportion of detected peptides restricted by the HLA-I molecules investigated. But notably in our setting, HLA-B*27:05 was disfavored presenting only a small fraction of the identified peptides. This phenomenon has to be HIV-1 independent, as the proportion of HLA-B*27:05-restricted peptides did not change after infection. As TAP contributes to epitope selection, one potential mechanism could be the selective peptide transport by TAP, leading to a more efficient peptide supply for some HLA-I alleles. But according to this hypothesis HLA-B*27:05 would have been favored, whereas HLA-A*02:01 would have been disfavored as described by Daniel et al. (156). This is not reflected in the results of this study and can be excluded as explanation. There might be technical issues beyond my current understanding that could be responsible for the disfavoring of HLA-B*27:05. One potential biological explanation is that HLA-B*27:05 has been described to form homodimers presenting

peptides in the absence of β2m (157). This could lead to a decreased number of presented peptides due to two free HLA-B*27:05 heavy chains forming one homodimer presenting one peptide. Additionally, annotation of peptides can be difficult as peptides can carry multiple HLA-I binding motifs. In cases of multiple possible annotations, the HLA-I allotype yielding the lowest NetMHC rank was selected in this study. This could have led to the disfavoring of HLA-B*27:05.

Previous studies of HLA-I-presented peptides on virus-infected cells showed one consistent observation; only a very small fraction of peptides are actually derived from the virus (145,146,158,159). In the current study, I observed similar results with only 0.2 % of the overall identified peptides presented on HIV-1-infected cells being of viral origin. Remarkably, 6 of these peptides were consistently detected during the two independent experiments within the over 5600 peptides identified by LC-MS/MS analyses on sHIVCD4$^+$ T cells, suggesting a high level of reproducibility in their presentation and detection. Half of the identified HIV-1 peptides were allocated to HLA-B*40:01, in line with the overall increased fraction of HLA-B*40:01-restricted peptides on infected cells, and three HIV-1 peptides were restricted by HLA-A*02:01, representing the largest fraction of HLA-I-presented peptides. This might indicate that the higher the proportion of sampled peptides, the higher the chance of presentation of HIV-1-derived peptides. One peptide, RSLFGSDPSSQ, could not be assigned to any HLA-I allele with the algorithm used, but was previously identified as being presented via HLA-A*02:01 on HIV-1-infected primary human CD4$^+$ T cells (160). Three of the HLA-A*02:01-restricted HIV-1 peptides (AVLSIVNRV, FLGKIWPS, VLAEAMSQV) and one of the HLA-B*40:01-restricted HIV-1 peptides (KELYPLASL) represented previously described CTL epitopes (161–163) (http://www.hiv.lanl.gov/), while the three remaining peptides (GENTSLLHPVSL, SESAIRNTI and SESAIRNTIL) have not been reported before. Interestingly, the HLA-A*02:01-restricted peptide SESAIRNTIL was detected at high relative quantity on HIV-1-infected cells during both runs, suggesting a potentially immune-dominant role in inducing virus-specific CD8$^+$ T cell responses.

While virus-derived peptides constituted only a small minority of infection-induced alterations in the immunopeptidome of HIV-1 infected $CD4^+$ T cells, I observed very clear differences on host-derived peptides between infected and uninfected cells, including over 800 peptides uniquely detected on HIV-1-infected $CD4^+$ T cells. Additionally, over 2000 peptides were identified that were detected both on $sHIVCD4^+$ T cells and $sCD4^+$ T cells, but not on $nCD4^+$ T cells. To evaluate whether the presentation of these host-derived stress peptides can influence recognition of infected cells by KIR^+ NK cells, I focused further studies on HLA-C*03:04-restricted peptides, as HLA-C*03:04 is the ligand of the inhibitory receptor KIR2DL2/3, and changes in HLA-C*03:04/KIR2DL interactions are associated with differential NK cell-mediated control of HIV-1 replication (94,144,164). Furthermore, we previously showed that HIV-1 can carry sequence polymorphisms within virus-derived peptides presented by HLA-C*03:04 able to restore engagement to inhibitory KIR2DL2/3 offering a possible way to escape from NK cell-mediated immune pressure (94,144). Using a subset of 32 peptides selected from each group based on consistent detection during both experiments and/or high *in silico* binding scores to HLA-C*03:04, I demonstrated that while all peptides showed similar binding affinities to HLA-C*03:04, peptides uniquely presented on resting $CD4^+$ T cells led to significantly stronger binding of KIR2DL3. Specifically the most abundant peptide, VIYPARISL (n3), mediated the highest binding of KIR2DL3, while the most abundant peptide presented on HIV-1-infected $CD4^+$ T cells, YAIQATETL (h9) did not induce KIR2DL3-binding. Furthermore, peptides identified on $nCD4^+$ T cells strongly stimulated $KIR2DL3\zeta^+$ Jurkat reporter cells, whereas peptides identified on $sHIVCD4^+$ T cells did significantly less. VIYPARISL, the most abundant peptide on resting $CD4^+$ T cells, arises from the source protein DNAJB1. DNAJB1 is a negative regulator of the heat shock response and belongs to the family of Hsp40 (165). Interestingly, it is described that HIV-1 subtype B Nef leads to an upregulation of Hsp40 expression (166). This seems to be contraindicative to the results of this study in which VIYPARISL is completely absent in the presentome of HIV-1 infected cells. But Nef does not only induce Hsp40 expression, but also physically interacts with HSP40 (167). Nef might therefore protect DNAJB1/HSP40 from degradation, so that no degradation product is available for presentation. The source protein of YAIQATETL, the most abundant peptide on HIV-1-infected cells and absent on non-infected,

non-stimulated cells, is the C-C chemokine receptor type 4 (CCR4). It was shown that CCL22, a ligand for CCR4, has antiviral activity and that the viral protein gp120 can interact with CCR4 (168–170) and might compete with CCL22 for binding to CCR4. But to date the exact mechanisms how CCR4 influences HIV-1 infection is not known. But it is likely that HIV-1 infection leads to an upregulation of CCR4, explaining the presentation of the degradation product YAIQATETL on the cell surface. All in all these results support a model in which HLA-I-presented host-derived peptides on non-stressed cells provide a strong inhibitory signal to NK cells expressing inhibitory KIRs, and infection-induced stress leads to changes in the presented peptide repertoire resulting in reduced engagement of inhibitory KIRs, facilitating NK cell activation. This activation can lead to killing of infected cells by the release of perforin and granzyme or, as NK cells also possess immunomodulatory functions, also result in enhanced immune activation through the release of cytokines.

As the current study was limited by a small sample size, the necessity of stimulating $CD4^+$ T cells prior to infection with HIV-1, and by the use of *in vitro* systems limiting the investigated interactions to one inhibitory NK cell receptor and its HLA-C ligand, additional studies using different infection models and different HLA-I allotypes will be required to confirm whether infection-induced changes in HLA-I-presented peptides represents an innate mechanism to render infected cells more susceptible to NK cell-mediated lysis by reducing engagement of inhibitory NK cell receptors.

To further characterize the structural components that resulted in reduced KIR2DL3-binding to HLA-C*03:04-restricted peptide presented on HIV-1-infected cells compared to non-stimulated non-infected cells, I used molecular dynamic simulations of the HLA-C*03:04/KIR2DL3 complexes with the dominant peptides presented on $nCD4^+$ T cells (VIYPARISL, n3) and $sHIVCD4^+$ T cells (YAIQATETL, h9). This modeling revealed that VIYPARISL binds with almost twice the equilibrated contact area to KIR2DL3 as compared to YAIQATETL. This increased contact area was mainly attributable to interactions at P6 and P9 of the 9mer peptide that provided more advantageous single point vdW and electrostatic energies at the peptide n3-KIR interface. P6 and P9 having critical relevance in the context of HLAI/peptide/KIR

interactions was not expected. Especially, given that previous studies based on crystal structures of KIR2DL1 (152), KIR2DL2 (171), KIR2DL3 (172) and KIR2DS2 (153) had demonstrated that peptide residues P7 and P8 had the most significant impact on KIR/HLA-I interactions (173). However, we previously showed that peptide residue P9 can impact KIR/HLA-I interactions, as changes in P9 affected binding of HLA-C*06:02 to KIR2DL1 and KIR2DS1, even though affinity to HLA-C*06:02 was not impacted (174). This suggests that changes in additional residues of HLA-I-presented peptides can have an important impact on KIR-binding due to consequences for tertiary peptide structures, as also described for TCR engagement (175). Taken together the results of this study demonstrate that HIV-1-mediated cellular stress results in alterations in HLA-I-presented peptide repertoires leading to reduced engagement of inhibitory KIRs, facilitating NK cell activation and offering a mechanism of innate immune-surveillance of virus-infected cells.

In conclusion the results of this thesis help to unravel the mechanisms how KIR^+ NK cells influence the course of viral infections. First, an inhibitory KIR-mediated accumulation or expansion of KIR^+ NK cells after viral infection is unlikely. Second, the results suggest that viral infections lead to the presentation of host-derived stress peptides, recognized by inhibitory KIR^+ NK cells leading to activation of the respective NK cell subset and elimination of virus-infected cells thereby influencing disease outcome.

References

1. Barre-Sinoussi, F., Chermann, J. C., Rey, F., et al. (2004) Isolation of a T-lymphotropic retrovirus from a patient at risk for acquired immune deficiency syndrome (AIDS). 1983. *Rev. Invest. Clin.*, **56**, 126–129.

2. Burton, D. R., Ahmed, R., Barouch, D. H., et al. (2012) A blueprint for HIV vaccine discovery. A blueprint for HIV vaccine discovery. *Cell Host Microbe* **(2012)** , *12*, 396–407.

3. Duncan, J. D., Urbanowicz, R. A., Tarr, A. W., et al. (2020) Hepatitis C virus vaccine: Challenges and prospects. Hepatitis C virus vaccine: Challenges and prospects. *Vaccines* **(2020)** , *8*.

4. Jost, S. and Altfeld, M. (2013) Control of Human Viral Infections by Natural Killer Cells. *Annu. Rev. Immunol.*, **31**, 163–194.

5. Khakoo, S. I., Thio, C. L., Martin, M. P., et al. (2004) HLA and NK cell inhibitory receptor genes in resolving hepatitis C virus infection. *Science*, **305**, 872–4.

6. Martin, M. P., Gao, X., Lee, J.-H., et al. (2002) Epistatic interaction between KIR3DS1 and HLA-B delays the progression to AIDS. *Nat. Genet.*, **31**, 429–434.

7. Alter, G., Martin, M. P., Teigen, N., et al. (2007) Differential natural killer cell-mediated inhibition of HIV-1 replication based on distinct KIR/HLA subtypes. *J. Exp. Med.*, **204**, 3027–36.

8. Cooper, M. A., Fehniger, T. A., Fuchs, A., et al. (2004) NK cell and DC interactions. *Trends Immunol.*, **25**, 47–52.

9. Cooper, M. A., Fehniger, T. A., Turner, S. C., et al. (2001) Human natural killer cells: A unique innate immunoregulatory role for the CD56bright subset. *Blood*, **97**, 3146–3151.

10. Waggoner, S. N., Cornberg, M., Selin, L. K., et al. (2011) Natural killer cells act as rheostats modulating antiviral T cells. *Nature*, **481**, 394–8.

11. Knapp, S., Warshow, U., Hegazy, D., et al. (2010) Consistent beneficial effects of killer cell immunoglobulin-like receptor 2DL3 and group 1 human leukocyte antigen-C following exposure to hepatitis C virus. *Hepatology*, **51**, 1168–1175.

12. Barré-Sinoussi, F. (2010) HIV: a discovery opening the road to novel scientific knowledge and global health improvement. *Virology*, **397**, 255–9.

13. Janeway CA Jr, Travers P, Walport M, S. M. (2001) Immunobiology: The Immune System in Health and Disease. *Immunobiology: The Immune System in Health and Disease.*; 5th ed.; New York: Garland Science, (2001) .

14. Weiss, R. A. (2001) Gulliver's travels in HIVland. *Nature*, **410**, 963–7.

15. Arts, E. J. and Hazuda, D. J. (2012) HIV-1 antiretroviral drug therapy. *Cold Spring Harb. Perspect. Med.*, **2**.

16. Simmonds, P. (2013) The origin of hepatitis C virus. *Curr. Top. Microbiol. Immunol.*, **369**, 1–15.

17. Lindenbach, B. D., Meuleman, P., Ploss, A., et al. (2006) Cell culture-grown hepatitis C virus is infectious in vivo and can be recultured in vitro. *Proc. Natl. Acad. Sci. U. S. A.*, **103**, 3805–9.

18. Dustin, L. B., Bartolini, B., Capobianchi, M. R., et al. (2016) Hepatitis C virus: life cycle in cells, infection and host response, and analysis of molecular markers influencing the outcome of infection and response to therapy. Hepatitis C virus: life cycle in cells, infection and host response, and analysis of molecular markers influencing the outcome of infection and response to therapy. *Clin. Microbiol. Infect.* **(2016)** , *22*, 826–832.

19. Penin, F., Dubuisson, J., Rey, F. A., et al. (2004) Structural Biology of Hepatitis C Virus. Structural Biology of Hepatitis C Virus. *Hepatology* **(2004)** , *39*, 5–19.

20. Pawlotsky, J. M., Feld, J. J., Zeuzem, S., et al. (2015) From non-A, non-B hepatitis to hepatitis C virus cure. From non-A, non-B hepatitis to hepatitis C virus cure. *J. Hepatol.* **(2015)** , *62*, S87–S99.

21. Sulkowski, M. S., Gardiner, D. F., Rodriguez-Torres, M., et al. (2014) Daclatasvir plus sofosbuvir for previously treated or untreated chronic HCV infection. *N. Engl. J. Med.*, **370**, 211–221.

22. Monath, T. P. (2008) Treatment of yellow fever. Treatment of yellow fever. *Antiviral Res.* **(2008)** , *78*, 116–124.

23. Verma, R., Khanna, P. and Chawla, S. (2014) Yellow fever vaccine: An effective vaccine for travelers. *Hum. Vaccines Immunother.*, **10**, 126–128.

24. Kaufmann, B. and Rossmann, M. G. (2011) Molecular mechanisms involved in the early steps of flavivirus cell entry. Molecular mechanisms involved in the early steps of flavivirus cell entry. *Microbes Infect.* **(2011)** , *13*, 1–9.

25. Collins, N. D. and Barrett, A. D. T. (2017) Live Attenuated Yellow Fever 17D Vaccine: A Legacy Vaccine Still Controlling Outbreaks In Modern Day. Live Attenuated Yellow Fever 17D Vaccine: A Legacy Vaccine Still Controlling Outbreaks In Modern Day. *Curr. Infect. Dis. Rep.* **(2017)** , *19*, 14.

26. Marquardt, N., Ivarsson, M. A., Blom, K., et al. (2015) The Human NK Cell Response to Yellow Fever Virus 17D Is Primarily Governed by NK Cell Differentiation Independently of NK Cell Education. *J. Immunol.*, **195**, 3262–72.

27. Wilkins, C. and Gale, M. J. (2010) Recognition of viruses by cytoplasmic sensors. *Curr. Opin. Immunol.*, **22**, 41–47.

28. Janeway, C. A. J. and Medzhitov, R. (2002) Innate immune recognition. *Annu. Rev. Immunol.*, **20**, 197–216.

29. French, A. R. and Yokoyama, W. M. (2003) Natural killer cells and viral infections. Natural killer cells and viral infections. *Curr. Opin. Immunol.* **(2003)** .

30. Cullen, S. P. and Martin, S. J. (2008) Mechanisms of granule-dependent killing. *Cell Death Differ.*, **15**, 251–62.

31. Jassoy, C., Harrer, T., Rosenthal, T., et al. (1993) Human immunodeficiency virus type 1-specific cytotoxic T lymphocytes release gamma interferon, tumor necrosis factor alpha (TNF-alpha), and TNF-beta when they encounter their target antigens. *J. Virol.*, **67**, 2844–2852.

32. Biron, C. A., Nguyen, K. B., Pien, G. C., et al. (1999) NATURAL KILLER CELLS IN ANTIVIRAL DEFENSE: Function and Regulation by Innate Cytokines. *Annu. Rev. Immunol.*, **17**, 189–220.

33. Boehm, U., Klamp, T., Groot, M., et al. (1997) CELLULAR RESPONSES TO INTERFERON-γ. *Annu. Rev. Immunol.*, **15**, 749–795.

References

34. Schroder, K., Hertzog, P. J., Ravasi, T., et al. (2004) Interferon-γ: an overview of signals, mechanisms and functions. *J. Leukoc. Biol.*, **75**, 163–189.

35. Chu, W. M. (2013) Tumor necrosis factor. Tumor necrosis factor. *Cancer Lett.* **(2013)** , *328*, 222–225.

36. Verbist, K. C. and Klonowski, K. D. (2012) Functions of IL-15 in anti-viral immunity: multiplicity and variety. *Cytokine*, **59**, 467–478.

37. Mattei, F., Schiavoni, G., Belardelli, F., et al. (2001) IL-15 is expressed by dendritic cells in response to type I IFN, double-stranded RNA, or lipopolysaccharide and promotes dendritic cell activation. *J. Immunol.*, **167**, 1179–1187.

38. Smith, K. M., Pottage, L., Thomas, E. R., et al. (2000) Th1 and Th2 CD4 + T Cells Provide Help for B Cell Clonal Expansion and Antibody Synthesis in a Similar Manner In Vivo . *J. Immunol.*, **165**, 3136–3144.

39. Alter, G. and Altfeld, M. (2009) NK cells in HIV-1 infection: evidence for their role in the control of HIV-1 infection. *J. Intern. Med.*, **265**, 29–42.

40. Herberman, R. B., Nunn, M. E., Holden, H. T., et al. (1975) Natural cytotoxic reactivity of mouse lymphoid cells against syngeneic and allogeneic tumors. II. Characterization of effector cells. *Int. J. Cancer*, **16**, 230–239.

41. Kiessling, R., Klein, E. and Wigzell, H. (1975) „Natural" killer cells in the mouse. I. Cytotoxic cells with specificity for mouse Moloney leukemia cells. Specificity and distribution according to genotype. *Eur. J. Immunol.*, **5**, 112–117.

42. Cooper, M. A., Fehniger, T. A. and Caligiuri, M. A. (2001) The biology of human natural killer-cell subsets. *Trends Immunol.*, **22**, 633–40.

43. Mace, E. M. and Orange, J. S. (2019) Emerging insights into human health and NK cell biology from the study of NK cell deficiencies. Emerging insights into human health and NK cell biology from the study of NK cell deficiencies. *Immunol. Rev.* **(2019)** , *287*, 202–225.

44. Biron, C. A., Byron, K. S. and Sullivan, J. L. (1989) Severe Herpesvirus Infections in an Adolescent without Natural Killer Cells. *N. Engl. J. Med.*, **320**, 1731–1735.

45. Orr, M. T. and Lanier, L. L. (2010) Natural Killer Cell Education and Tolerance. Natural Killer Cell Education and Tolerance. *Cell* **(2010)** , *142*, 847–856.

46. O'Leary, J. G., Goodarzi, M., Drayton, D. L., et al. (2006) T cell- and B cell-independent adaptive immunity mediated by natural killer cells. *Nat. Immunol.*, **7**, 507–16.

47. Sun, J. C., Beilke, J. N. and Lanier, L. L. (2009) Adaptive immune features of natural killer cells. *Nature*, **457**, 557–561.

48. Cooper, M. A., Elliott, J. M., Keyel, P. A., et al. (2009) Cytokine-induced memory-like natural killer cells. *Proc. Natl. Acad. Sci. U. S. A.*, **106**, 1915–9.

49. Elliott, J. M. and Yokoyama, W. M. (2011) Unifying concepts of MHC-dependent natural killer cell education. *Trends Immunol.*, **32**, 364–372.

50. Kim, S., Poursine-Laurent, J., Truscott, S. M., et al. (2005) Licensing of natural killer cells by host major histocompatibility complex class I molecules. *Nature*, **436**, 709–713.

51. Seidel, U. J. E., Schlegel, P. and Lang, P. (2013) Natural killer cell mediated antibody-dependent cellular cytotoxicity in tumor immunotherapy with therapeutic antibodies. Natural killer cell mediated antibody-dependent cellular cytotoxicity in tumor immunotherapy with therapeutic antibodies. *Front. Immunol.* **(2013)** , *4*, 76.

52. Waggoner, S. N., Cornberg, M., Selin, L. K., et al. (2011) Natural killer cells act as rheostats modulating antiviral T cells. *Nature*, **481**, 394–8.

53. Maini, M. K. and Peppa, D. (2013) NK cells: a double-edged sword in chronic hepatitis B virus infection. *Front. Immunol.*, **4**, 57.

54. Yokoyama, W. M., Kim, S. and French, A. R. (2004) The Dynamic Life of Natural Killer Cells. *Annu. Rev. Immunol.*, **22**, 405–429.

55. Ljunggren, H. G. and Kärre, K. (1990) In search of the "missing self": MHC molecules and NK cell recognition. *Immunol. Today*, **11**, 237–44.

56. Arnon, T. I., Markel, G. and Mandelboim, O. (2006) Tumor and viral recognition by natural killer cells receptors. Tumor and viral recognition by natural killer cells receptors. *Semin. Cancer Biol.* **(2006)** , *16*, 348–358.

57. Niehrs, A., Garcia-Beltran, W. F., Norman, P. J., et al. (2019) A subset of HLA-DP molecules serve as ligands for the natural cytotoxicity receptor NKp44. A subset of HLA-DP molecules serve as ligands for the natural cytotoxicity receptor NKp44. *Nat. Immunol.* **(2019)** , *20*, 1129–1137.

58. Lanier, L. L. (2015) NKG2D receptor and its ligands in host defense. *Cancer Immunol. Res.*, **3**, 575–582.

59. Garcia-Beltran, W. F., Holzemer, A., Martrus, G., et al. (2016) Open conformers of HLA-F are high-affinity ligands of the activating NK-cell receptor KIR3DS1. *Nat. Immunol.*, **17**, 1067–1074.

60. Horowitz, A., Stegmann, K. A. and Riley, E. M. (2012) Activation of natural killer cells during microbial infections. Activation of natural killer cells during microbial infections. *Front. Immunol.* **(2012)** , *2*.

61. Carrington, M. and Norman, P. (2003) The KIR Gene Cluster. *Clin. Transplant.*, 1–48.

62. Leddon, S. A. and Sant, A. J. (2010) Generation of MHC class II-peptide ligands for CD4 T-cell allorecognition of MHC class II molecules. Generation of MHC class II-peptide ligands for CD4 T-cell allorecognition of MHC class II molecules. *Curr. Opin. Organ Transplant.* **(2010)** , *15*, 505–511.

63. Hölzemer, A., Garcia-Beltran, W. F. and Altfeld, M. (2017) Natural Killer Cell Interactions with Classical and Non-Classical Human Leukocyte Antigen Class I in HIV-1 Infection. *Front. Immunol.*, **8**, 1496.

64. Ranasinghe, S., Lamothe, P. A., Soghoian, D. Z., et al. (2016) Antiviral CD8+ T Cells Restricted by Human Leukocyte Antigen Class II Exist during Natural HIV Infection and Exhibit Clonal Expansion. *Immunity*, **45**, 917–930.

65. Neefjes, J., Jongsma, M. L. M., Paul, P., et al. (2011) Towards a systems understanding of MHC class i and MHC class II antigen presentation. Towards a systems understanding of MHC class i and MHC class II antigen presentation. *Nat. Rev. Immunol.* **(2011)** , *11*, 823–836.

66. Shiina, T., Hosomichi, K., Inoko, H., et al. (2009) The HLA genomic loci map: Expression,

interaction, diversity and disease. The HLA genomic loci map: Expression, interaction, diversity and disease. *J. Hum. Genet.* **(2009)** , *54*, 15–39.

67. Gleimer, M. and Parham, P. (2003) Stress Management: MHC Class I and Class I-like Molecules as Reporters of Cellular Stress. *Immunity*, **19**, 469–477.

68. Hughes, A. L. and Nei, M. (1988) Pattern of nucleotide substitution at major histocompatibility complex class I loci reveals overdominant selection. *Nature*, **335**, 167–70.

69. Parham, P. (1987) Functional sites of human class I MHC molecules: paradigms a dozen? *Immunol. Res.*, **6**, 153–78.

70. Stevanović, S., Lemmel, C., Häntschel, M., et al. (2003) Generating data for databases--the peptide repertoire of HLA molecules. *Novartis Found. Symp.*, **254**, 143–55; discussion 155-64, 216–22, 250–2.

71. Theodossis, A., Guillonneau, C., Welland, A., et al. (2010) Constraints within major histocompatibility complex class I restricted peptides: presentation and consequences for T-cell recognition. *Proc. Natl. Acad. Sci. U. S. A.*, **107**, 5534–9.

72. Yewdell, J. W., Reits, E. and Neefjes, J. (2003) Making sense of mass destruction: quantitating MHC class I antigen presentation. *Nat. Rev. Immunol.*, **3**, 952–961.

73. Bassani-Sternberg, M., Pletscher-Frankild, S., Jensen, L. J., et al. (2015) Mass spectrometry of human leukocyte antigen class I peptidomes reveals strong effects of protein abundance and turnover on antigen presentation. *Mol. Cell. Proteomics*, **14**, 658–73.

74. Granados, D. P., Tanguay, P.-L., Hardy, M.-P., et al. (2009) ER stress affects processing of MHC class I-associated peptides. *BMC Immunol.*, **10**, 10.

75. Nover, L. (1991) Heat shock response. .

76. Patil, C. and Walter, P. (2001) Intracellular signaling from the endoplasmic reticulum to the nucleus: the unfolded protein response in yeast and mammals. *Curr. Opin. Cell Biol.*, **13**, 349–355.

77. Bukau, B., Cell, A. H.- and 1998, undefined The Hsp70 and Hsp60 chaperone machines. *cell.com*.

78. Welihinda, A., Tirasophon, W., expression, R. K.-G., et al. The cellular response to protein misfolding in the endoplasmic reticulum. *ingentaconnect.com*.

79. nutrition, K. W.-T. J. of and 1999, undefined Ubiquitin-dependent signaling: the role of ubiquitination in the response of cells to their environment. *academic.oup.com*.

80. Gleimer, M. and Parham, P. (2003) Stress Management: MHC Class I and Class I-like Molecules as Reporters of Cellular Stress. *Immunity*, **19**, 469–477.

81. Peruzzi, M., Wagtmann, N. and Long, E. O. (1996) A p70 killer cell inhibitory receptor specific for several HLA-B allotypes discriminates among peptides bound to HLA-B*2705. *J. Exp. Med.*, **184**, 1585–1590.

82. Fadda, L., Körner, C., Kumar, S., et al. (2012) HLA-Cw*0102-restricted HIV-1 p24 epitope variants can modulate the binding of the inhibitory KIR2DL2 receptor and primary NK cell function. *PLoS Pathog.*, **8**, e1002805.

83. Rajagopalan, S. and Long, E. O. (1997) The direct binding of a p58 killer cell inhibitory receptor to human histocompatibility leukocyte antigen (HLA)-Cw4 exhibits peptide selectivity. *J. Exp. Med.*,

185, 1523–8.

84. Silvestre, D., Kourilsky, F. M., Niccolai, M. G., et al. (1970) Presence of HL.A Antigens on human reticulocytes as demonstrated by electron microscopy. *Nature*, **228**, 67–68.

85. Pereyra, F., Jia, X., McLaren, P. J., et al. (2010) The major genetic determinants of HIV-1 control affect HLA class I peptide presentation. *Science (80-.).*, **330**, 1551–1557.

86. Dendrou, C. A., Petersen, J., Rossjohn, J., et al. (2018) HLA variation and disease. HLA variation and disease. *Nat. Rev. Immunol.* **(2018)** , *18*, 325–339.

87. González-Galarza, F. F., Takeshita, L. Y. C., Santos, E. J. M., et al. (2015) Allele frequency net 2015 update: New features for HLA epitopes, KIR and disease and HLA adverse drug reaction associations. *Nucleic Acids Res.*, **43**, D784–D788.

88. Frazier, W. R., Steiner, N., Hou, L., et al. (2013) Allelic variation in KIR2DL3 generates a KIR2DL2-like receptor with increased binding to its HLA-C ligand. *J. Immunol.*, **190**, 6198–208.

89. Knapp, S., Usama Warshow, Hegazy, D., et al. (2010) Consistent beneficial effects of killer cell immunoglobulin-like receptor 2dl3 and group 1 human leukocyte antigen-c following exposure to hepatitis c virus. *Hepatology*, **51**, 1168–1175.

90. Vidal-Castiñeira, J. R., López-Vázquez, A., Díaz-Peña, R., et al. (2010) Effect of killer immunoglobulin-like receptors in the response to combined treatment in patients with chronic hepatitis C virus infection. *J. Virol.*, **84**, 475–81.

91. Lunemann, S., Martrus, G., Hölzemer, A., et al. (2016) Sequence variations in HCV core-derived epitopes alter binding of KIR2DL3 to HLA-C∗03:04 and modulate NK cell function. *J. Hepatol.*, **65**, 252–8.

92. Alter, G., Heckerman, D., Schneidewind, A., et al. (2011) HIV-1 adaptation to NK-cell-mediated immune pressure. *Nature*, **476**, 96–100.

93. Apps, R., Qi, Y., Carlson, J. M., et al. (2013) Influence of HLA-C expression level on HIV control. *Science*, **340**, 87–91.

94. Hölzemer, A., Thobakgale, C. F., Jimenez Cruz, C. A., et al. (2015) Selection of an HLA-C*03:04-Restricted HIV-1 p24 Gag Sequence Variant Is Associated with Viral Escape from KIR2DL3+ Natural Killer Cells: Data from an Observational Cohort in South Africa. *PLOS Med.*, **12**, e1001900.

95. Ziegler, M. C., Grañana, F. B., Garcia-Beltran, W. F., et al. (2018) Stable Frequencies of HLA-C*03:04/Peptide-Binding KIR2DL2/3+ Natural Killer Cells Following Vaccination. *Front. Immunol.*, **9**, 2361.

96. Schüpbach, J. (2003) Viral RNA and p24 antigen as markers of HIV disease and antiretroviral treatment success. Viral RNA and p24 antigen as markers of HIV disease and antiretroviral treatment success. *Int. Arch. Allergy Immunol.* **(2003)** , *132*, 196–209.

97. Nelde, A., Kowalewski, D. J. and Stevanovic, S. (2019) Purification and Identification of Naturally Presented MHC Class I and II Ligands. *Methods Mol. Biol.*, **1988**, 123–136.

98. Nelde, A., Kowalewski, D. J., Backert, L., et al. (2018) HLA ligandome analysis of primary chronic lymphocytic leukemia (CLL) cells under lenalidomide treatment confirms the suitability of lenalidomide for combination with T-cell-based immunotherapy. *Oncoimmunology*, **7**, e1316438.

References

99. Kowalewski, D. J., Schuster, H., Backert, L., et al. (2015) HLA ligandome analysis identifies the underlying specificities of spontaneous antileukemia immune responses in chronic lymphocytic leukemia (CLL). *Proc. Natl. Acad. Sci.*, **112**, E166–E175.

100. Eng, J. K., McCormack, A. L. and Yates, J. R. (1994) An approach to correlate tandem mass spectral data of peptides with amino acid sequences in a protein database. *J. Am. Soc. Mass Spectrom.*, **5**, 976–989.

101. Käll, L., Canterbury, J. D., Weston, J., et al. (2007) Semi-supervised learning for peptide identification from shotgun proteomics datasets. *Nat. Methods*, **4**, 923–925.

102. Nielsen, M. and Andreatta, M. (2016) NetMHCpan-3.0; improved prediction of binding to MHC class I molecules integrating information from multiple receptor and peptide length datasets. *Genome Med.*, **8**, 33.

103. Hoof, I., Peters, B., Sidney, J., et al. (2009) NetMHCpan, a method for MHC class I binding prediction beyond humans. *Immunogenetics*, **61**, 1–13.

104. Rasmussen, M., Harndahl, M., Stryhn, A., et al. (2014) Uncovering the Peptide-Binding Specificities of HLA-C: A General Strategy To Determine the Specificity of Any MHC Class I Molecule. *J. Immunol.*, **193**, 4790–4802.

105. Rasmussen, M., Harndahl, M., Stryhn, A., et al. (2014) Uncovering the Peptide-Binding Specificities of HLA-C: A General Strategy To Determine the Specificity of Any MHC Class I Molecule. *J. Immunol.*, **193**, 4790–4802.

106. Rasmussen, M., Harndahl, M., Stryhn, A., et al. (2014) Uncovering the Peptide-Binding Specificities of HLA-C: A General Strategy To Determine the Specificity of Any MHC Class I Molecule. *J. Immunol.*, **193**, 4790–4802.

107. Adams, N. M., Geary, C. D., Santosa, E. K., et al. (2019) Cytomegalovirus Infection Drives Avidity Selection of Natural Killer Cells. *Immunity*, **50**, 1381-1390.e5.

108. Boyington, J. C., Motyka, S. A., Schuck, P., et al. (2000) Crystal structure of an NK cell immunoglobulin-like receptor in complex with its class I MHC ligand. *Nature*, **405**, 537–43.

109. Béziat, V., Traherne, J., Malmberg, J.-A., et al. (2014) Tracing dynamic expansion of human NK-cell subsets by high-resolution analysis of KIR repertoires and cellular differentiation. *Eur. J. Immunol.*, **44**, 2192–6.

110. Shimizu, Y. and DeMars, R. (1989) Production of human cells expressing individual transferred HLA-A,-B,-C genes using an HLA-A,-B,-C null human cell line. *J. Immunol.*, **142**, 3320–8.

111. Alter, G., Malenfant, J. M. and Altfeld, M. (2004) CD107a as a functional marker for the identification of natural killer cell activity. *J. Immunol. Methods*, **294**, 15–22.

112. Ziegler, M. C., Nelde, A., Weber, J. K., et al. (2020) HIV-1-induced changes in HLA-C*03: 04-presented peptide repertoires lead to reduced engagement of inhibitory NK cell receptors. *AIDS*.

113. Simms, P. E. and Ellis, T. M. (1996) Utility of flow cytometric detection of CD69 expression as a rapid method for determining poly- and oligoclonal lymphocyte activation. *Clin. Diagn. Lab. Immunol.*, **3**, 301–304.

114. Alter, G. and Altfeld, M. (2009) NK cells in HIV-1 infection: evidence for their role in the control of HIV-1 infection. *J. Intern. Med.*, **265**, 29–42.

115. Koup, R. A., Safrit, J. T., Cao, Y., et al. (1994) Temporal association of cellular immune responses with the initial control of viremia in primary human immunodeficiency virus type 1 syndrome. *J. Virol.*, **68**, 4650–4655.

116. Bertoletti, A. and Ferrari, C. (2003) Kinetics of the immune response during HBV and HCV infection. Kinetics of the immune response during HBV and HCV infection. *Hepatology* **(2003)** , *38*, 4–13.

117. Biron, C. A. (1999) Initial and innate responses to viral infections - Pattern setting in immunity or disease. Initial and innate responses to viral infections - Pattern setting in immunity or disease. *Curr. Opin. Microbiol.* **(1999)** .

118. Carrington, M. and O'Brien, S. J. (2003) The Influence of HLA Genotype on AIDS . *Annu. Rev. Med.*, **54**, 535–551.

119. Knapp, S., Warshow, U., Hegazy, D., et al. (2010) Consistent beneficial effects of killer cell immunoglobulin-like receptor 2DL3 and group 1 human leukocyte antigen-C following exposure to hepatitis C virus. *Hepatology*, **51**, 1168–1175.

120. Rajagopalan, S. and Long, E. O. (1997) The direct binding of a p58 killer cell inhibitory receptor to human histocompatibility leukocyte antigen (HLA)-Cw4 exhibits peptide selectivity. *J. Exp. Med.*, **185**, 1523–8.

121. Hölzemer, A., Thobakgale, C. F., Jimenez Cruz, C. A., et al. (2015) Selection of an HLA-C*03:04-Restricted HIV-1 p24 Gag Sequence Variant Is Associated with Viral Escape from KIR2DL3+ Natural Killer Cells: Data from an Observational Cohort in South Africa. *PLOS Med.*, **12**, e1001900.

122. Sun, P. D., Boyington, J. C., Motyka, S. A., et al. (2000) Crystal structure of an NK cell immunoglobulin-like receptor in complex with its class I MHC ligand. *Nature*, **405**, 537–543.

123. Vivian, J. P., Duncan, R. C., Berry, R., et al. (2011) Killer cell immunoglobulin-like receptor 3DL1-mediated recognition of human leukocyte antigen B. *Nature*, **479**, 401–5.

124. Kiepiela, P., Leslie, A. J., Honeyborne, I., et al. (2004) Dominant influence of HLA-B in mediating the potential co-evolution of HIV and HLA. *Nature*, **432**, 769–775.

125. Co, M. D. T., Kilpatrick, E. D. and Rothman, A. L. (2009) Dynamics of the CD8 T-cell response following yellow fever virus 17D immunization. *Immunology*, **128**, e718-27.

126. Townsley, E., O'Connor, G., Cosgrove, C., et al. (2016) Interaction of a dengue virus NS1-derived peptide with the inhibitory receptor KIR3DL1 on natural killer cells. *Clin. Exp. Immunol.*, **183**, 419–30.

127. Colantonio, A. D., Bimber, B. N., Neidermyer, W. J., et al. (2011) KIR Polymorphisms Modulate Peptide-Dependent Binding to an MHC Class I Ligand with a Bw6 Motif. .

128. Dokun, A. O., Kim, S., Smith, H. R. C., et al. (2001) Specific and nonspecific NK cell activation during virus infection. *Nat. Immunol.*, **2**, 951–956.

129. Gumá, M., Angulo, A. and López-Botet, M. (2006) NK cell receptors involved in the response to human cytomegalovirus infection. *Curr. Top. Microbiol. Immunol.*, **298**, 207–23.

130. Björkström, N. K., Lindgren, T., Stoltz, M., et al. (2011) Rapid expansion and long-term persistence of elevated NK cell numbers in humans infected with hantavirus. *J. Exp. Med.*, **208**, 13–21.

References

131. Alter, G., Rihn, S., Walter, K., et al. (2009) HLA class I subtype-dependent expansion of KIR3DS1+ and KIR3DL1+ NK cells during acute human immunodeficiency virus type 1 infection. *J. Virol.*, **83**, 6798–805.

132. Tarazona, R., Casado, J. G., Delarosa, O., et al. (2002) Selective depletion of CD56(dim) NK cell subsets and maintenance of CD56(bright) NK cells in treatment-naive HIV-1-seropositive individuals. *J. Clin. Immunol.*, **22**, 176–83.

133. Morishima, C., Paschal, D. M., Wang, C. C., et al. (2006) Decreased NK cell frequency in chronic hepatitis C does not affectex vivo cytolytic killing. *Hepatology*, **43**, 573–580.

134. Vossen, M. T. M., Biezeveld, M. H., de Jong, M. D., et al. (2005) Absence of Circulating Natural Killer and Primed CD8 $^{+}$Cells in Life-Threatening Varicella. *J. Infect. Dis.*, **191**, 198–206.

135. Alter, G., Rihn, S., Walter, K., et al. (2009) HLA class I subtype-dependent expansion of KIR3DS1+ and KIR3DL1+ NK cells during acute human immunodeficiency virus type 1 infection. *J. Virol.*, **83**, 6798–6805.

136. Kim, S., Sunwoo, J. B., Yang, L., et al. HLA alleles determine differences in human natural killer cell responsiveness and potency. .

137. Gaucher, D., Therrien, R., Kettaf, N., et al. (2008) Yellow fever vaccine induces integrated multilineage and polyfunctional immune responses. *J. Exp. Med.*, **205**, 3119–31.

138. Béziat, V., Dalgard, O., Asselah, T., et al. (2012) CMV drives clonal expansion of NKG2C $^{+}$ NK cells expressing self-specific KIRs in chronic hepatitis patients. *Eur. J. Immunol.*, **42**, 447–457.

139. Fausther-Bovendo, H., Wauquier, N., Cherfils-Vicini, J., et al. (2008) NKG2C is a major triggering receptor involved in the Vδ1 T cell-mediated cytotoxicity against HIV-infected CD4 T cells. *AIDS*, **22**, 217–226.

140. Béziat, V., Sleiman, M., Goodridge, J. P., et al. (2015) Polyclonal Expansion of NKG2C(+) NK Cells in TAP-Deficient Patients. *Front. Immunol.*, **6**, 507.

141. Daëron, M., Jaeger, S., Du Pasquier, L., et al. (2008) Immunoreceptor tyrosine-based inhibition motifs: a quest in the past and future. *Immunol. Rev.*, **224**, 11–43.

142. Arlettaz, L., Degermann, S., De Rham, C., et al. (2004) Expression of inhibitory KIR is confined to CD8+ effector T cells and limits their proliferative capacity. *Eur. J. Immunol.*, **34**, 3413–22.

143. Béziat, V., Traherne, J. A., Liu, L. L., et al. (2013) Influence of KIR gene copy number on natural killer cell education. *Blood*, **121**, 4703–4707.

144. van Teijlingen, N. H., Hölzemer, A., Körner, C., et al. (2014) Sequence variations in HIV-1 p24 Gag-derived epitopes can alter binding of KIR2DL2 to HLA-C*03. *AIDS*, **28**, 1399–1408.

145. Ternette, N., Yang, H., Partridge, T., et al. (2016) Defining the HLA class I-associated viral antigen repertoire from HIV-1-infected human cells. *Eur. J. Immunol.*, **46**, 60–9.

146. Hickman, H. D., Luis, A. D., Bardet, W., et al. (2003) Cutting Edge: Class I Presentation of Host Peptides Following HIV Infection. *J. Immunol.*, **171**, 22–26.

147. Verhoef, C. M., Van Roon, J. A., Vianen, M. E., et al. (1999) Lymphocyte stimulation by CD3-CD28 enables detection of low T cell interferon-gamma and interleukin-4 production in rheumatoid arthritis. *Scand. J. Immunol.*, **50**, 427–32.

148. Chong, C., Marino, F., Pak, H., et al. (2018) High-throughput and Sensitive Immunopeptidomics Platform Reveals Profound Interferonγ-Mediated Remodeling of the Human Leukocyte Antigen (HLA) Ligandome. *Mol. Cell. Proteomics*, **17**, 533–548.

149. Gfeller, D., Guillaume, P., Michaux, J., et al. (2018) The Length Distribution and Multiple Specificity of Naturally Presented HLA-I Ligands. *J. Immunol.*, **201**, 3705–3716.

150. Rist, M. J., Theodossis, A., Croft, N. P., et al. (2013) HLA peptide length preferences control CD8+ T cell responses. *J. Immunol.*, **191**, 561–71.

151. Pymm, P., Illing, P. T., Ramarathinam, S. H., et al. (2017) MHC-I peptides get out of the groove and enable a novel mechanism of HIV-1 escape. *Nat. Struct. Mol. Biol.*, **24**, 387–394.

152. Fan, Q. R., Long, E. O. and Wiley, D. C. (2001) Crystal structure of the human natural killer cell inhibitory receptor KIR2DL1–HLA-Cw4 complex. *Nat. Immunol.*, **2**, 452–460.

153. Liu, J., Xiao, Z., Ko, H. L., et al. (2014) Activating killer cell immunoglobulin-like receptor 2DS2 binds to HLA-A*11. *Proc. Natl. Acad. Sci. U. S. A.*, **111**, 2662–7.

154. Remesh, S. G., Andreatta, M., Ying, G., et al. (2017) Unconventional Peptide Presentation by Major Histocompatibility Complex (MHC) Class I Allele HLA-A*02:01: BREAKING CONFINEMENT. *J. Biol. Chem.*, **292**, 5262–5270.

155. McMurtrey, C., Trolle, T., Sansom, T., et al. (2016) Toxoplasma gondii peptide ligands open the gate of the HLA class I binding groove. *Elife*, **5**.

156. Daniel, S., Brusic, V., Caillat-Zucman, S., et al. (1998) Relationship between peptide selectivities of human transporters associated with antigen processing and HLA class I molecules. *J. Immunol.*, **161**, 617–24.

157. Allen, R. L., O'Callaghan, C. A., McMichael, A. J., et al. (1999) Cutting edge: HLA-B27 can form a novel beta 2-microglobulin-free heavy chain homodimer structure. *J. Immunol.*, **162**, 5045–8.

158. Yaciuk, J. C., Skaley, M., Bardet, W., et al. (2014) Direct interrogation of viral peptides presented by the class I HLA of HIV-infected T cells. *J. Virol.*, **88**, 12992–3004.

159. Rucevic, M., Kourjian, G., Boucau, J., et al. (2016) Analysis of Major Histocompatibility Complex-Bound HIV Peptides Identified from Various Cell Types Reveals Common Nested Peptides and Novel T Cell Responses. *J. Virol.*, **90**, 8605–8620.

160. Rucevic, M., Kourjian, G., Boucau, J., et al. (2016) Analysis of Major Histocompatibility Complex-Bound HIV Peptides Identified from Various Cell Types Reveals Common Nested Peptides and Novel T Cell Responses. *J. Virol.*, **90**, 8605–20.

161. Altfeld, M. A., Livingston, B., Reshamwala, N., et al. (2001) Identification of novel HLA-A2-restricted human immunodeficiency virus type 1-specific cytotoxic T-lymphocyte epitopes predicted by the HLA-A2 supertype peptide-binding motif. *J. Virol.*, **75**, 1301–11.

162. Levitz, L., Koita, O. A., Sangare, K., et al. (2012) Conservation of HIV-1 T cell epitopes across time and clades: validation of immunogenic HLA-A2 epitopes selected for the GAIA HIV vaccine. *Vaccine*, **30**, 7547–60.

163. Llano, A., WILLIAMS, A., OLVERA, A., et al. (2013) Best-characterized HIV-1 CTL epitopes: the 2013 update. Best-characterized HIV-1 CTL epitopes: the 2013 update **(2013)** .

References

164. Körner, C., Simoneau, C. R., Schommers, P., et al. (2017) HIV-1-Mediated Downmodulation of HLA-C Impacts Target Cell Recognition and Antiviral Activity of NK Cells. *Cell Host Microbe*, **22**, 111-119.e4.

165. Shi, Y., Mosser, D. D. and Morimoto, R. I. (1998) Molecular chaperones as HSF1-specific transcriptional repressors. *Genes Dev.*, **12**, 654–66.

166. Solis, M., Wilkinson, P., Romieu, R., et al. (2006) Gene expression profiling of the host response to HIV-1 B, C, or A/E infection in monocyte-derived dendritic cells. *Virology*, **352**, 86–99.

167. Kumar, M. and Mitra, D. (2005) Heat shock protein 40 is necessary for human immunodeficiency virus-1 Nef-mediated enhancement of viral gene expression and replication. *J. Biol. Chem.*, **280**, 40041–50.

168. Pal, R., Garzino-Demo, A., Markham, P., et al. Inhibition of HIV-1 infection by the β-chemokine MDC. *science.sciencemag.org*.

169. Cota, M., Mengozzi, M., … E. V.-P. of the, et al. Selective inhibition of HIV replication in primary macrophages but not T lymphocytes by macrophage-derived chemokine. *Natl. Acad Sci.*

170. Agrawal, L., Vanhorn-Ali, Z. and Alkhatib, G. (2002) Multiple determinants are involved in HIV coreceptor use as demonstrated by CCR4/CCL22 interaction in peripheral blood mononuclear cells (PBMCs). *J. Leukoc. Biol.*, **72**, 1063–1074.

171. Boyington, J. C., Motyka, S. A., Schuck, P., et al. (2000) Crystal structure of an NK cell immunoglobulin-like receptor in complex with its class I MHC ligand. *Nature*, **405**, 537–43.

172. Maenaka, K., Juji, T., Stuart, D. I., et al. (1999) Crystal structure of the human p58 killer cell inhibitory receptor (KIR2DL3) specific for HLA-Cw3-related MHC class I. *Structure*, **7**, 391–8.

173. Boyington, J. C. and Sun, P. D. (2002) A structural perspective on MHC class I recognition by killer cell immunoglobulin-like receptors. *Mol. Immunol.*, **38**, 1007–1021.

174. Chapel, A., Garcia-Beltran, W. F., Hölzemer, A., et al. (2017) Peptide-specific engagement of the activating NK cell receptor KIR2DS1. *Sci. Rep.*, **7**, 2414.

175. Singh, N. K., Riley, T. P., Baker, S. C. B., et al. (2017) Emerging Concepts in TCR Specificity: Rationalizing and (Maybe) Predicting Outcomes. *J. Immunol.*, **199**, 2203–2213.

Appendix

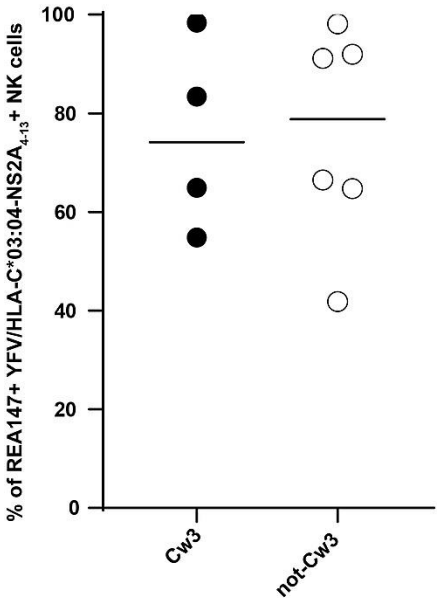

SUP 1 Frequencies of YFV/HLA-C*03:04-NS2A$_{4\text{-}13}^{+}$ KIR2DL2/3^{+} in HLA-C*03:04^{+} vs HLA-C*03:04^{neg} individuals (95).

Appendix

SUP 2 HLA-C*03:04-restricted peptides with sequence and protein classification used for analysis (112).

Name	Sequence	Lenght	# Proteins	Protein Group Accessions	Protein	best NetMHC Allele Rank	best NetMHC Rank
peptides on naive cells							
n1	FITESYQTL	9	1	P14921	Protein C-ets-1	C0304	0.05
n2	VVNGAFMVL	9	1	Q96JK2	DDB1- and CUL4-associated factor 5	C0304	0.15
n3	VIYPARISL	9	1	P25685	DnaJ homolog subfamily B member 1	C0304	0.25
n4	VAKAVTQAL	9	1	Q9Y490	Talin-1	C0304	0.25
n5	YIIDPQNGL	9	1	Q9NRH2	SNF-related serine/threonine-protein kinase	C0304	0.25
n6	FIMEAGVKL	9	2	Q8N1B3;	Cyclin-Q	C0304	0.04
				P0C7Q3	Putative cyclin-related protein FAM58B		
n7	IAIGSQPVL	9	1	Q96DZ1	Endoplasmic reticulum lectin 1	C0304	0.05
n8	LAALPGVSL	9	1	Q9H400	Lck-interacting transmembrane adapter 1	C0304	0.05
n9	TAIERSQTL	9	1	Q9NRY5	Protein FAM114A2	C0304	0.07
n10	FLVGVFTTM	9	1	O15050	TPR and ankyrin repeat-containing protein 1	C0304	0.12
n11	FSTGNFNVL	9	1	Q15629	Translocating chain-associated membrane protein 1	C0304	0.01
n12	FIYTSELEL	9	1	Q53GT1	Kelch-like protein 22	C0304	0.05
n13	FIMGKVPVF	9	1	Q14156	Protein EFR3 homolog A	C0304	0.17
n14	YVAIQAVLSL	10	9	P62736	Actin, aortic smooth muscle	C0304	0.17
				Q562R1	Beta-actin-like protein 2		
				Q9BYX7	Putative beta-actin-like protein 3		
				P60709	Actin, cytoplasmic 1		
				P68032	Actin, alpha cardiac muscle 1		
				P63261	Actin, cytoplasmic 2		
				P63267	Actin, gamma-enteric smooth muscle		
				P68133	Actin, alpha skeletal muscle		
				A5A3E0	POTE ankyrin domain family member F		
n15	VATEGSREL	9	1	Q96C10	Probable ATP-dependent RNA helicase DHX58	C0304	0.12
n16	MVLENVKEM	9	1	P62316	Small nuclear ribonucleoprotein Sm D2	C0304	0.15
peptides on HIV-1-infected cells							
h1	LAMRPLASL	9	1	Q9NUQ8	ATP-binding cassette sub-family F member 3	C0304	0.01
h2	LAIESANEL	9	1	Q7L014	Probable ATP-dependent RNA helicase DDX46	C0304	0.01
h3	HAVFPTSSM	9	1	P35612	Beta-adducin	C0304	0.04
h4	VVVQPYNSL	9	2	P23258	Tubulin gamma-1 chain	C0304	0.3
				Q9NRH3	Tubulin gamma-2 chain		
h5	FIEVTTQEL	9	1	Q13936	Voltage-dependent L-type calcium channel subunit alpha-1C	C0304	0.4
h6	ILSQPTPSL	9	1	Q6PL18	ATPase family AAA domain-containing protein 2	C0304	0.5
h7	LAMVLTSAL	9	1	P15248	Interleukin-9	C0304	0.01
h8	YAFPVSNNL	9	1	Q13614	Myotubularin-related protein 2	C0304	0.01
h9	YAIQATETL	9	1	P51679	C-C chemokine receptor type 4	C0304	0.01
h10	FARPASPSL	9	1	Q8WUF5	RelA-associated inhibitor	C0304	0.02
h11	FAVGSFHTL	9	1	Q9P2H3	Intraflagellar transport protein 80 homolog	C0304	0.01
h12	FVAHPVSSL	9	1	Q5SRE5	Nucleoporin NUP188 homolog	C0304	0.01
h13	LALETTNSL	9	1	Q8IX01	SURP and G-patch domain-containing protein 2	C0304	0.01
h14	YAISKPEVL	9	1	Q6NUN9	Zinc finger protein 746	C0304	0.01
h15	YAYETKDAL	9	3	P32298	G protein-coupled receptor kinase 4	C0304	0.01
				P34947	G protein-coupled receptor kinase 5		
				P43250	G protein-coupled receptor kinase 6		
h16	FAINNSKSF	9	1	P01111	GTPase NRas	C0304	0.02

Acknowledgements

This thesis could not have been possible without the help of many people. Therefore I would like to thank:

First and foremost I want to thank **Marcus Altfeld**, who gave me the opportunity to work on this awesome topic in his group. He was key for this project, as he did not only provide funding and the scientific freedom to implement my own ideas, but also supported my research by creating a nice work environment with helpful ideas and inspiring thoughts. Thank you for your trust in me and your excellent guidance.

I would also like to thank my second supervisor **Chris Meier** for scientific discussions and advice during the time of my Ph.D.

I thank the **NIH tetramer core facility** for kindly providing HLA-I-tetramers.

I would like to thank **Sebastian Lunemann**, for his constant helpful support, explaining me the scientific world and for being a perfect coffee provider

I would like to thank **Christian Hoffmann**, **Julian Schulze zur Wiesch** and **Anne Rechtien** for providing patient samples.

I would like to thank the **participants of the healthy blood cohort**. Without you this project would not have been possible.

Many thanks go to **Annika Nelde, Christian Schreitmüller, Daniel Kowalewski** and **Jeffrey K Weber** for being excellent collaboration partners.

I want to thank **Gloria Martrus** for her patience in answering my questions and circulating her knowledge.

I thank the core facility Fluorescence Cytometry at the HPI, especially **Arne Düsedau** and **Jana Hennesen,** for helpful support.

Big hug to **Caroline Pfeifer** and **Sven Hagen** for personal support in difficult as well as happy times.

Last but not least I would like to express my heartfelt thanks to all of my **colleagues** of the department of **virus immunology**. Thank you for your experimental help and scientific suggestions at various points of my research and especially for creating such a cooperative and enjoyable atmosphere.

Acknowledgements

List of hazardous substances used according to GHS

Product name	**CAS number**	**Hazard pictogram**	**Hazard an precautionary statments**
Ethylendiamin-tetraessigsäure (EDTA)	0-00-4	 Harmful	H: 319 P: 305+351+338
Paraformaldehyd (PFA)	30525-89-4	 Flammable  Health hazard  Corrosive  Harmful	H: 301 + 311 + 314 + 317 + 331 + 341 +350 P: 201, 202, 260, 261, 264, 270, 271, 272, 280, 281, 301+310, 301+330+331, 302+352, 303+361+353, 304+340, 305+351+338, 308+313, 310, 311, 312, 321, 322, 330, 333+313, 361, 363, 403+233, 405, 501
3-((3-Cholamidopropyl)dimethyl-ammonium)-1-propanesulfonate (CHAPS)	331717-45-4	 Harmful	H: 315 + 319 + 335 P: 261, 264, 271, 280, 302+352, 304+340, 305+351+338, 312, 321, 332+313, 337+313, 362, 403+233, 405, 501
Trypan blue	72-57-1	 Harmful	H: 350 P: 201, 202, 281, 308+313, 405, 501

Eidesstattliche Versicherung

Declaration on oath

„Hiermit versichere ich, Maja Christiane Ziegler, an Eides statt, die vorliegende Dissertation selbst verfasst und keine anderen als die angegebenen Hilfsmittel benutzt zu haben. Die eingereichte schriftliche Fassung entspricht der auf dem elektronischen Speichermedium. Ich versichere, dass diese Dissertation nicht in einem früheren Promotionsverfahren eingereicht wurde."

I, Maja Christiane Ziegler, hereby declare, on oath, that I have written the present dissertation by my own and have not used other than the acknowledged resources and aids. The submitted written version corresponds to that on the electronic storage medium. I assure you that this dissertation was not submitted in a previous doctoral procedure. "

Kiel 17.07.2020
Ort und Datum
City and date

M. Ziegler
Unterschrift
signature